SSC-282
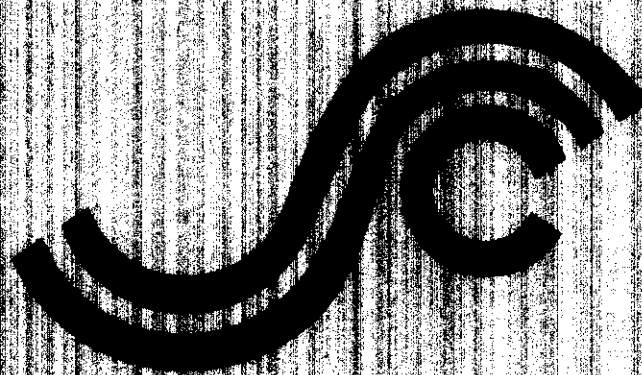# (SL-7-24)

COMPARISON OF STRESSES
CALCULATED USING THE
DAISY SYSTEM TO THOSE
MEASURED ON THE
SL-7 CONTAINERSHIP PROGRAM

Ship Structure Committee

An Interagency Advisory Committee
Dedicated to Improving the Structure of Ships

SR-1236

APRIL 1979

This report is one of a group of Ship Structure Committee Reports which describes the SL-7 Instrumentation Program. This program, a jointly funded undertaking of Sea-Land Service, Inc., the American Bureau of Shipping and the Ship Structure Committee, represents an excellent example of cooperation between private industry, regulatory authority and government. The goal of the program is to advance understanding of the performance of ships' hull structures and the effectiveness of the analytical and experimental methods used in their design. While the experiments and analyses of the program are keyed to the SL-7 Containership and a considerable body of the data developed relates specifically to that ship, the conclusions of the program will be completely general, and thus applicable to any surface ship structure.

The program includes measurement of hull stresses, accelerations and environmental and operating data on the S.S. SEA-LAND MCLEAN, development and installation of a microwave radar wavemeter for measuring the seaway encountered by the vessel, a wave tank model study and a theoretical hydrodynamic analysis which relate to the wave induced loads, a structural model study and a finite element structural analysis which relate to the structural response, and installation of long term stress recorders on each of the eight vessels of the class.

Results of each of the program elements are being made available through the National Technical Information Service, each identified by an SL-7 number and an AD-number. A list of all SL-7 reports available to date is included on the back cover of this report.

This report discusses the results of the finite element structural analysis program. Comparisons are made to the measured full-scale strain-gauge data at sea and while undergoing dockside calibration measurements. This is part of the effort to develop correlations of the results of the several program elements.

Henry H. Bell
Rear Admiral, U. S. Coast Guard
Chairman, Ship Structure Committee

SSC-282

(SL-7-24)

FINAL REPORT

on

Project SR-1236

"SL-7 Stress Calculations Compared

With Full-Scale Measured Values"

COMPARISON OF STRESSES CALCULATED

USING THE DAISY SYSTEM TO THOSE

MEASURED ON THE SL-7 CONTAINERSHIP PROGRAM

by

Hsien-Yun Jan
Kuan-Tao Chang
Matias E. Wojnarowski

AMERICAN BUREAU OF SHIPPING

under

Department of Transportation
United States Coast Guard
Contract No. DOT-CG-63176-A

U. S. Coast Guard Headquarters
Washington, D.C.
1979

1. Report No. SSC-282 - (SL-7-24)	2. Government Accession No.	3. Recipient's Catalog No.

4. Title and Subtitle Comparison of Stresses Calculated Using the DAISY System to Those Measured on the SL-7 Containership Program	5. Report Date January 1979
	6. Performing Organization Code ABS

7. Author's) Hsien-Yun Jan, Kuan-Tao Chang, Matias E. Wojnarowski	8. Performing Organization Report No. RD-78005

9. Performing Organization Name and Address American Bureau of Shipping Ocean Engineering Division 45 Broad Street New York, NY 10004	10. Work Unit No. (TRAIS)
	11. Contract or Grant No. DOT-CG-63176 A

12. Sponsoring Agency Name and Address Commandant (G-DSA) U.S. Coast Guard Headquarters Office of Research & Development Washington, D.C. 20590	13. Type of Report and Period Covered Final Report December 1976 to May 1978
	14. Sponsoring Agency Code G-DSA-1

15. Supplementary Notes

16. Abstract

A comparison of stresses calculated using the ABS/DAISY system with those measured on board the SL-7 Containership is undertaken to verify the analytical procedures used in assessing the strength of ships in a seaway. The comparisons and evaluations are performed for four different and progressively more severe technical conditions: dockside calibration, RMS stresses in head seas, instantaneous stresses in head seas and instantaneous stresses in oblique seas.

The overall comparison between calculated and measured stresses for the dockside calibration is good where thermal effects were small but inconclusive elsewhere. The comparison of RMS stresses in head seas is generally satisfactory, using both the spectrum analysis approach and the equivalent regular wave approach, and the comparison of instantaneous stresses in head seas and in oblique seas is also good for the wave conditions considered.

The results show that the existing analytical tools for predicting wave loads and structural responses are suitable to assess the overall strength of the hull-girder. All the measured and calculated hull-girder stresses are of low magnitude, and no modifications to the present hull-girder strength standard are deemed necessary.

17. Key Words Finite Element Analysis, Full-Scale Instrumentation, Dock-Side Calibration, Comparison of Dynamic Stresses, Shipmotion, Dynamic Pressure, Spectrum Analysis, Instantaneous Stresses, RMS Stresses, Containership	18. Distribution Statement Document is available to the public through the National Technical Information Service, Springfield, VA 22161.

19. Security Classif. (of this report) UNCLASSIFIED	20. Security Classif. (of this page) UNCLASSIFIED	21. No. of Pages 102	22. Price

Form DOT F 1700.7 (8-72)   Reproduction of completed page authorized

SHIP STRUCTURE COMMITTEE

The SHIP STRUCTURE COMMITTEE is constituted to prosecute a research program to improve the hull structures of ships and other marine structures by an extension of knowledge pertaining to design, materials and methods of construction.

RADM H. H. Bell   (Chairman)
Chief, Office of Merchant Marine
    Safety
U. S. Coast Guard Headquarters

Mr. P. M. Palermo
Assistant for Structures
Naval Ship Engineering Center
Naval Sea Systems Command

Mr. W. N. Hannan
Vice President
American Bureau of Shipping

Mr. M. Pitkin
Assistant Administrator for
    Commercial Development
Maritime Administration

Mr. R. B. Krahl
Chief, Branch of Marine Oil and
    Gas Operations
U. S. Geological Survey

Mr. C. J. Whitestone
Chief Engineer
Military Sealift Command

LCDR T. H. Robinson, U. S. Coast Guard (Secretary)

SHIP STRUCTURE SUBCOMMITTEE

The SHIP STRUCTURE SUBCOMMITTEE acts for the Ship Structure Committee on technical matters by providing technical coordination for the determination of goals and objectives of the program, and by evaluating and interpreting the results in terms of structural design, construction and operation.

U. S. COAST GUARD

Cdr. J. C. Card
Lcdr S. H. Davis
Capt C. B. Glass
Dr. W. C. Dietz

NAVAL SEA SYSTEMS COMMAND

Mr. R. Chiu
Mr. R. Johnson
Mr. G. Sorkin
Mr. J. B. O'Brien (Contracts Admin.)

MARITIME ADMINISTRATION

Mr. F. J. Dashnaw
Mr. N. O. Hammer
Mr. F. Seibold
Mr. M. Touma

**NATIONAL ACADEMY OF SCIENCES
    SHIP RESEARCH COMMITTEE**

Mr. O. H. Oakley - Liaison
Mr. R. W. Rumke - Liaison

**SOCIETY OF NAVAL ARCHITECTS &
    MARINE ENGINEERS**

Mr. A. B. Stavovy - Liaison

WELDING RESEARCH COUNCIL

Mr. K. H. Koopman - Liaison

MILITARY SEALIFT COMMAND

Mr. T. W. Chapman
Mr. A. B. Stavovy
Mr. D. Stein
Mr. J. Torresen

AMERICAN BUREAU OF SHIPPING

Dr. H. Y. Jan
Mr. D. Liu
Mr. I. L. Stern
Mr. S. G. Stiansen (Chairman)

U. S. GEOLOGICAL SURVEY

Mr. R. Giangerelli
Mr. J. Gregory

INTERNATIONAL SHIP STRUCTURES CONGRESS

Prof. J. H. Evans - Liaison

AMERICAN IRON & STEEL INSTITUTE

Mr. R. H. Sterne - Liaison

STATE UNIV. OF NEW YORK MARITIME COLLEGE

Dr. W. R. Porter - Liaison

U. S. COAST GUARD ACADEMY

Capt W. C. Nolan - Liaison

U. S. NAVAL ACADEMY

Dr. R. Battacharyya - Liaison

U. S. MERCHANT MARINE ACADEMY
Dr. Chin-Bea Kim - Liaison

METRIC CONVERSION FACTORS

Approximate Conversions to Metric Measures

Symbol	When You Know	Multiply by	To Find	Symbol

LENGTH

Symbol	When You Know	Multiply by	To Find	Symbol
in	inches	*2.5	centimeters	cm
ft	feet	30	centimeters	cm
yd	yards	0.9	meters	m
mi	miles	1.6	kilometers	km

AREA

Symbol	When You Know	Multiply by	To Find	Symbol
in^2	square inches	6.5	square centimeters	cm^2
ft^2	square feet	0.09	square meters	m^2
yd^2	square yards	0.8	square meters	m^2
mi^2	square miles	2.6	square kilometers	km^2
	acres	0.4	hectares	ha

MASS (weight)

Symbol	When You Know	Multiply by	To Find	Symbol
oz	ounces	28	grams	g
lb	pounds	0.45	kilograms	kg
	short tons (2000 lb)	0.9	tonnes	t

VOLUME

Symbol	When You Know	Multiply by	To Find	Symbol
tsp	teaspoons	5	milliliters	ml
Tbsp	tablespoons	15	milliliters	ml
fl oz	fluid ounces	30	milliliters	ml
c	cups	0.24	liters	l
pt	pints	0.47	liters	l
qt	quarts	0.95	liters	l
gal	gallons	3.8	liters	l
ft^3	cubic feet	0.03	cubic meters	m^3
yd^3	cubic yards	0.76	cubic meters	m^3

TEMPERATURE (exact)

Symbol	When You Know	Multiply by	To Find	Symbol
°F	Fahrenheit temperature	5/9 (after subtracting 32)	Celsius temperature	°C

*1 in = 2.54 (exactly). For other exact conversions and more detailed tables, see NBS Misc. Publ. 286, Units of Weights and Measures, Price $2.25, SD Catalog No. C13.10 286.

Approximate Conversions from Metric Measures

Symbol	When You Know	Multiply by	To Find

LENGTH

Symbol	When You Know	Multiply by	To Find
mm	millimeters	0.04	inches
cm	centimeters	0.4	inches
m	meters	3.3	feet
m	meters	1.1	yards
km	kilometers	0.6	miles

AREA

Symbol	When You Know	Multiply by	To Find
cm^2	square centimeters	0.16	square inches
m^2	square meters	1.2	square yards
km^2	square kilometers	0.4	square miles
ha	hectares (10,000 m^2)	2.5	acres

MASS (weight)

Symbol	When You Know	Multiply by	To Find
g	grams	0.035	ounces
kg	kilograms	2.2	pounds
t	tonnes (1000 kg)	1.1	short tons

VOLUME

Symbol	When You Know	Multiply by	To Find
ml	milliliters	0.03	fluid ounces
l	liters	2.1	pints
l	liters	1.06	quarts
l	liters	0.26	gallons
m^3	cubic meters	35	cubic feet
m^3	cubic meters	1.3	cubic yards

TEMPERATURE (exact)

Symbol	When You Know	Multiply by	To Find
°C	Celsius temperature	9/5 (then add 32)	Fahrenheit temperature

```
°F
  -40      0    |32  40      98.6  80      120     160    20
                                   |
   |   |   |   |   |   |   |   |   |   |   |   |   |   |   |
  -40    -20    0      20    |40    60      80
°C                           37
```

TABLE OF CONTENTS

LIST OF TABLES

LIST OF FIGURES

This report summarizes the work performed by the Research and Development Department of the American Bureau of Shipping under U.S. Coast Guard Contract No. DOT-CG-63176-A. This project is jointly sponsored by the Ship Structure Committee and the American Bureau of Shipping, and is part of the comprehensive SL-7 Containership Research Program of ship loads, model testing, structural analysis, response analysis, full-scale measurements and data correlation.

The long-range objective of the SL-7 Research Program is to advance the understanding of the responses of hull structures at sea and to verify the current design criteria. Emphasis is focused on the correlation of experimental (full-scale and model) data and theoretical predictions at different phases of the program. The overall research plan, historical background and the interface of various phases of the program were presented and discussed in Reference [1]*. The SL-7 Research Program was sponsored by the Ship Structure Committee, the American Bureau of Shipping and Sea-Land Services, Inc. The major phases which have been completed, either directly under the SL-7 program or associated with it, can be summarized as follows:

1. Full-scale Instrumentation

To investigate the structural responses of a high-speed open-deck containership at sea, an extensive full-scale instrumentation system was installed on board the SL-7 class containership S.S. SEA-LAND McLEAN to measure wave heights, ship motions, accelerations and wave-induced stresses in many critical areas. The detailed information for this system is given in Reference [2]. In addition, a micro-wave radar was developed and installed to measure wave elevations. A finite element analysis of the entire ship [3], using the ABS/DAISY system of computer programs [4], and a steel structural model test [5] were carried out at the planning and installation stage of the instrumentation program. The results of these two research projects were utilized to identify critical regions for strain-gage locations.

After the instrumentation installation was completed, a dockside calibration was carried out by Teledyne Materials Research Company and reported in Reference [6]. Subsequently, a large amount of stress data has been acquired for three

---

* Numbers in brackets designate References listed at the end of the report.

1

consecutive winter seasons, between September 1972 and March 1975. Some sample results are presented in Reference [7]. The wave-meter data was analyzed by Dalzell [8].

2. Correlation of Calculated Structural Responses and Steel Model Experimental Data

Although the finite element method utilized in predicting structural responses to quasi-static loads has been well tested and verified with full-scale and model experimental results in recent years, it is still desirable to validate the analysis procedure and modeling techniques in dealing with a special structure, such as an open-deck containership. Accordingly, the American Bureau of Shipping has performed a structural analysis of the SL-7 Steel Model, using the ABS/DAISY system. The calculated results together with a comparison with experimental data were presented by Elbatouti, Jan and Stiansen [9]. The predicted hull-girder responses to both bending and torsional loads were generally found to be in good agreement with the measured data. Consequently, the ABS/DAISY system and the current modeling practice employed at ABS are considered satisfactory in dealing with containerships.

3. Correlation of Ship-Motion Calculations and Model Experiments

Another significant phase of the SL-7 program was to verify the wave-load prediction. Under the sponsorship of the Ship Structure Committee, a ship-motion computer program, SCORES, was developed in 1972 based on the two-dimensional strip theory [10]. It was generally understood that the strip theory was valid for full-form vessels, but its application to fine-form ships was questionable.

To assess ship motions and wave loads, an SL-7 model was tested in oblique seas in 1974 [11]. The first comparison of the model test data with the SCORES results [12] showed significant discrepancies between the RAOs (Response Amplitude Operators) of ship motions and wave loads. Subsequently, Oceanics Incorporated introduced a speed correction factor in the existing SCORES program and obtained good agreement of the RAO between the model experimental data and the theoretical predictions [13].

Based on the results of the above three phases of the SL-7 research program, it can be seen that the finite element techniques and wave-load predictions have been generally validated. The final phase in the verification of the analytical procedure in assessing ship strength is a correlation of dynamic stresses of ships at sea.

2

The objective of this phase of the SL-7 program is to compare the stresses calculated using the ABS/DAISY system to those measured on the SL-7, in corresponding sea and dockside conditions, and to evaluate the results through each of four different and progressively more severe technical conditions. Accordingly, the work was divided into the following four tasks:

TASK I - Comparison of the results of the DAISY stress analysis with the results of the full-scale dockside calibration.

TASK II - Comparison of the stress spectra calculated from the DAISY analysis results with the selected full-scale at-sea stress spectra.

TASK III - Comparison of the DAISY stress analysis results, using measured acceleration and a specific, selected wave profile estimated from the wave radar data in head seas, with the instantaneous measured stresses taken simultaneously while the wave profile was developed.

TASK IV - Investigation of TASK III for oblique sea conditions.

ANALYSIS PROCEDURE

The procedure utilized in the performance of this study relies heavily on the ABS/DAISY system of computer programs. A brief description of the system and the interface of the associated element programs are presented in Appendix A. The analysis comprises the following four steps:

1. Selection of Record Intervals and Acquisition of the Wave and Full-Scale Stress Data

To compare the measured stress data with theoretical predictions for a ship at sea, it is essential to have reliable information about the actual wave environment. Two wave-measuring meters were installed on-board the SEA-LAND McLEAN, a Tucker wave meter and a micro-wave radar. A correlation and verification study [8] of the wave-meter data shows that the Tucker meter data is in error for the high ship speeds of interest, and the radar wave data appears to be more realistic. Since there was no meaningful stress data recorded with the ship in a "hove-to" condition or at "near zero" speed, the Tucker wave meter data could not be directly utilized for this study. Consequently, the wave environment was solely determined based on recorded signals of the wave radar, as presented by Dalzell [8]. However, it should be noted that the radar wave data has not yet been fully verified. Any possible errors incurred in the wave-measuring system or in the data reduction procedure would be essentially carried through the analysis and might cause stress deviations in the calculation.

The selection of record intervals was based on the availability of the measured stress data, the relative wave angle and the relative directions of the wave and the swell.

Regarding the full-scale stress data, the RMS values, stress spectra and stress-time histories of the midship average bending sensor (LVB) are presented in Reference [8] for all the selected record intervals at sea. For other strain gages, the required stress data was reduced by Teledyne.

For Task I (dockside calibration), all the test conditions were taken into consideration. The detailed information about loading conditions, gage locations and the measured data are presented in Reference [6].

4

2. Approximation of the Wave Environment and Prediction
   of Wave Loads

   For each selected record interval, the wave environ-
ment was approximated either by an equivalent regular wave
or a wave-spectrum approach, depending upon the methods
utilized for each individual task. Details are discussed
under Tasks II and III.

   Once the wave environment was determined, the ABS/
SHIPMOTION and ABS/DYNPRE computer programs were used to
predict ship motions, wave loads and hydrodynamic pressures
for input to the finite element structural model. The ABS/
SHIPMOTION program is a revised version of SCORES. ABS/
DYNPRE which is an extended subroutine of the SHIPMOTION
program calculates the hydrodynamic pressure distribution
on the wet surface of a ship's hull.

   As mentioned in the introduction, the revised version
of SCORES, modified with a speed correction factor, has
been validated with a model test. This modified version
is not available to the public. In the present study, the
ABS version of the SCORES program (designated ABS/SHIPMOTION)
was utilized for wave-load predictions. A speed correction
factor similar to that introduced by Oceanics has been in-
corporated into the ABS version. A sample comparison of the
RAO with the model test data is shown in Figures A-2 and A-3
of Appendix A, which shows that the comparison of the RAO
for the vertical bending moments at midship is very good.
However, the calculated RAO for the lateral bending moment
at midship are generally less than those reduced from model
experiments.

3. Generation of Finite Element Structural Models and
   Calculation of Structural Responses

   In calculating the hull-girder responses, the entire ship
was first represented by a three-dimensional coarse-mesh
finite element model. Subsequently, fine-mesh three-dimen-
sional models were utilized to determine the stress distribution
at selected strain-gage locations. The ABS/DAISY computer
program was used for this step of the analysis. The struc-
tural models and the boundary conditions used in the analysis
are discussed in the following section.

5

4. Analysis of Calculated Results and Comparison with
   Measured Data

    After the completion of the fine-mesh DAISY runs for
each task, a selective output containing strains and stresses
for the selected strain gage locations was printed out.
The analysis of the calculated results varies task by task.
The detailed analysis methods and the comparison with the
measured data are discussed separately under each individual
task.

The SL-7 is an 880'-6" x 105'-6" x 68'-6" twin-screw containership with a displacement of 50,315 long tons at 34'-0" draft. A general arrangement is shown in Figure 1.

The structural analysis for the SL-7 Containership was performed using the ABS/DAISY system of finite element computer programs (see Appendix A) for one coarse-mesh model comprising the entire ship and six fine-mesh models representing detailed structures of selected strain gage regions.
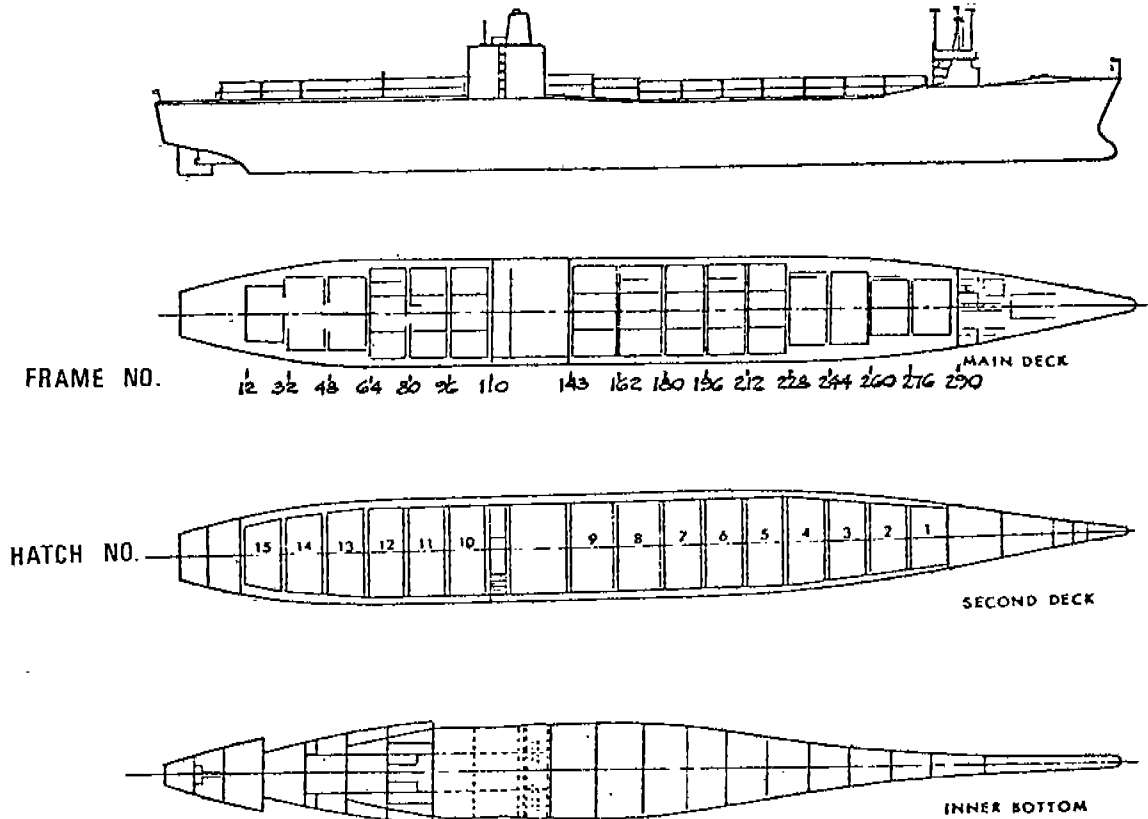
FIGURE 1 - SL-7 GENERAL ARRANGEMENT (FROM REFERENCE [3])

Three-dimensional Coarse-Mesh Model

The coarse-mesh model consists of 2602 nodal points and 9866 degrees of freedom. The major structural members are represented by rods, beams, membrane plates and bending plates,

with a total of 7122 elements. The model comprised only the port side of the vessel because of structural symmetry about the centerline plane. A three-dimensional isometric plot of this model is shown in Figure 2. Computer plots of the decks, bottom, side shell and the centerline profile are shown in Figure 3. Typical transverse bulkheads and web frames in the model are shown in Figure 4. For asymmetric loadings, the loads are divided into symmetric and anti-symmetric loading conditions, as shown in Figure 5, with appropriate boundary restraints at the centerline plane, as shown in Figure 6. In order to prevent rigid body movements due to the possible unbalanced forces on the model, certain additional boundary restraints must be imposed on the model, as shown in Figure 6. LOADER, one of the "DAISY" preprocessor programs, automatically redistributes the unbalanced forces in the model, therefore minimizing the effect of these local boundary restraints on the accuracy of the results.

Three-dimensional Fine-Mesh Models

Six fine-mesh models in the vicinity of selected sensor locations, as shown in Figure 7, are utilized to determine stress distributions and to facilitate comparisons between the calculated results and those obtained from measurements. Computer plots for these six models are shown in Figures 8 through 13, together with sensor locations and designations as specified in Reference [6]. Detailed information about all the sensors installed on board the S.S. SEA-LAND McLEAN is given in Appendix B. Each fine-mesh model consists of rods, beams and bending plates, and has the characteristics described in Table 1. Displacements obtained from the coarse-mesh analysis are used as boundary conditions in the analysis of the fine-mesh models.

8
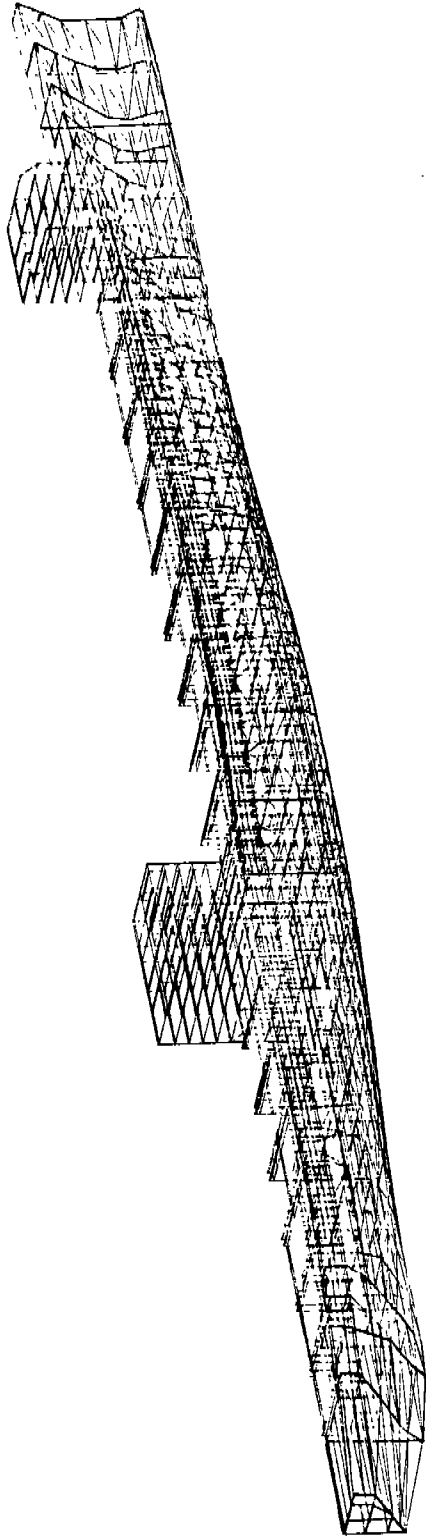
FIGURE 2. – ISOMETRIC PLOT OF FINITE ELEMENT COARSE–MESH MODEL

9

MAIN DECK

SECOND DECK

Z
↑
└→X

BOTTOM

Y
↑
└→X

SIDE SHELL

| | | | | | | | | | | | | | | | |
18   38   70   96 112   142   172   195½   238   258 270   293   311 328

CENTERLINE PROFILE
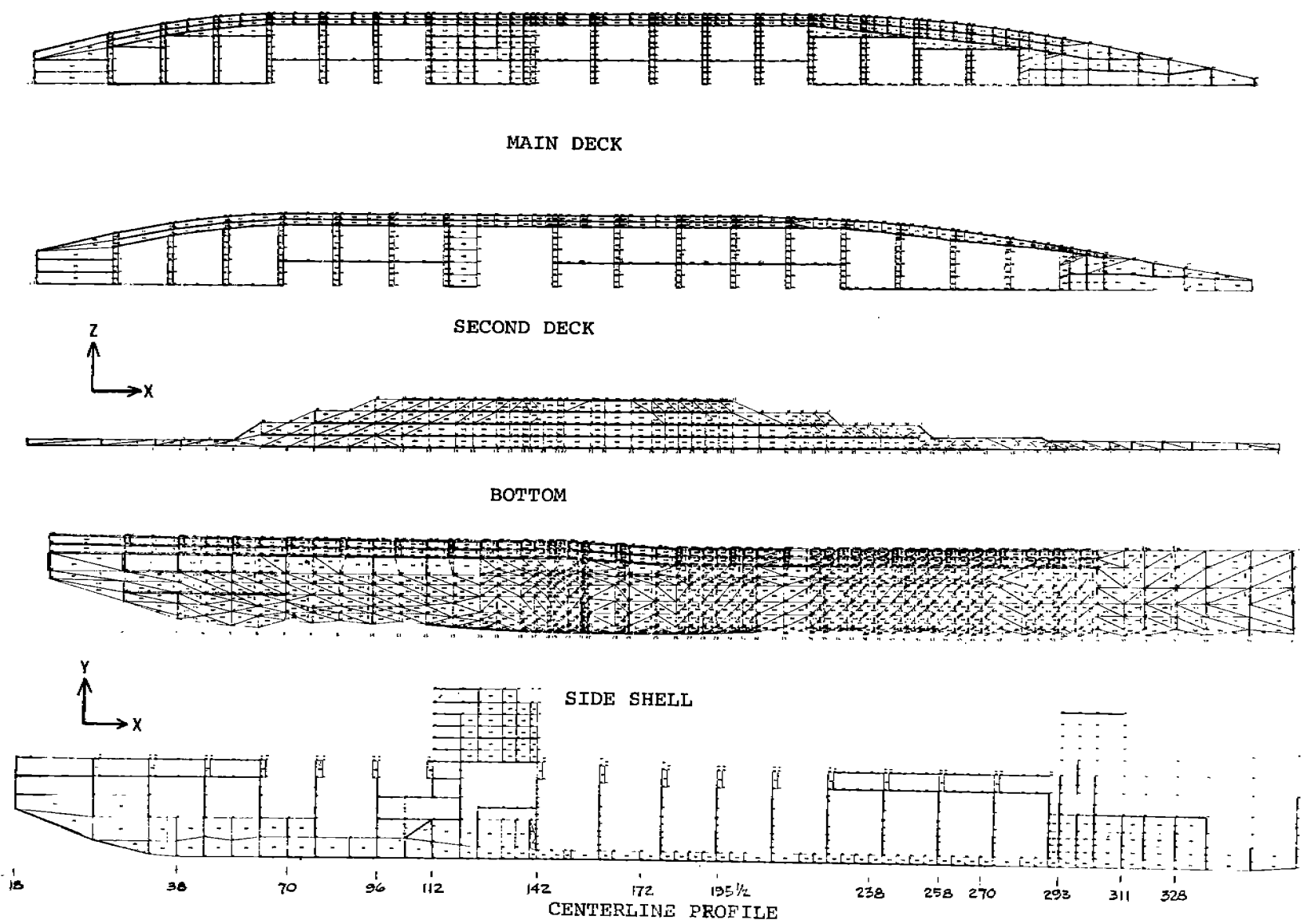
FIGURE 3 – PROJECTIONS OF FINITE ELEMENT COARSE-MESH MODEL

10

Frame 18   Frame 38   Frame 70   Frame 96

Frame 112   Frame 142   Frame 172   Frame 186

FRAME 190   FRAME 195 1/2   FRAME 238   FRAME 258

FRAME 270   FRAME 293   FRAME 311   FRAME 328
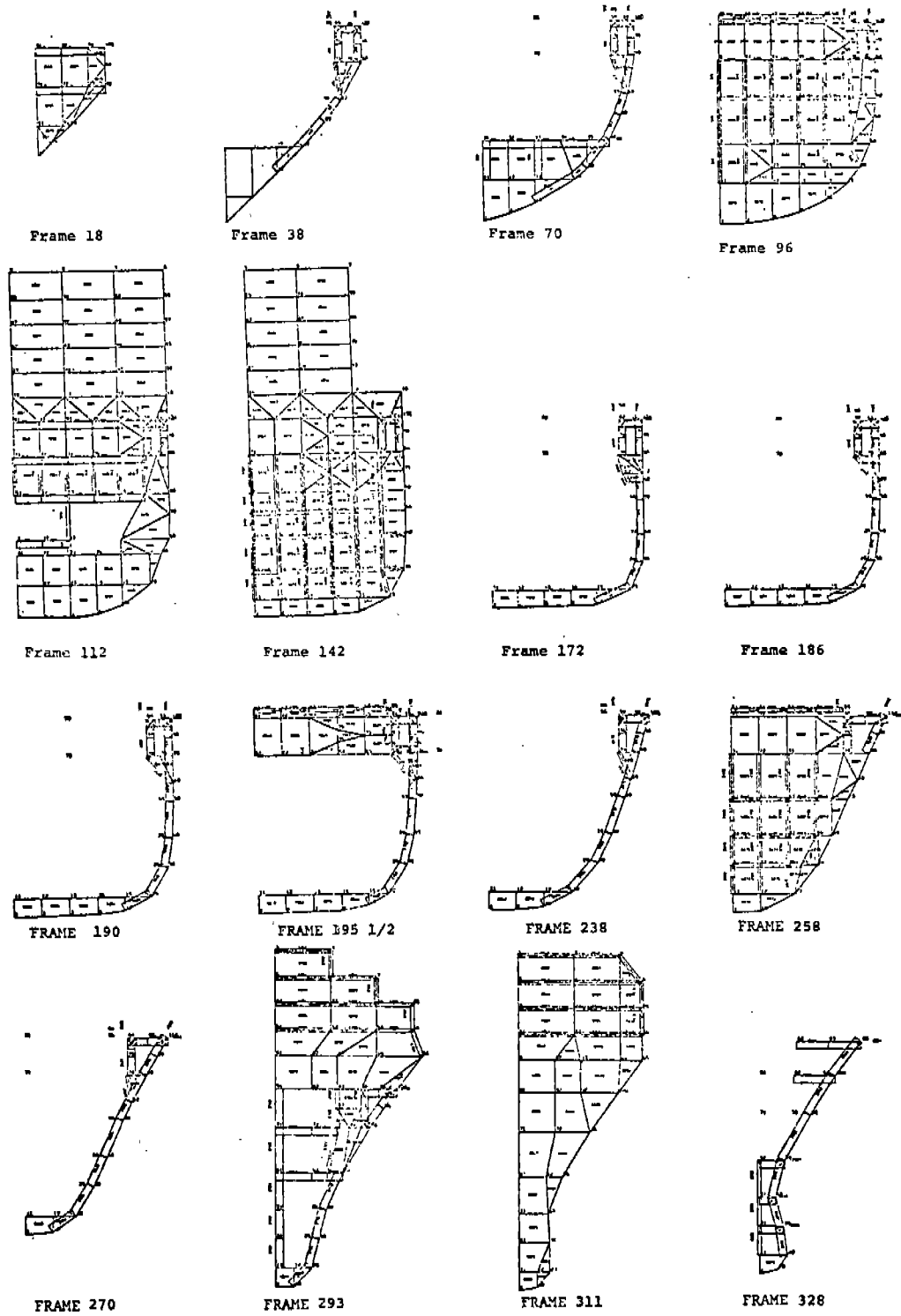
FIGURE 4 - TRANSVERSE FRAMES AND BULKHEADS

11

12

$$P_{sym}(x) = \frac{P(x) + P(-x)}{2}$$

$$P_{sym} = \frac{P_2 + P_1}{2}$$

$$P_{antisym}(x) = \frac{P(x) - P(-x)}{2}$$

$$P_{antisym} = \frac{P_1 - P_2}{2}$$

$$P_{stbd} = P_{symmetry} - P_{antisymmetry}$$

$$P_{port} = P_{symmetry} + P_{antisymmetry}$$
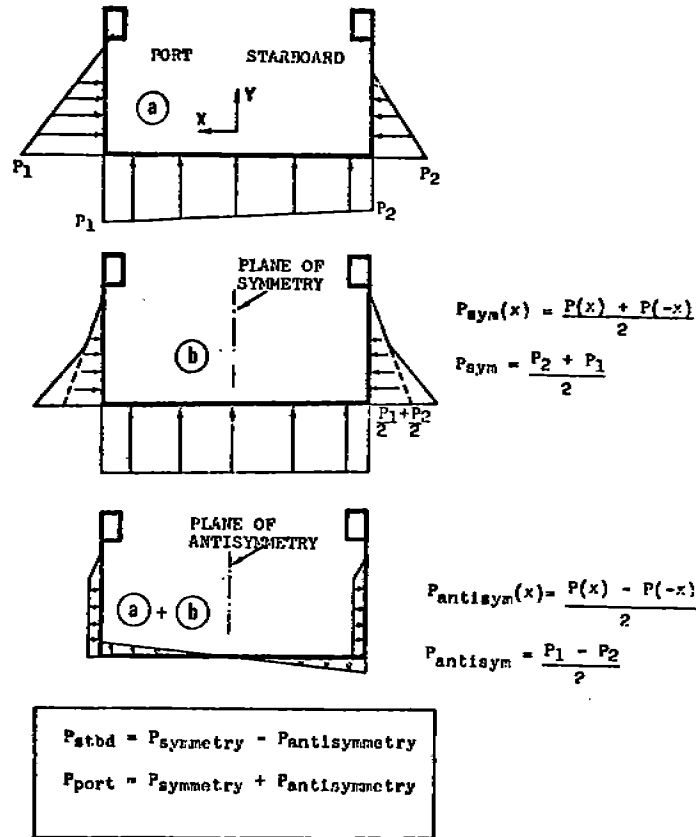
FIGURE 5 – DECOMPOSITION OF A LOAD INTO SYMMETRIC AND ANTI-SYMMETRIC COMPONENTS (FROM REFERENCE [3])

1) Symmetric Loading Condition

$\delta_x, \delta_y, \delta_z$ – Displacement in x,y,z direction

$\theta_x, \theta_y, \theta_z$ – Rotation in x,y,z direction

FR10   FR210   FR311

Manually Suppressed
Freedoms $\delta_y=0$ $\delta_z=0$ $\delta_y=0$
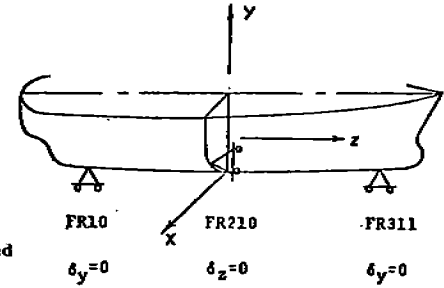
Automatically Suppressed Freedoms
at y-z centerline plane. $\delta_x = \theta_y = \theta_z = 0$

2) Anti-Symmetric Loading Condition

FR10   FR210   FR311

Manually Suppressed
Freedoms $\delta_x=0$ $\delta_y=0$ $\delta_x=0$
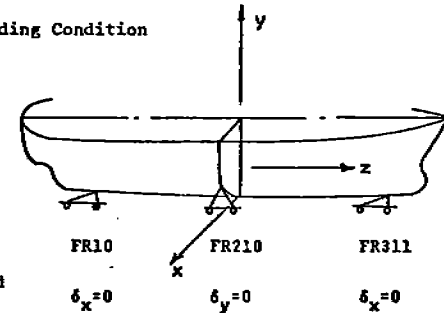
Automatically Suppressed Freedoms
at y-z centerline plane. $\delta_y = \delta_z = \theta_x = 0$

FIGURE 6 – BOUNDARY RESTRAINTS FOR SYMMETRIC AND ANTI-SYMMETRIC LOADING CONDITIONS
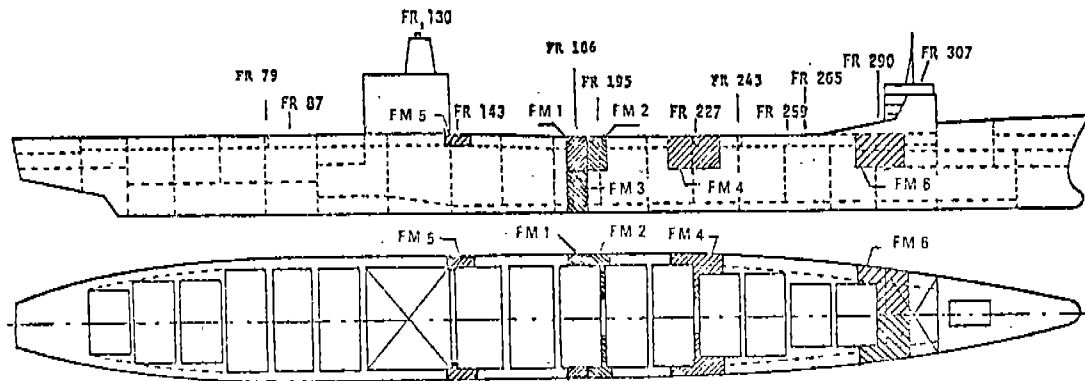
Fine-Mesh Models

FM 1
FM 2
FM 3
FM 4
FM 5
FM 6

FIGURE 7 - LOCATION OF FINE-MESH MODELS

TABLE 1   CHARACTERISTICS OF FINE MESH FINITE ELEMENT MODELS

Model Designation	Model Location	Number of Nodes	Number of Elements	Number of Degrees of Freedom
FM1	FR.182-190 (above str.no.1)	314	502	1507
FM2	FR.190-198	432	802	2030
FM3	FR.182-190 (below str.no.1)	391	536	1565
FM4	FR.218-238	318	680	1764
FM5	FR.140-150	326	522	1350
FM6	FR.282-298	393	541	1405

13

SENSOR 28 (BGSB)

MAIN DECK

SENSOR 1 (LVB)
SENSOR 15 (LSTS)
SENSOR 18 (LSTP)
SENSOR 27 (BGST)

SECOND DECK

SIDE SHELL

FRAME 182

FRAME 190

LONGITUDINAL BHD.
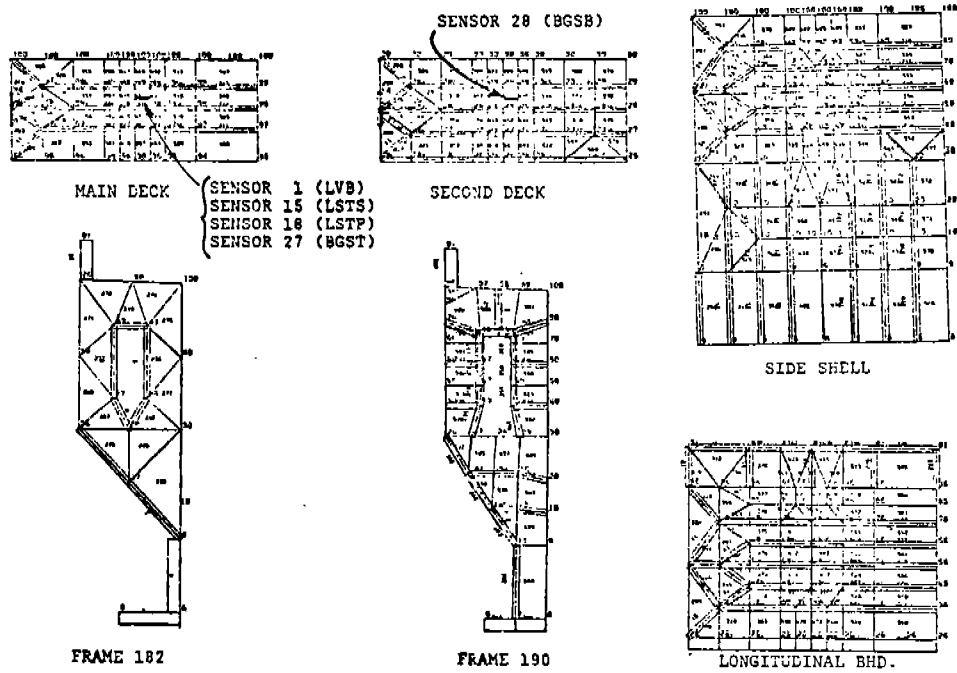
FIGURE 8 - FINE MESH MODEL 1 (FRAMES 182 - 190, ABOVE STRINGER NO. 1)

SENSOR 101
(TCMSX)

MAIN DECK

SENSOR 99
(TGMS2X)

SECOND DECK

SIDE SHELL

SENSOR 97
(TGMS4)
SENSOR 105
(TGSSdX)
SENSOR 100
(TGMS3X)
SENSOR 104
(TGSS3X)
SENSOR 96
(TGMS3)

SENSOR 94 (TGMS1)
SENSOR 102(TGSS1X)

SENSOR 98
(TCMS1X)
SENSOR 103
(TGSS2X)
SENSOR 95
(TGMS2)

FRAME 194

FRAME 195 1/2

LONGITUDINAL BHD.
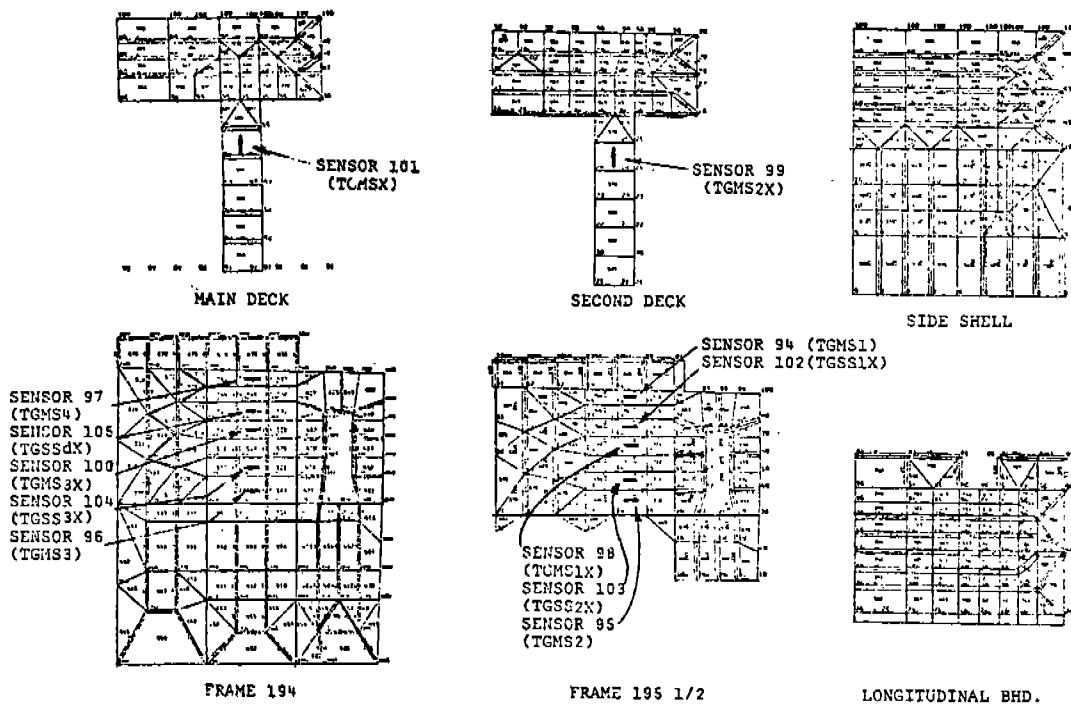
FIGURE 9 - FINE MESH MODES 2 (FRAMES 190 - 198, ABOVE STRINGER NO. 1)

14

SIDE SHELL

SENSOR 19 (LSMP)
SENSOR 16 (LSMS)

TANK TOP

SENSOR 17 (LSBS)
SENSOR 20 (LSBP)

BOTTOM

FRAME 182   FRAME 190
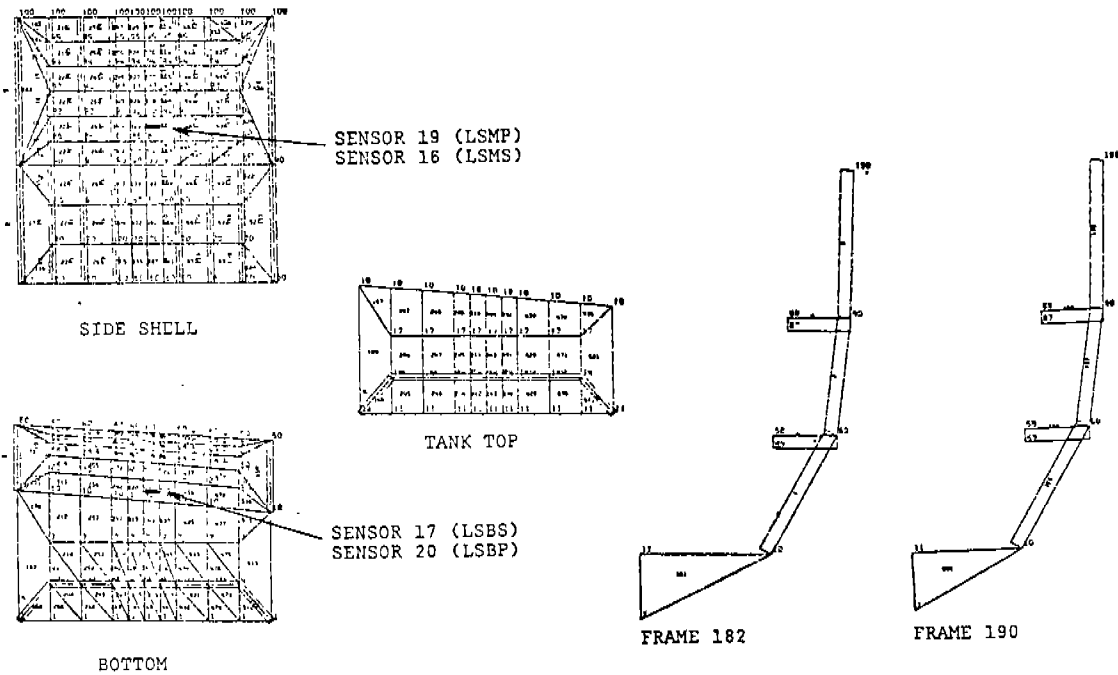
FIGURE 10 - FINE MESH MODEL 3 (FRAMES 182 - 190, BELOW STRINGER NO. 1)

SENSOR 82,83,84 (R14A,14B,14C)

SENSOR 79,80,81
(R13A,13B,13C)
SENSOR 76,77,78
(R12A,12B,12C)
SENSOR 73,74,75
(R11A,11B,11C)
SENSOR 70,71,72
(R10A,10B,10C)

MAIN DECK

SECOND DECK   FRAME 222

SIDE SHELL   FRAME 226   FRAME 230
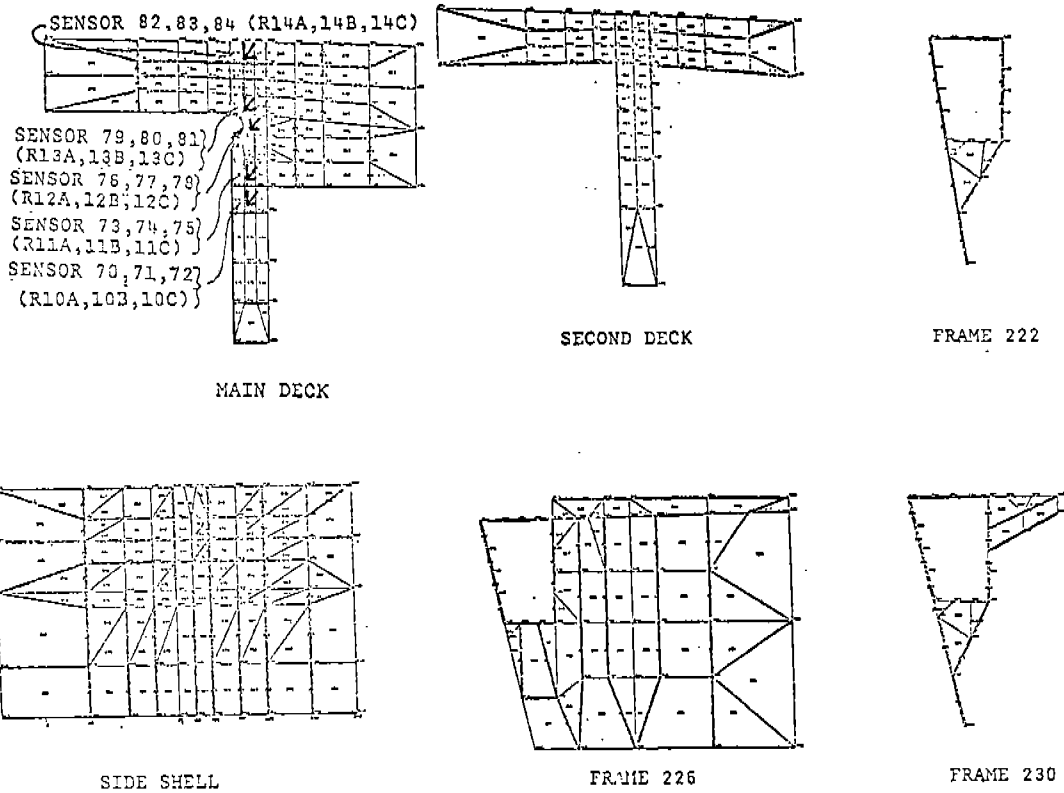
FIGURE 11 - FINE MESH MODEL 4 (FRAMES 218 - 238, ABOVE STRINGER NO. 1)

15

SENSOR 39,40,41 (AR4A,4B,4C)

MAIN DECK

(SENSOR 36,37,38
(AR3A,3B,3C)
SENSOR 33,34,35
(AR2A,2B,2C)(STBD)
SENSOR 30,31,32
(AR1A,1B,1C)(PORT)

FRAME 150

SECOND DECK

SIDE SHELL
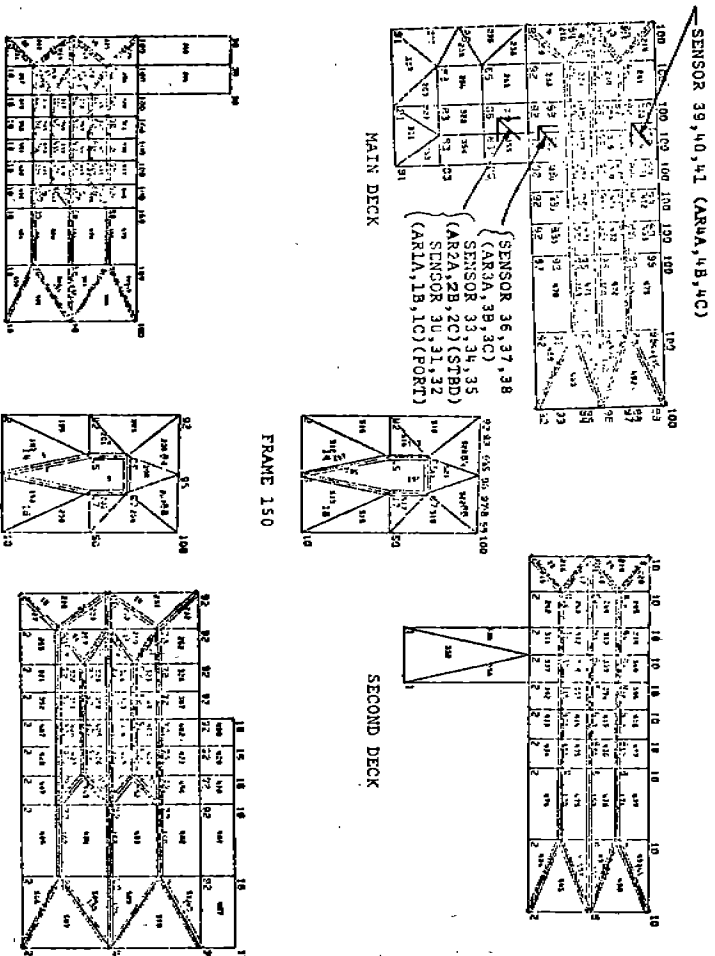
FIGURE 12 — FINE MESH MODEL 5 (FRAMES 140 - 150, BOX GIRDER)

FRAME 140

LONGITUDINAL BHD.

SENSOR 43,44,45 MAIN DECK
(R1A,1B,1C)(PORT)
SENSOR 46,47,48
(R2A,2B,2C)(STBD)

SENSOR 52,53,54
(R4A, 4B, 4C) (STBD)

SENSOR 49,50,51
(R3A, 3B, 3C) (STBD)

SECOND DECK

SIDE SHELL
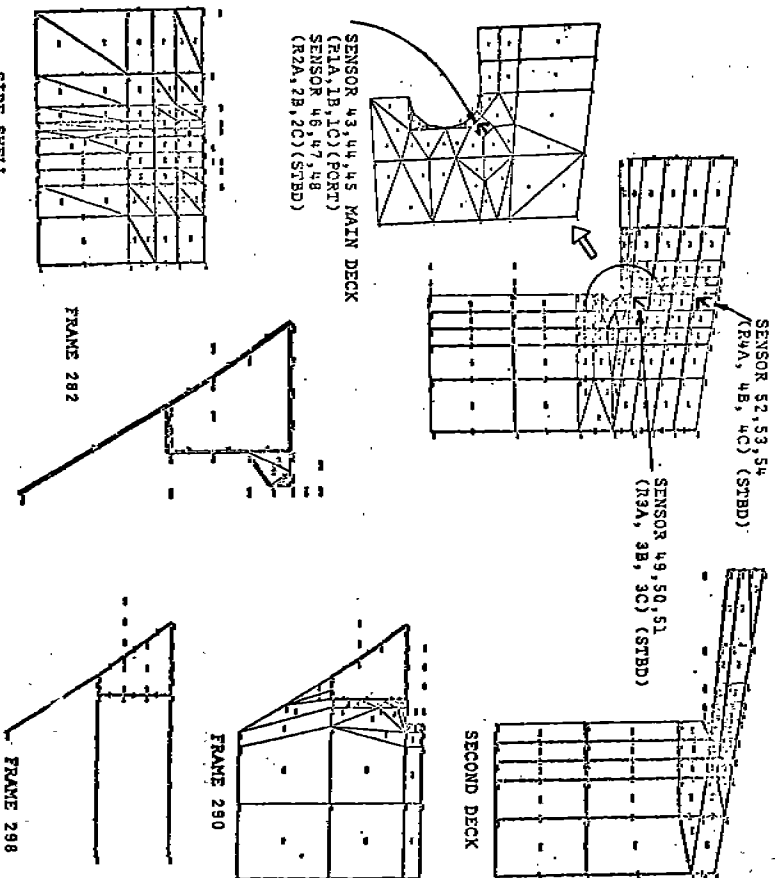
FIGURE 13 — FINE MESH MODEL 6 (FRAMES 282 - 298, ABOVE STRINGER NO. 1)

FRAME 282

FRAME 290

FRAME 298

TASK I - DOCKSIDE CALIBRATION

1. Loading Conditions

The following six calibration loading conditions have been analyzed:

Condition 1

Dockside initial loading condition, with all cargo hold and deck containers, except holds beneath Hatches 3, 10 and 14.

Condition 3

Deck containers removed from Hatches 1 through 4 and 12 through 15.

Condition 4

Remaining deck containers on Hatches 5 through 11 removed.

Condition 5

Approximately one-half of containers removed from starboard side of Hatches 1 through 7 and from the port side of Hatches 8 through 15, generating a torsional moment. Hatch covers placed asymmetrically to contribute to the torsional moment.

Condition 6

Completion of unloading described in Condition 5. This represents the maximum torsional load.

Condition 7

Nominally empty ship except for one propeller (47 long tons) loaded into Hatch 3 and one propeller in Hatch 4, all hatch covers on.

Loading conditions 1, 3, 4 and 7 are symmetric about the centerline plane; loading conditions 5 and 6 are asymmetric and include torsional loadings.

Note: The designated loading cases are identical with those used in Reference [6]. Loading condition 2 was not used during the calibration test.

17

The "SHIPMOM" program was used to calculate static bending moments and to generate hydrostatic pressures for the DAISY model. These SHIPMOM results were compared with the results of a previous less refined SHIPMOM computer run with fewer stations, described in Reference [6]. The comparison indicated very little difference between the two runs.

2. Comparison of Calculated Stresses and Measured Data – Longitudinal Stresses

The comparison of stresses measured by strain gages and those calculated at corresponding gage locations is presented in Tables 2 and 3. In Table 2 the comparison was made by subtracting loading condition 1 from each loading condition, taking loading condition 1 as a datum loading. Similarly, Table 3 takes loading condition 4 as the datum loading.

A preliminary investigation of the experimental and analytical stress results indicates some instances of agreement, and some instances of disagreement. The correlation of full-scale measurements and computed results can only be established after carefully verifying the data and the environmental conditions.

The experimental data for midship sensors 1 (LVB), 15 (LSTS) and 18 (LSTP), where LVB measures the average longitudinal vertical bending stress of port and starboard, LSTP and LSTS measure the longitudinal stress at top, port and starboard respectively, show some discrepancies.

Sensor number 1 should average the values of the longitudinal stress components of the LSTS and LSTP sensors. However, differences in the comparative stress values appear with the change in the reference of datum loading condition, or the so-called zero-stress reference case. Table 4 illustrates these differences when referring loading condition 7 to loading conditions 1, 3 or 4.

Loading condition 1 represents no change in mechanical loading of the ship from the initial calibration condition (zero reading for the strain gages) that took place when the ship was navigating through the Maas river, but the measured stresses range between -2677 and 1654 psi (Reference [6]).

Loading condition 7 is predominantly a symmetric loading case, but the measured stresses from the symmetrically located sensors 15 and 18 indicate asymmetric response, especially in loading condition 7-4.

18

TABLE 2   COMPARISON OF CALCULATED AND MEASURED STRESSES (PSI)
USING LOADING CONDITION 1 AS DATUM LOADING

Sensor		(3-1) Calc.	(3-1) Meas.	(4-1) Calc.	(4-1) Meas.	(5-1) Calc.	(5-1) Meas.	(6-1) Calc.	(6-1) Meas.	(7-1) Calc.	(7-1) Meas.
FM1	1(LVB)	-1058	-1148	104	-133	890	574	1352	883	2746	2119
	15(LSTS)	-1058	-1756	104	-1486	791	-495	1103	-180	2746	2252
	18(LSTP)	-1058	-1369	104	-88	988	782	1600	1286	2746	1789
FM 2	94(TGMS1)	75	467	437	2451	-940	409	-1622	-583	435	2568
	95(TGMS2)	142	993	-112	386	-1399	-3033	-1988	-2041	71	-1600
	96(TGMS3)	119	228	471	-684	1569	-342	2191	114	561	-1483
	97(TGMS4)	-107	396	-9	1016	1803	4230	2795	5245	753	1974
	98(TGMS1X)	237	1322	125	680	-1191	-1421	-1833	-1888	-291	38
	99(TGMS2X)	43	1225	115	-429	88	-621	148	-1532	601	-484
	100(TGMS3X)	170	376	109	-365	1189	-822	1803	-365	-24	-993
	101(TGMS4X)	-123	-1882	246	248	621	1037	863	1150	984	1094
FM 3	17(LSBS)	531	1785	16	1648	-236	961	-267	1099	-1146	183
	20(LSBP)	531	589	16	453	-453	272	-802	589	-1146	226
FM 4	73(R11A)	-85	-115	102	-343	59	-115	-10	399	486	798
	76(R12A)	-133	142	78	-77	402	687	515	687	671	796
	79(R13A)	-525	-1096	341	76	1872	2653	2420	3257	2865	3141
	82(R14A)	-454	-1864	301	-1032	1061	-307	1300	-195	2391	864
FM 5	30(AR1A)	-719	-593	-277	-209	1033	1217	1476	1491	507	-758
	33(AR2A)	-719	152	-277	1592	-975	-592	-1297	-1125	507	-334
	36(AR3A)	-1362	-1084	-471	1882	-1425	-513	-1884	-1939	1003	912
	39(AR4A)	-1212	-1964	-459	-982	171	1363	266	1145	892	600
FM 6	43(R1A)	85	-937	170	-334	-568	-1870	-1136	-2418	710	-1102
	46(R2A)	85	-725	170	-1562	1150	390	1974	948	710	335
	49(R3A)	98	-513	202	-1825	835	0	1386	343	814	199
	52(R4A)	111	-163	230	-382	-57	-1145	-246	-1254	902	-436

19

TABLE 3 COMPARISON OF CALCULATED AND MEASURED STRESSES (PSI) USING LOADING CONDITION 4 AS DATUM LOADING

Loading Cond. Sensor		(5-4) Calc.	(5-4) Meas.	(6-4) Calc.	(6-4) Meas.	(7-4) Calc.	(7-4) Meas.
FM1	1 (LVB)	786	707	1249	1016	2643	2252
	15 (LSTS)	687	-991	1000	1306	2643	3738
	18 (LSTP)	885	870	1497	1374	2643	1877
FM2	94 (TGMS1)	-1377	-2042	-2059	-3034	-3	117
	95 (TGMS2)	-1287	-3419	-1876	-2427	183	-1986
	96 (TGMS3)	1098	342	1720	798	89	-799
	97 (TGMS4)	1812	3214	2803	4229	761	958
	98 (TGMS1X)	-1316	-2101	-1958	-2568	-416	-642
	99 (TGMS2X)	-27	-192	33	-1103	486	-55
	100 (TGMS3X)	1079	-457	1694	0	-133	-628
	101 (TGMS4X)	375	789	617	902	738	846
FM3	17 (LSBS)	-251	-687	-283	-549	-1162	-1465
	20 (LSBP)	-469	-181	-818	136	-1162	-227
FM4	73 (R11A)	-43	228	-112	742	384	1141
	76 (R12A)	324	764	437	764	593	873
	79 (R13A)	1531	2577	2079	3181	2524	3071
	82 (R14A)	760	-1339	999	837	2089	1896
FM5	30 (AR1A)	1310	1426	1753	1700	784	-549
	33 (AR2A)	-698	-2184	-1020	-2717	784	-1926
	36 (AR3A)	-953	-2395	-1412	-3821	1475	-970
	39 (AR4A)	623	2345	718	2127	1350	1582
FM6	43 (R1A)	-738	-1536	-1306	-2084	540	-768
	46 (R2A)	980	1952	1803	2510	540	1898
	49 (R3A)	633	1825	1184	2168	612	2024
	52 (R4A)	-270	-763	-462	-872	672	-54

20

It can be seen that the degree of agreement between the measured and calculated results varies significantly from Table 2 to Table 3. This indicates some inconsistencies of the measured data between different loading conditions, probably due to changes in ambient temperatures.

According to Table IV of Reference [6], a temperature difference of 15° F between port and starboard sides was recorded during the calibration test. A temperature difference of 21° F between the deck and sea water was also recorded. With these magnitudes of temperature gradient, the thermal stress could be as high as 1500 psi. However, due to the lack of sufficient information about the temperature distribution during the calibration test, it is impossible to incorporate thermal stresses into the analysis.

To evaluate the effects of these temperature changes, longitudinal stresses measured at 17 selected sensors are shown in Figures 14 through 16. The sensors are described in Table 5.

Figure 14 shows the longitudinal stresses for calibration loading conditions 3 through 7, utilizing loading condition 1 as the datum loading. The deviations of the measured stresses from the calculated values are generally within a bandwidth of + 1,500 psi. Based on the temperature differential recorded during the calibration test, shown in Table 6, the maximum thermal stress may be as high as 1,500 psi. With this thermal stress margin in mind, the overall comparison of the measured and computed stresses shown in Figure 14 is reasonably good.

In an attempt to minimize the possible thermal effects, changes in stresses between two loading conditions with the least temperature differential were also examined. The results of loading case 4-3, which represents pure vertical bending, are shown in Figure 15, With a few exceptions, the stress deviations fall within a bandwidth of + 400 psi. This magnitude of deviation is regarded as acceptable, considering the sensibility and reliability of strain-gage readings. The results of loading case 7-6, which reflects both vertical bending and torsion, are shown in Figure 16. With the exception of Sensors 30 and 39, the stress comparison is generally good.

To minimize the possible thermal effects, it is advisable, for the future calibration tests, that other means of loading be used to create appreciable mechanical strains and that complete steel temperature data of the deck and side shell (port and starboard) be recorded.

21

TABLE 4   MEASUREMENTS OF LONGITUDINAL STRESSES (PSI) IN
         MIDSHIP SENSORS

Loading Condition Sensor No.	(7-1)	(7-3)	(7-4)
15(LSTS)	2252	4008	3738
18(LSTP)	1789	3158	1877
Average of 15 and 18	2020.5	3583	2807.5
1(LVB)	2119	3267	2252

TABLE 5   SELECTED SENSOR LIST

SENSOR NUMBER	SENSOR NOMEN.	SIGNAL NOMENCLATURE
1	LVB	Longitudinal Vertical Bending
15	LSTS	Longitudinal Stress Top Starboard
18	LSTP	Longitudinal Stress Top Port
17	LSBS	Longitudinal Stress Bottom Starboard
20	LSBP	Longitudinal Stress Bottom Port
73	R11A	R = Foreward Rosettes on the Main Deck, See Figure 11
76	R12A	
79	R13A	
82	R14A	
30	AR1A	AR = Aft Rosettes on the Main Deck, See Figure 12
33	AR2A	
36	AR3A	
39	AR4A	
43	R1A	R = Forward Rosettes on the Main Deck, See Figure 13
46	R2A	
49	R3A	
52	R4A	

22

TABLE 6   ENVIRONMENTAL CONDITIONS AT CALIBRATION
(FROM REFERENCE [6])

Cond.	Time	Temperatures, °F [a]					Location of Sun, degrees		Wind	
		Air, Dry	Air Wet	Water	Port Tunnel	Stbd Tunnel [a]	Elevation	Azimuth [b]	Speed, mph	Direction
	9 Apr'73									
1	0900	49.5	43	43	51	52	45 (Overcast)	50 Stbd	15	60° Port
3	1300	58	50.5	43	49	64	60 (Clear)	100 Stbd	20	60° Port
4	1725	49	44	43	49	63	30 (Clear)	Aft	10	110° Port
5	2130	38	36	43	45	52	-	-	8	90° Port
	10 Apr'73									
6	0105	36.5	35	43	43	46	-	-	12	60° Port
7	0830	40	-	42	40	46	-	-	10	90° Port

Notes:

a Measured on hull plating backside
b Relative to ship

Dockside

Heading
083

Sun Direction with Reference
to Ship
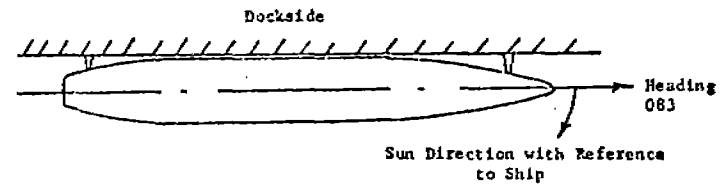
Another uncertainty in comparing the measured and calculated stresses is the influence of plate unfairness and local plate bendings. So far as the longitudinal stresses in the hull structures are concerned, this kind of influence is considered insignificant. All the longitudinal strain gages were installed on very thick plates where the effect of unfairness, if any, would not be generally noticeable. Where local plate bending was apparent, such as the bottom hull plating, the strain gages were located at the quarter span between frames (floors) to minimize local plate bending. In addition, all the primary plating was represented by bending plate elements in the fine-mesh models. Panel bendings are also included in the calculation. Consequently, the plate unfairness and local plate bending should not be regarded as an influential parameter to the stress discrepancies in this case.
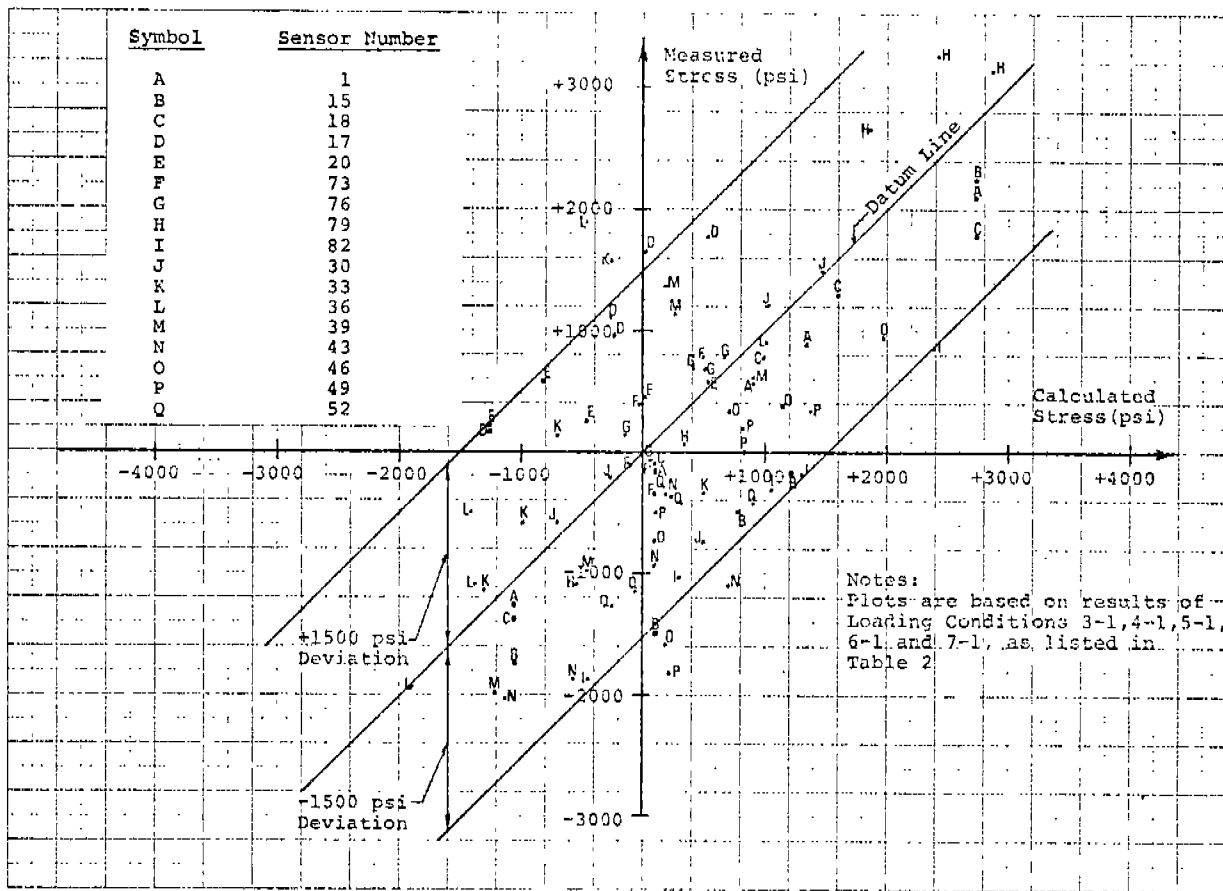
FIGURE 14 - DEVIATION OF MEASURED LONGITUDINAL STRESSES FROM CALCULATED VALUES

Symbol	Sensor Number
A	1
B	15
C	18
D	17
E	20
F	73
G	76
H	79
I	82
J	30
K	33
L	36
M	39
N	43
O	46
P	49
Q	52

Environmental Temperatures °F

Loading Case	Water	Port Tunnel	Stbd Tunnel
3	43	49	64
4	43	49	63
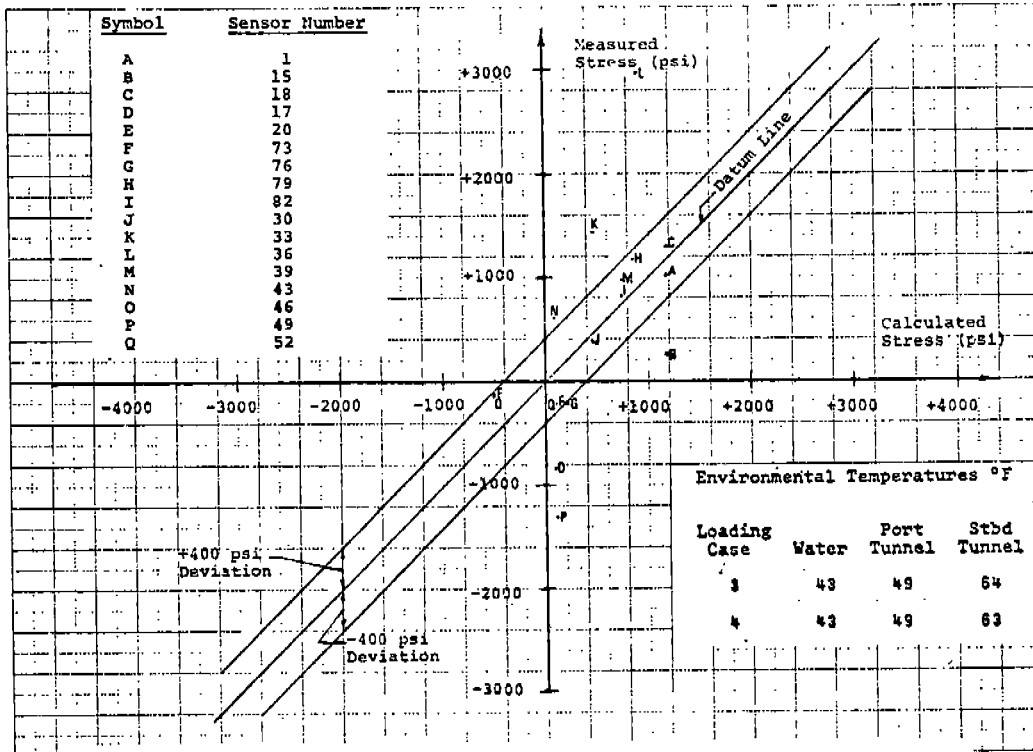
FIGURE 15 - DEVIATION OF MEASURED LONGITUDINAL STRESSES FROM CALCULATED VALUES
PLOTS ARE BASED ON LOADING CONDITION 4 MINUS 3

Symbol	Sensor Number
A	1
B	15
C	18
D	17
E	20
F	73
G	76
H	79
I	82
J	30
K	33
L	36
M	39
N	43
O	46
P	49
Q	52

Environmental Temperatures °F

Loading Case	Water	Port Tunnel	Stbd Tunnel
6	43	43	46
7	42	40	46
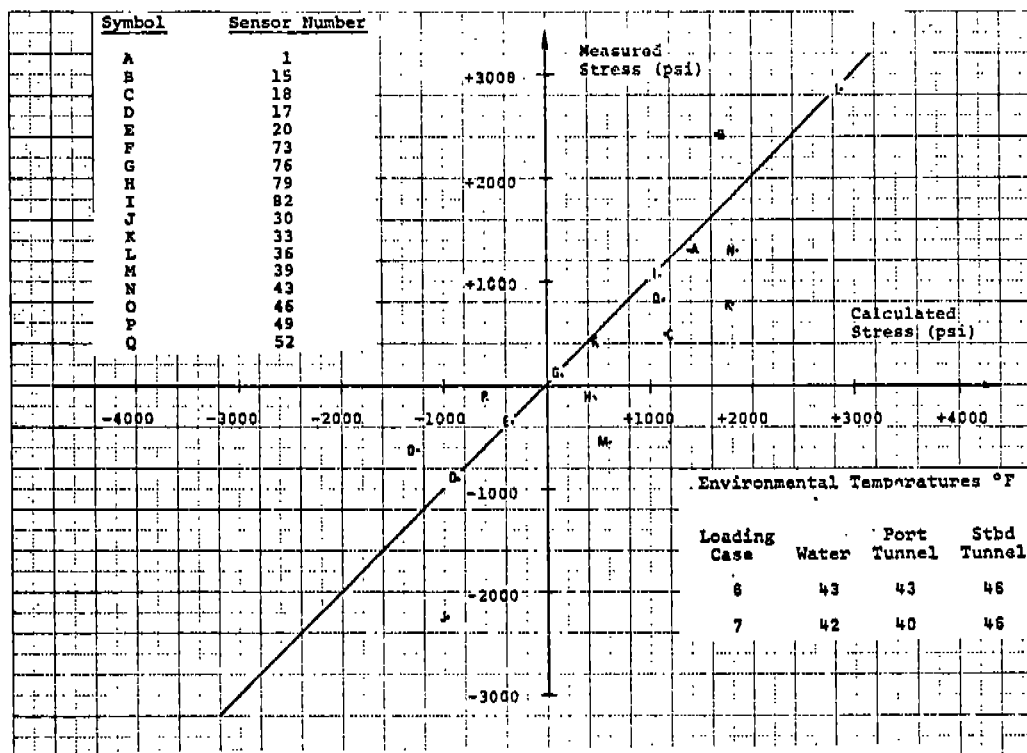
FIGURE 16 - DEVIATION OF MEASURED LONGITUDINAL STRESSES FROM CALCULATED VALUES,
PLOTS ARE BASED ON LOADING CONDITION 7 MINUS 6

25

3. Comparison of Calculated Stresses and Measured Data - Transverse Stresses

The calculated and measured transverse stresses in the transverse box girder at Fr. 194-196 are plotted in Figure 17 for loading cases 3-1, 4-1, 5-1, 6-1 and 7-1. Regarding the difference between the measured and calculated stresses at each gage location, these figures show approximately the same results as those shown in Table 2. However, by comparing the stress distribution patterns, it can be seen that the measured data reflects generally a higher degree of bending and torsion loads, probably caused by thermal expansions.

To minimize the thermal effect, loading cases 4-3 and 7-6 were again selected for comparison. The results are shown in Figure 18. No improvement in stress agreement can be gained for loading case 4-3, which represents a pure longitudinal bending load.
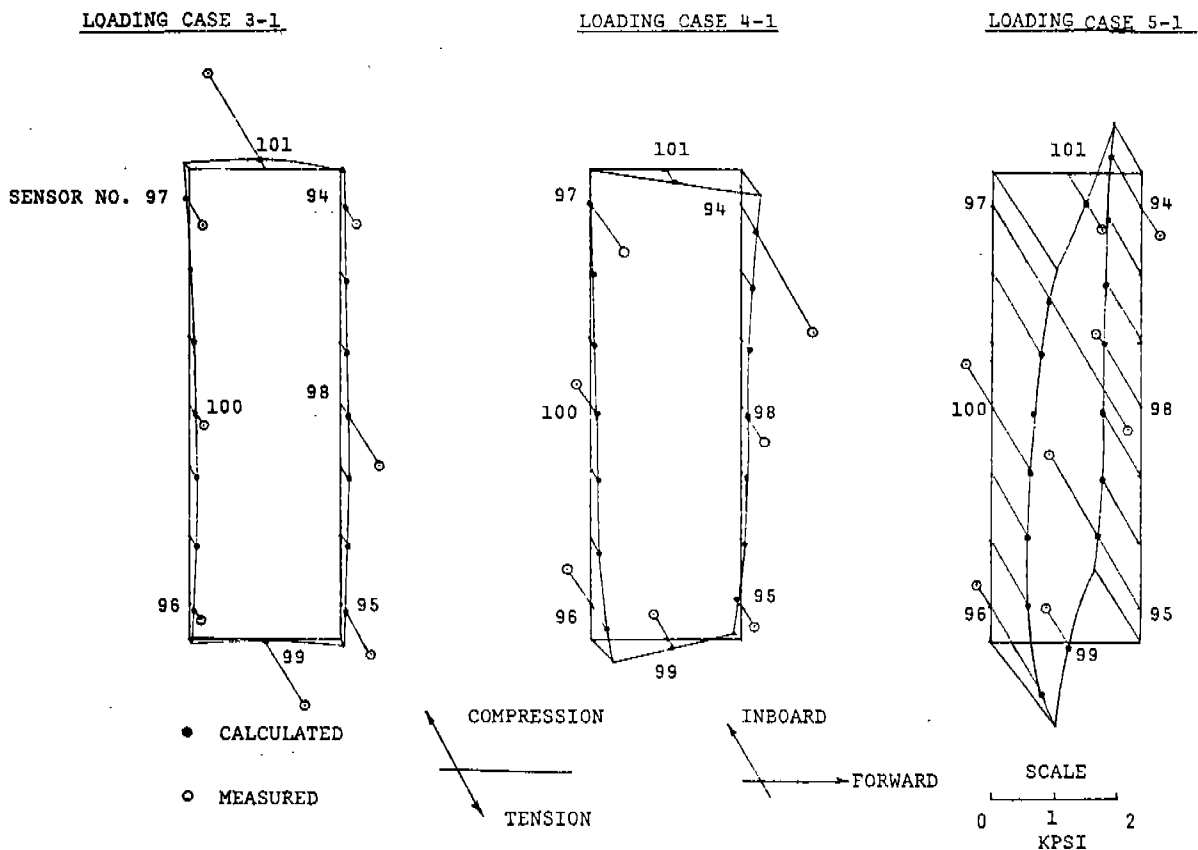
FIGURE 17 - COMPARISON OF CALCULATED AND MEASURED TRANSVERSE STRESSES IN THE TRANSVERSE BOX-GIRDER AT FR. 194-196

LOADING CASE 6-1   LOADING CASE 7-1

SENSOR NO. 97

- CALCULATED   COMPRESSION   INBOARD   SCALE
o MEASURED   TENSION   FORWARD   0   1   2
                                              KPSI

FIGURE 17 – COMPARISON OF CALCULATED AND MEASURED TRANSVERSE STRESSES IN THE
TRANSVERSE BOX-GIRDER AT FR. 194-196 (CONT'D)

LOADING CASE 4-3   LOADING CASE 7-6

SENSOR NO. 97

• CALCULATED   COMPRESSION   INBOARD
o MEASURED   TENSION   FORWARD   SCALE
                                         0   1   2
                                              KPSI
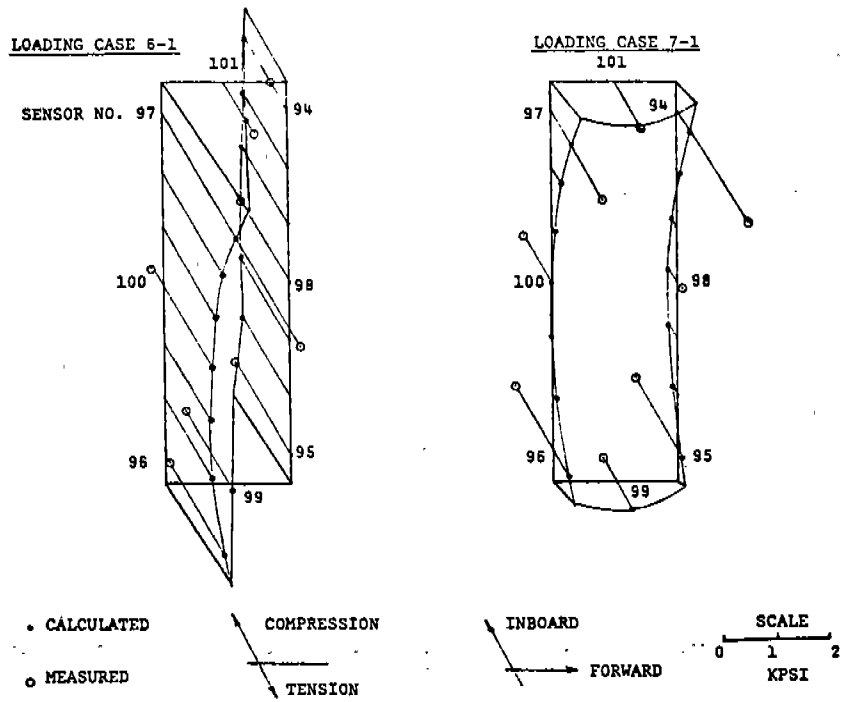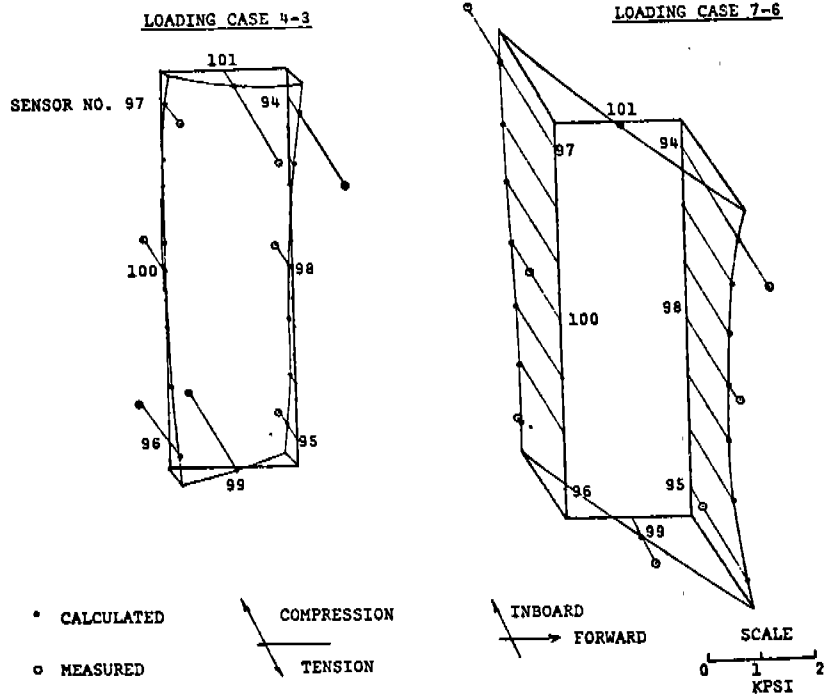
FIGURE 18 – COMPARISON OF CALCULATED AND MEASURED TRANSVERSE STRESSES IN THE
TRANSVERSE BOX-GIRDER AT FR. 194-196

27

Since the primary loads of the transverse box girder are induced by hull-girder bending and twisting, in addition to thermal loads, manufacturing imperfections could also contribute to the deviations of the measured data. Furthermore, the strain gages have a single element which measures the strain in the transverse direction only. The measured stress data does not account for the Poisson's effect which may cause significant stress variations. However, a reasonably good agreement, particularly of the stress distribution patterns, can be seen for loading case 7-6, with the only exception of Sensor 95.

In conclusion, a reasonably good agreement of the measured stresses and the calculated values has been obtained for several selected calibration conditions by minimizing the possible thermal effects.

For Task II, a stress comparison between the calculated and measured RMS values in head seas was carried out by an equivalent regular wave approach and by a spectrum analysis, based on a study of the relationship between computed wave-induced stresses and wave heights.

In order to examine this relationship, a regular wave with a length of 808.5 feet and with its crest at the midship was selected for ship motion and stress calculations. Three different wave heights as shown in Table 7 were taken into consideration, with a ship speed of 10.9 knots in head seas.

TABLE 7   WAVE CHARACTERISTICS AND SHIP MOTION DATA - LINEARITY STUDY

Wave Cond.	(a) Load-ing Cond.	Ship Speed (knots)	Wave Length (ft.)	Wave Height (Peak-to-Trough) (ft.)	(b) Heave (ft.)	(c) Pitch (deg.)	Location of Wave Crest Forward From A.P. (ft.)
1	8	10.9	808.5	3.28	0.62	0.32	440.0
2	9	10.9	808.5	9.84	1.85	0.97	440.0
3	10	10.9	808.5	20.92	3.93	2.06	440.0

Notes:

[a] All conditions consist of full cargo loads and head waves
[b] Heave is positive down
[c] Pitch is positive bow up

The ship's motions and accelerations which are required as part of the finite element model input were calculated using the SHIPMOTION computer program. A set of quasi-static pressures (still-water plus wave profile) and inertia forces corresponding to the calculated accelerations were applied on the finite element model and a correction was made to ensure that the applied vertical shearing forces and bending moments were generally identical to those obtained directly from the SHIPMOTION program.

The calculated results are shown in Figures 19, 20, and 21 at three selected locations along the length of the ship. As shown in Figure 19, the wave-induced longitudinal and transverse stresses in the main deck plating at the midship section are approximately in direct proportion to the wave height. They depart from linearity at stations remote from the midship section (Figures 20 and 21), even though the hull-girder shearing forces and bending moments vary linearly with wave heights, as predicted by a ship motion calculation.

The non-linearity is due to the combination of the local bending in the transverse direction and the wave-induced forces in the longitudinal direction.

Recent model experiments in towing tanks indicate that the motions and wave loads do not vary linearly with wave heights. A realistic trend cannot yet be defined due to the lack of sufficient experimental data. Based on the results shown in Figures 20 and 21, it can be seen that the hull-girder responses (wave-induced stresses) exhibit a non-linear pattern even with linear shear and bending loads.
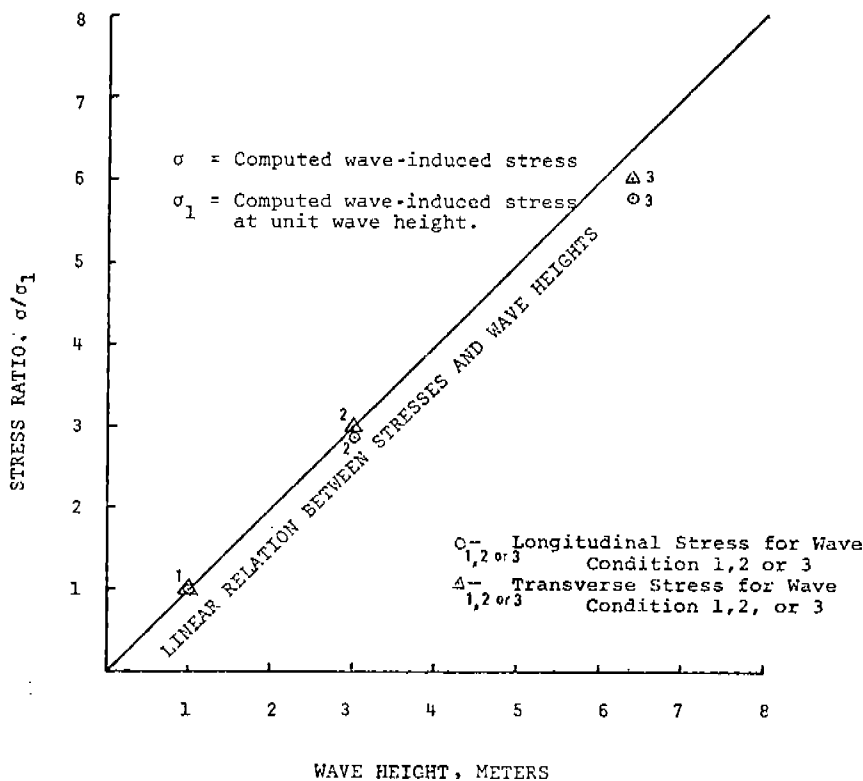
FIGURE 19 - WAVE-INDUCED STRESSES VS WAVE HEIGHTS -
MAIN DECK PLATING AT THE MIDSHIP SECTION

30
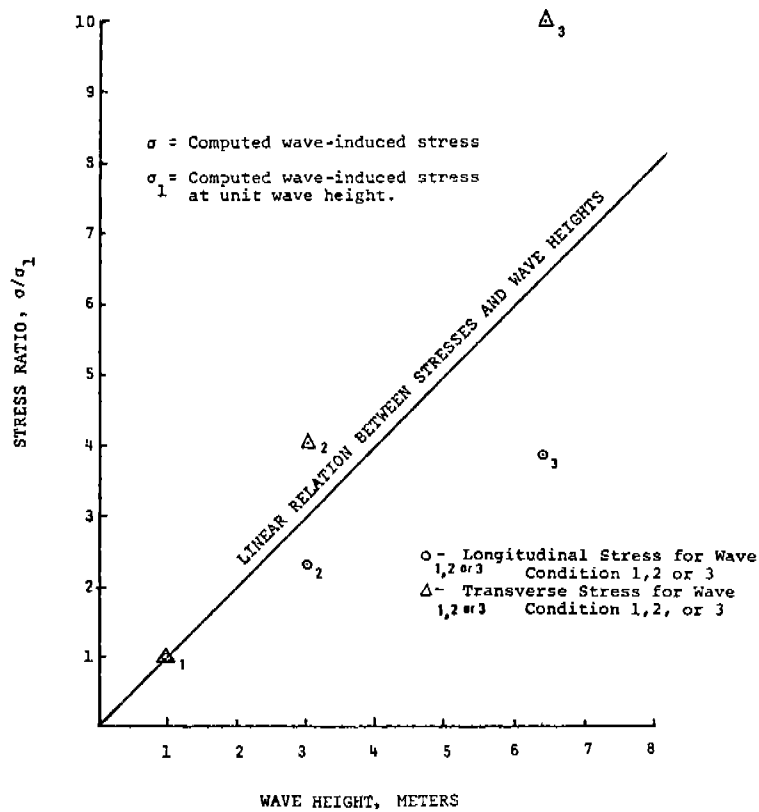
FIGURE 20 - WAVE-INDUCED STRESSES VS WAVE HEIGHTS -
MAIN DECK PLATING BETWEEN FRAMES 226 and 228
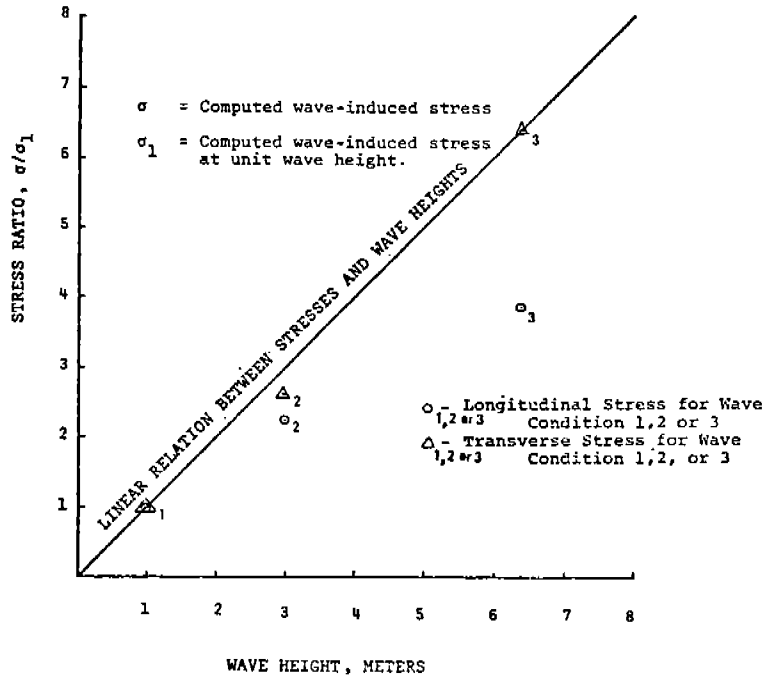
FIGURE 21 - WAVE-INDUCED STRESSES VS WAVE HEIGHTS -
MAIN DECK PLATING AT FRAME 290

31

In the equivalent regular wave method, a given wave spectrum can be approximated by a regular wave with equivalent energy. With this approach, no assumption concerning the relation between stresses and wave heights is necessary. On the other hand, this equivalent regular wave approach will not account for the variation in responses to different wave frequencies.

A spectrum analysis, which depends completely upon an assumption of linearity between stresses and wave heights, is valid for performing stress comparisons only in the midship region.

After a thorough review of these two methods, it was decided to perform the RMS stress comparison using both approaches selectively. Three recorded intervals were selected for the equivalent regular wave approach. For comparison, the same intervals were also used for the spectrum analysis. Because of the non-linear effects, the spectrum analysis was carried out for the longitudinal stresses at midship only. The stress RAO (Response Amplitude Operator) generated for these three intervals was then utilized to calculate the stress spectrum for other selected intervals.

The detailed procedures of these two approaches and the computed results are discussed in the following sections.

1. Method 1 - Equivalent Regular Wave Approach

    A. Description of Method

        a. Calculation of Equivalent Regular Waves

        The equivalent wave encounter frequency, wave height and wave length of the regular waves were calculated based on the radar wave spectrum shown in Reference [8], using the following formulas

$$\text{Equivalent wave encounter frequency} = \frac{\int_{\omega_{e1}}^{\omega_{e2}} \omega_e S_\zeta(\omega_e)\, d\omega_e}{\int_{\omega_{e1}}^{\omega_{e2}} S_\zeta(\omega_e)\, d\omega_e} \qquad (1)$$

$$\text{Equivalent wave height} = 2.5 \left[\int_{\omega_{e1}}^{\omega_{e2}} S_\zeta(\omega_e)\, d\omega_e \right]^{1/2} \qquad (2)$$

32

Equivalent wave length = $\dfrac{2\pi g}{\omega^2}$ (3)

ω is derived from the equation

$$\omega_e = \omega - \dfrac{u\ \cos\beta}{g}\ \omega^2$$ (4)

where g = gravity constant

ω = Wave frequency

ω_e = encounter frequency, measured directly
from the time history

β = heading angle

u = ship's speed

$S_\zeta(\omega_e)$ = wave spectrum in the frequency domain

ω_{e1}, ω_{e2} = lower and upper bounds of frequency
within the domain under consideration

Three wave conditions were selected for this task. The detailed information and the equivalent waves for these three wave conditions are shown in Table 8.

TABLE 8 WAVE CONDITIONS SELECTED FROM REFERENCE [8] FOR
COMPARISON OF RMS STRESSES IN HEAD SEAS

Wave Condition	Tape	Index	Interval	Run No.	Ship Speed (knots)	Equivalent Wave Length (ft.)	Equivalent Wave Height (ft.)
4	145	18	5	405	10.9	808.5	20.92
5	145	24	29	429	18.7	808.5	21.97
6	145	29	50	450	28.1	561.5	16.47

b. Calculation of Wave-Induced Loads

A computer subroutine was developed by ABS for the calcu-
lation of hydrodynamic pressures (ABS/DYNPRE) acting on the
ship in a seaway. However, it was found that the wave-induced
vertical bending moments obtained from an integration of the
hydrodynamic pressures were not in full agreement with those
obtained from the ABS/SHIPMOTION program. In order to elim-
inate such differences, the following two modifications were
utilized to correct the vertical bending moments obtained by
integration of the imposed pressures and inertial forces.

Method 1A - Quasi-static Pressures

A quasi-static pressure approach was used to calculate
the input load for the ABS/DAISY runs. In this approach, the
quasi-static pressures and the inertia forces at the instan-
taneous ship position as determined by the ship motion
calculation were first applied to the structural model. Then,
the bottom pressures were modified to make the vertical wave
bending moments comparable with those obtained from the ship
motion program. This was the procedure used in the determin-
ation of the relationship between computed wave-induced stresses
and wave heights described at the beginning of Task II.

Method 1B - Hydrodynamic Pressures

The hydrodynamic pressure coefficients obtained from the
ABS External Pressure subroutine (DYNPRE) were modified at
each ship station to make the vertical wave bending moments
comparable with those obtained from the ship motion calculation.

In both the ship motion and the external pressure calcu-
lations, information is obtained only for regions of the ship
under the still-water line. To account for the actual wave
profile, the external pressures were linearly extended up or
deleted down to the wave surface, depending on whether the
wave surface was above or below the still-water line. By so
doing, the total external pressure, which includes both the
hydrodynamic and the static components, becomes zero at the
wave surface. The typical pressure distributions for wave
surfaces above and below the still-water line are shown in
Figures 22 and 23 respectively. The wave characteristics and
ship motion data used for Methods 1A and 1B are shown in Table 9.

c. Structural Analysis

After the calculation of dynamic and static loads, the
stress analyses for coarse-mesh and subsequently for fine-
mesh models were performed by using the ABS/DAISY finite
element program. For the comparison of wave-induced stresses,

34

W.S.
(Wave Surface)

S.W.L.
(Still-water Line)

Boundary of
Total Pressure

Static Pressure

Dynamic Pressure

Extended Pressure

0   10 psi   20 psi

Scale
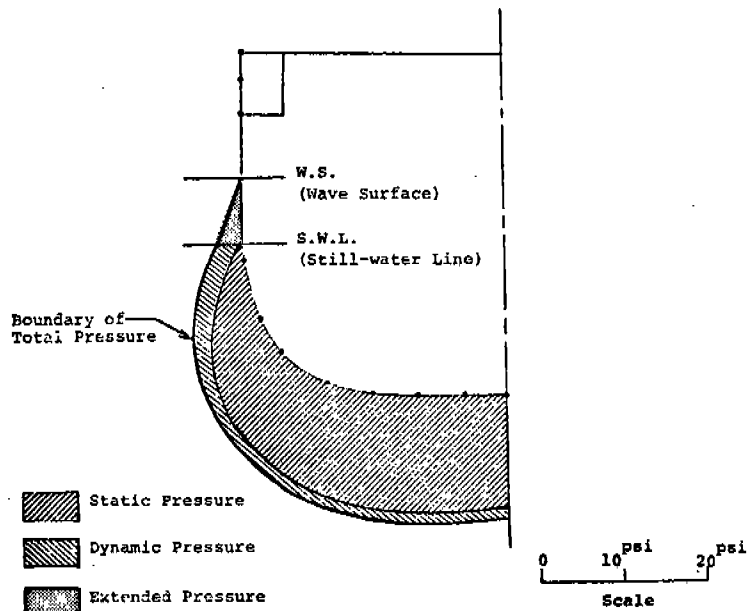
Frame 14 (Ship Frame 120)

FIGURE 22 - DISTRIBUTION OF STATIC AND WAVE-INDUCED DYNAMIC
PRESSURES IN HEAD SEAS, W.S. > S.W.L.

S.W.L.
(Still-water Line)

W.S.
(Wave Surface)

Boundary of
Total Pressure

Static Pressure

Dynamic Pressure

Deleted Pressure

0   10 psi   20 psi

Scale
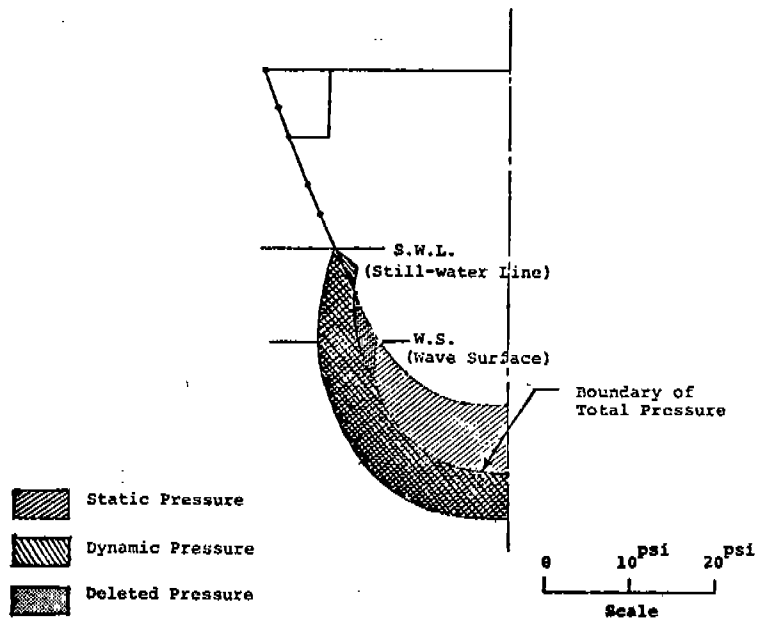
Frame 44 (Ship Frame 258)

FIGURE 23 - DISTRIBUTION OF STATIC AND WAVE-INDUCED DYNAMIC
PRESSURES IN HEAD SEAS, W.S. < S.W.L.

35

TABLE 9   WAVE CHARACTERISTICS AND SHIP MOTION DATA - METHOD 1 - TASK II

Method	Wave Cond.	(a) Load-ing Cond.	Ship Speed (knots)	Wave Length (ft.)	Wave Height (Peak-to-Trough) (ft.)	(b) Heave (ft.)	(c) Pitch (deg.)	Location of Wave Crest Forward From A.P. (ft.)
1A	4	11	10.9	808.5	20.92	-0.69	-2.30	220.0
		12	10.9	808.5	20.92	3.93	2.06	440.0
		13	10.9	808.5	20.92	-0.41	1.73	660.0
1B	4	11	10.9	808.5	20.92	-0.69	-2.30	220.0
		12	10.9	808.5	20.92	3.93	2.06	440.0
		13	10.9	808.5	20.92	-0.41	1.73	660.0
1B	5	14	18.7	808.5	21.97	1.02	-1.93	220.0
		15	18.7	808.5	21.97	7.30	3.27	440.0
		16	18.7	808.5	21.97	-2.65	1.2	660.0
1B	6	17	28.1	561.5	16.47	-0.63	0.13	220.0
		18	28.1	561.5	16.47	0.84	0.01	440.0
		19	28.1	561.5	16.47	-0.68	-0.15	660.0

Notes:

a, b, and c   see sign convention under Table 7

the net dynamic responses can be obtained simply by deducting the still-water response from the overall results for each wave loading condition.

d.   Generation of Stress-time History Curve

In order to determine the amplitude of the wave-induced stresses for each wave condition, a stress-time history of one complete stress cycle, as shown in Figure 24, was plotted based on three different wave-crest positions at the midship and the quarter points, and each wave-crest position was treated as a separate loading condition.
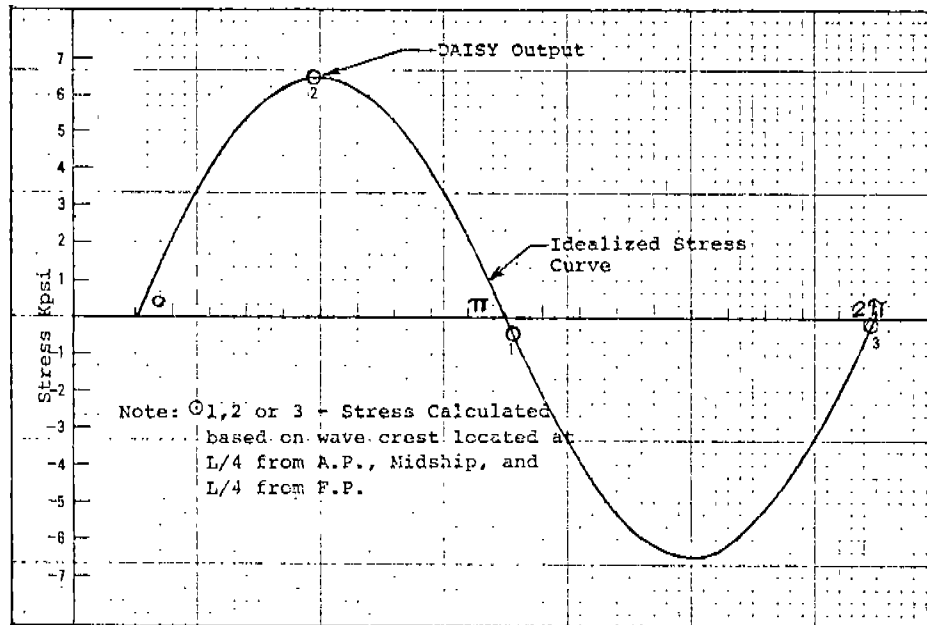
FIGURE 24 - IDEALIZED STRESS-TIME HISTORY CURVE, BASED ON
THREE WAVE CREST POSITIONS

Two assumptions were made in generating the stress-time history. First, the time variation of stress was assumed to be sinusoidal. Second, the calculated longitudinal wave-induced stress was assumed to be in phase with the wave-induced vertical bending moment at the ship station under consideration. In the comparison of the calculated and the measured RMS stresses, the double stress amplitude (peak-to-trough) was utilized.

B.   Calculated Results

For comparison, the calculated and measured RMS stresses for the three selected wave conditions are shown in Tables 10 and 11 and are also plotted in Figures 25, 26 and 27. The measured values were based on data reduction performed by Teledyne. The RMS stresses calculated by Methods 1A and 1B are generally in good agreement, as shown in Table 10. These stresses are generally of the same order of magnitude as the measured values. The calculated and measured RMS stresses for sensors AR1A, AR2A and AR3A in Table 11 show good agreement; however, sensor AR4A consistently shows that the measured data are much lower than the calculated values.

37

Wave Condition	Sensor No.	Location	Calc. RMS Stress (Method 1B)	Meas. RMS Stress
4	1 (LVB)	MN.DK.MID- SHIP SEC. (AVG. OF STBD. AND PORT)	9,673	6,743
5			8,469	6,344
6			6,887	5,368
6	15 (LSTS)	MN.DK.MID- SHIP SEC. (STBD)	6,887	5,840
4	17 (LSBS)	NEAR-BOTTOM PL. (STBD)	4,570	4,164
6			3,039	3,297
4	18 (LSTP)	MN.DK.MID- SHIP SEC. (PORT)	9,673	5,367
6			6,887	5,529
4	20 (LSBP)	NEAR-BOTTOM PL. (PORT)	4,570	2,974
5			4,623	2,743
6			3,039	2,876
4	30 (AR1A)	MN.DK.FR. 143-144 (PORT)	5,285	5,027
5			5,850	4,769
6			3,433	4,649
4	33 (AR2A)	MN.DK.FR. 143-144 (STBD)	5,285	5,587
5			5,850	5,767
6			3,433	4,939
4	36 (AR3A)	MN.DK. FR. 143-144 (STBD)	10,505	7,537
5			11,657	7,563
6			6,844	6,576
4	39 (AR4A)	MN.DK.FR. 143-144 (STBD)	10,499	4,333
5			11,450	4,017
6			6,930	3,786

TABLE 11   COMPARISON OF CALCULATED AND MEASURED RMS
LONGITUDINAL STRESSES (PEAK-TO-TROUGH, PSI)

WAVE CONDITION 4

Sensor No.	Calculated RMS Stress		Measured RMS Stress
	Method 1A	Method 1B	
1 (LVB)	9,243	9,673	6,743
18 (LSTP)	9,243	9,673	5,367
17 (LSBS)	4,320	4,570	4,164
20 (LSBP)	4,320	4,570	2,974
30 (AR1A)	6,121	5,285	5,027
33 (AR2A)	6,121	5,285	5,587
36 (AR3A)	10,566	10,505	7,537
39 (AR4A)	9,813	10,499	4,333
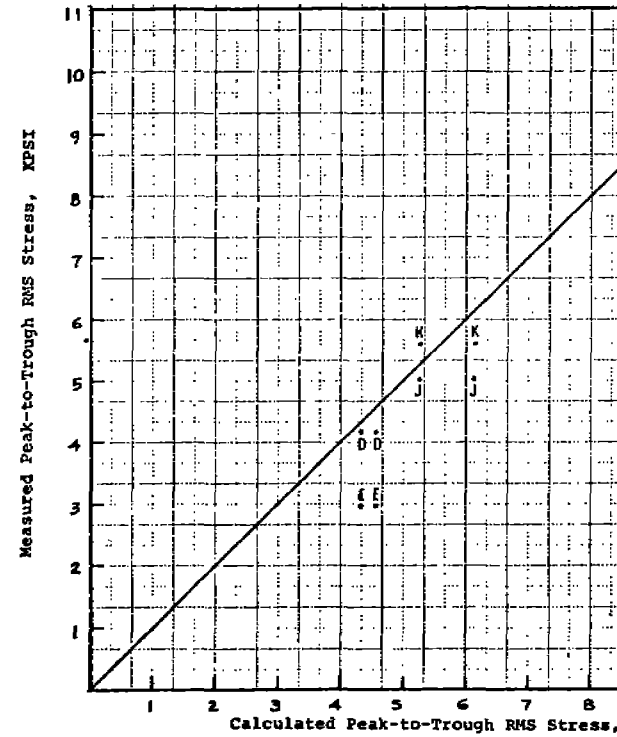
SENSOR	SYMBOL	CALCULATED STRESS (PSI)		MEA STI
		METHOD 1A	1B	
LSBS	D	4320	4570	
LSTP	C	9243	9673	
LSBP	E	4320	4570	
AR1A	J	6121	5285	
AR2A	K	6121	5285	
AR3A	L	10,566	10,505	
AR4A	M	9813	10,499	

FIGURE 25 -   DEVIATION OF CALCULATED PEAK-TO-TROUGH RMS S
VALUES (WAVE CONDITION 1, L_W = 808.5 FT., H_W

Calculated Peak-to-Trough, KPSI
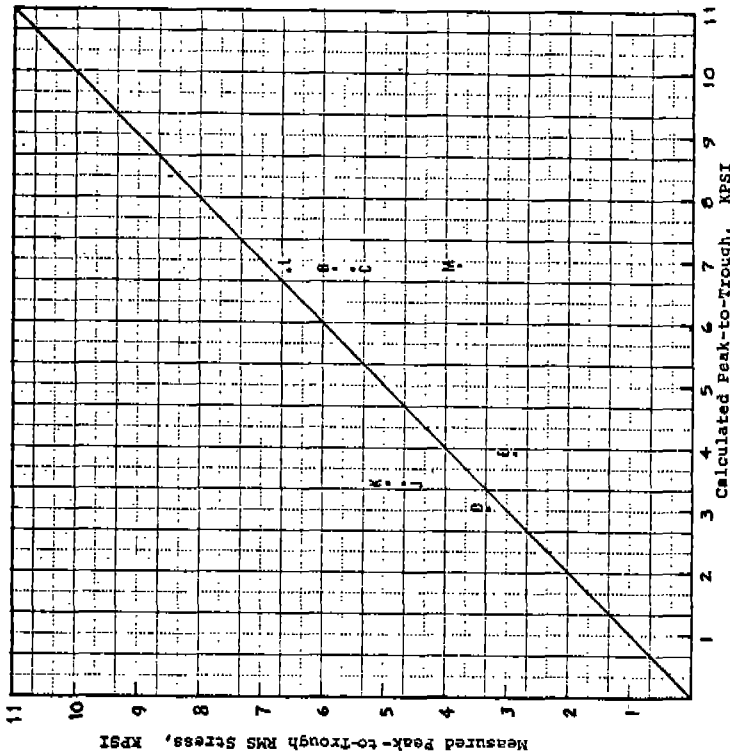
SENSOR	SYMBOL	CALCULATED STRESS (PSI) METHOD 1B	MEASURED STRESS (PSI)
LSTS	B	6887	5840
LSBS	D	3039	3297
LSTP	C	6887	5529
LSBP	E	3939	2876
AR1A	J	3433	4649
AR2A	K	3433	4939
AR3A	L	6844	6576
AR4A	M	6930	3786

FIGURE 27 — DEVIATION OF CALCULATED PEAK-TO-TROUGH RMS STRESSES FROM MEASURED VALUES (WAVE CONDITION 3, L_W = 561.4 FT., H_W = 16.47 FT.)

Calculated Peak-to-Trough RMS Stress, KPSI

SENSOR	SYMBOL	CALCULATED STRESS (PSI) METHOD 1B	MEASURED STRESS (PSI)
LSBS	D	4623	2743
AR1A	J	5850	4769
AR2A	K	5850	5767
AR3A	L	11,657	7563
AR4A	M	11,450	4017

FIGURE 26 — DEVIATION OF CALCULATED PEAK-TO-TROUGH RMS STRESSES FROM MEASURED VALUES (WAVE CONDITION 2, L_W = 808.5 FT., H_W = 21.97 FT.)

40

2. Method 2 - Stress Spectrum Approach

A. Description of Method

The procedures used to calculate wave-induced dynamic loads and to perform the structural analysis are the same as those described in the previous sections. For the external pressures, Method 1B was used in conjunction with wave spectra from Reference [8] for the selected wave conditions. Since the selected three basic intervals have three different ship speeds, ranging from 10.9 to 28.1 knots, a stress RAO curve has to be generated for each ship speed. In order to have sufficient points for each selected wave spectrum a total of 23 wave lengths, as shown in Table 12, was used. The wave lengths were determined in such a way that these three basic wave spectra could be closely represented.

For each wave length the relative wave-crest position was selected to maximize the vertical bending moment at the ship station under consideration. This information was readily available from the ship motion calculations. Assuming that the longitudinal stresses in the deck plating are in phase with the vertical bending moment, the stress amplitude could be directly calculated for each wave frequency.

In an attempt to minimize the possible stress deviations due to the non-linear relation between stresses and wave heights, an average wave height of 19.68 ft was used for all the different waves. The computed stresses were then divided by the wave amplitudes to generate the stress RAO. Once the RAO curve in terms of a unit wave amplitude for the selected stress sensor is constructed, a stress spectrum can be obtained by multiplying the ordinate of the wave spectrum by $(RAO)^2$. The measured wave spectrum has a low-frequency cut-off value, as illustrated in Figures 28 through 41, below which the data are unreliable.

B. Calculated Results

The calculated stress spectra for the three selected basic wave conditions are shown in Figures 28, 29 and 30 for sensor LVB and Figures 31, 32 and 33 for sensors LSBS and LSBP. The measured stress spectra reproduced from Reference [8] are also shown for comparison. The calculated RMS stresses, expressed in terms of $2\sqrt{2A}$ (where A is the area under the stress spectrum curve) are listed in Table 14.

In order to make a further comparison for sensor LVB, eight additional recorded intervals with nearly head sea conditions and comparable ship speeds were selected from Reference [8]. The particulars for these intervals are listed in Table 13.

41

TABLE 12 — WAVE CHARACTERISTICS AND SHIP MOTION DATA – METHOD 2 – TASK II
WAVE HEIGHT (PEAK-TO-TROUGH)= 19.68 FT. (6M)

Wave Cond.	(a) Loading Cond.	Ship Speed (knots)	Wave Encounter Frequency (rad./sec.)	Wave Length (ft.)	(b) Heave (ft.)	(c) Pitch (deg.)	Location of Wave Crest Forward From A.P. (ft.)
	20	10.9	.279	3366.9	9.32	0.19	471.7
	21	10.9	.451	1460.5	7.26	0.81	448.8
	22	10.9	.560	1015.85	5.21	1.42	439.0
4	23	10.9	.643	808.5	3.69	1.85	433.8
	24	10.9	.729	682.96	2.76	1.95	432.0
	25	10.9	.816	550.4	1.75	0.96	436.8
	26	10.9	1.088	350.8	-0.39	0.31	564.3
	27	18.7	.430	1901.8	8.31	0.87	496.8
	28	18.7	.548	1295.4	7.38	1.55	464.3
	29	18.7	.611	1093.14	6.97	2.00	452.0
5	30	18.7	.745	821.5	6.58	2.89	436.7
	31	18.7	.866	644.46	2.14	1.97	431.4
	32	18.7	1.019	509.33	1.75	0.02	431.8
	33	18.7	1.138	434.5	1.36	-0.05	426.8
	34	28.1	.305	3887.9	7.57	0.65	820.3
	35	28.1	.508	1758.7	8.23	1.51	541.2
	36	28.1	.479	1322.0	8.72	2.25	492.4
6	37	28.1	.712	1088.0	9.63	3.00	465.6
	38	28.1	.817	880.9	8.27	3.81	438.9
	39	28.1	.967	695.7	-1.52	1.30	433.4
	40	28.1	1.130	561.5	1.00	0.05	427.6
	41	28.1	1.273	478.4	1.03	-0.01	420.7
	42	28.1	1.579	359.3	-.14	0.0	578.2

Notes:

a, b, and c   see sign convention under Table 7

TABLE 13 PARTICULARS OF WAVES SELECTED FROM REFERENCE [8] FOR COMPARISON OF RMS STRESSES USING THE STRESS SPECTRUM APPROACH

Wave Condition	Ship Speed (knots)	Tape	Index	Interval	Run No.
7	32.6	143	9	36	337
8	32.5	145	27	41	441
9	32.3	153	4	15	815
10	32.4	153	8	29	829
11	31.8	153	12	45	845
12	31.2	155	17	1	901
13	32.6	157	12	45	1045
14	31.3	163	14	5	1305

TABLE 14 COMPARISON OF CALCULATED AND MEASURED RMS VERTICAL BENDING STRESSES (PEAK-TO-TROUGH, PSI) FOR SENSORS AT MIDSHIP

Wave Condition	Sensor	Calculated (Wave Spectrum Approach)	Measured
4	LVB	8343	6743
5		7295	6344
6		7183	5368
7		3547	2990
8		4192	3300
9		4544	4730
10		2542	2000
11		4252	3410
12		4766	4310
13		3188	3530
14		4595	5800
4	LSBS	3605	4101
5		2926	———
6		1954	3161
4	LSBS	3605	3261
5		2926	2729
6		1954	2732

Notes:

1. RMS values of stresses are defined as $2\sqrt{2A}$ where A is the area under the stress spectrum curve (Figures 28 through 41)

2. Stress RAO curve used for above Runs (except for Runs 405 and 429) is the same as that for Run 450 (Figure 30b)

43

Since these intervals have ship speeds comparable with wave condition 6, it is reasonable to use the stress RAO curve for wave condition 6, (Figure 30b) to calculate the stress spectra for the additional intervals. The calculated stress spectra together with the measured stress and wave spectra are shown in Figures 34 through 41. The calculated RMS stresses for these additional intervals, together with the measured values, are also listed in Table 14.

As shown in Figures 28 through 41, the calculated stress spectra generally exhibit shapes similar to those obtained from the measured data. Some of the calculated peak frequencies and peak amplitudes deviate significantly from the measured curves. However, the calculated RMS stresses as shown in Table 14 generally agree well with the measured values.

For a further comparison of the three different methods to calculate external pressures, some calculated and measured RMS longitudinal stresses in the main deck at midship (Sensor LVB) are shown in Table 15.

TABLE 15   COMPARISON ON CALCULATED AND MEASURED RMS VERTICAL BENDING STRESSES (PEAK-TO-TROUGH, PSI) FOR SENSOR LVB AT MIDSHIP

Wave Condition / Method	Calculated Equivalent Wave Approach		Stress Spectrum Approach	Measured
	Method 1A	Method 1B	(Method 2)	
4	9243	9673	8343	6743
5	7810	8469	7295	6344
6	7800	6887	7183	5368

3. Conclusions

Based on the results and comparison discussed above, the following conclusions can be drawn:

A. In general, both Method 1 and Method 2 give a reasonably good agreement between the calculated RMS stresses and the measured data in head seas.

44

B.   As shown in Tables 14 and 15, the RMS stresses calculated
by the spectrum analysis (Method 2) agree very well with those
obtained from the measured data.   On the other hand, at some
strain-gage locations (Table 10) the RMS stresses computed by
Method 1 are significantly greater than the measured values.
This may be attributed to the fact that the equivalent regu-
lar wave approach ignores the possible variations in structural
responses to different wave frequencies.   The spectrum analysis,
which accounts for all the significant wave frequencies, gives
a better average value.   It should be noted that the spectrum
analysis is valid only where the relation between the stresses
and wave lengths can be approximated as linear.

C.   The calculated stress spectra, as shown in Figures 28
through 41, assume similar shapes as those obtained from the
measured data.   However, the calculated peak frequency and peak
amplitude may deviate from the measured ones in some comparisons.

D.   The stresses calculated by Method 1A are, as expected,
comparable with those obtained by Method 1B for head sea
conditions.

45

FIGURE 29 – MEAN MIDSHIP VERTICAL BENDING STRESS (SENSOR LVB) RESPONSES TO IRREGULAR SEA, WAVE CONDITION 5
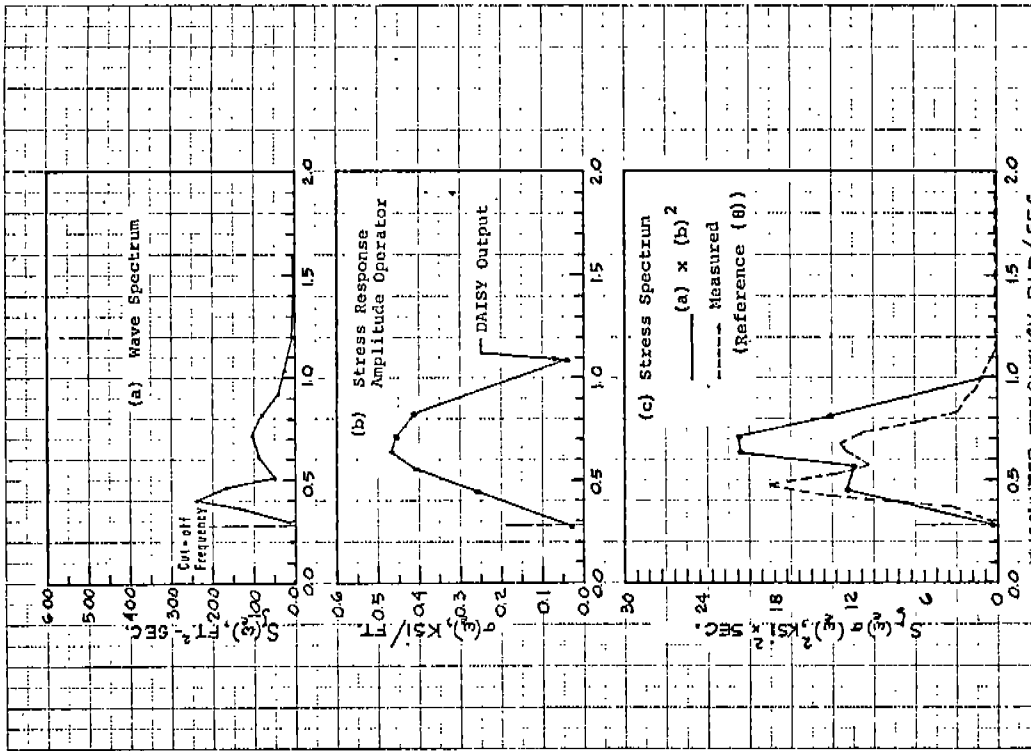
FIGURE 28 – MEAN MIDSHIP VERTICAL BENDING STRESS (SENSOR LVB) RESPONSES TO IRREGULAR SEA, WAVE CONDITION 4

FIGURE 31 – MIDSHIP VERTICAL BENDING STRESS (SENSORS LSBP AND LSBS) RESPONSES TO IRREGULAR SEA, WAVE CONDITION 4

FIGURE 30 – MEAN MIDSHIP VERTICAL BENDING STRESS (SENSOR LVB) RESPONSES TO IRREGULAR SEA, WAVE CONDITION 6

47
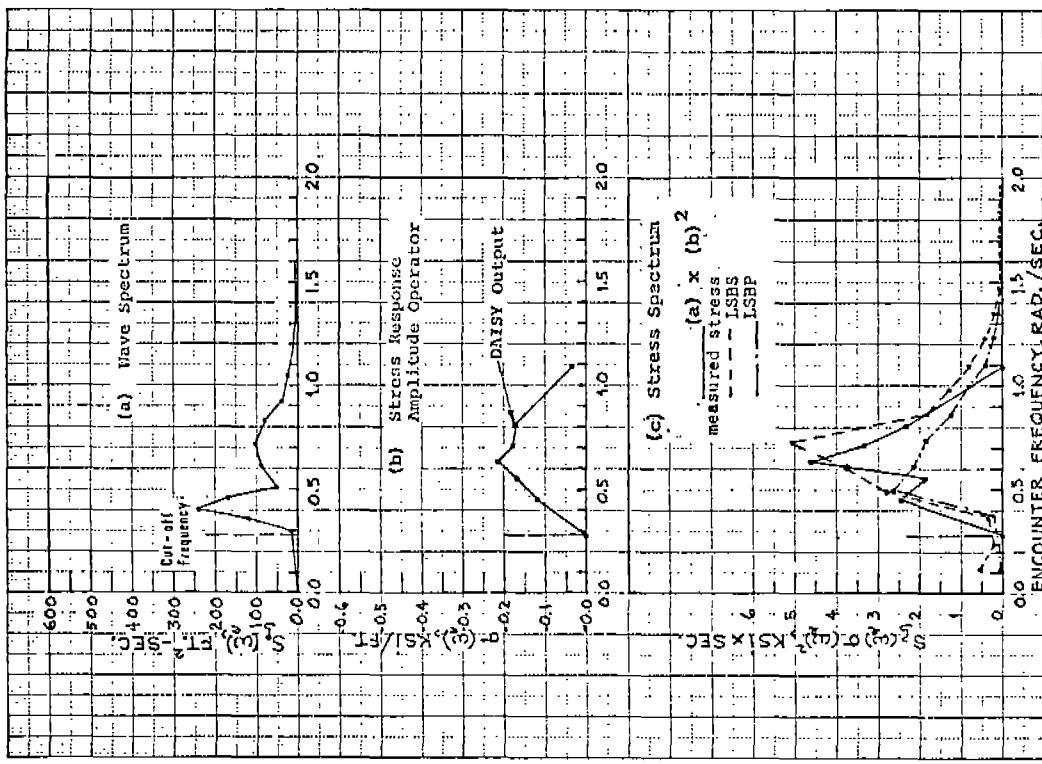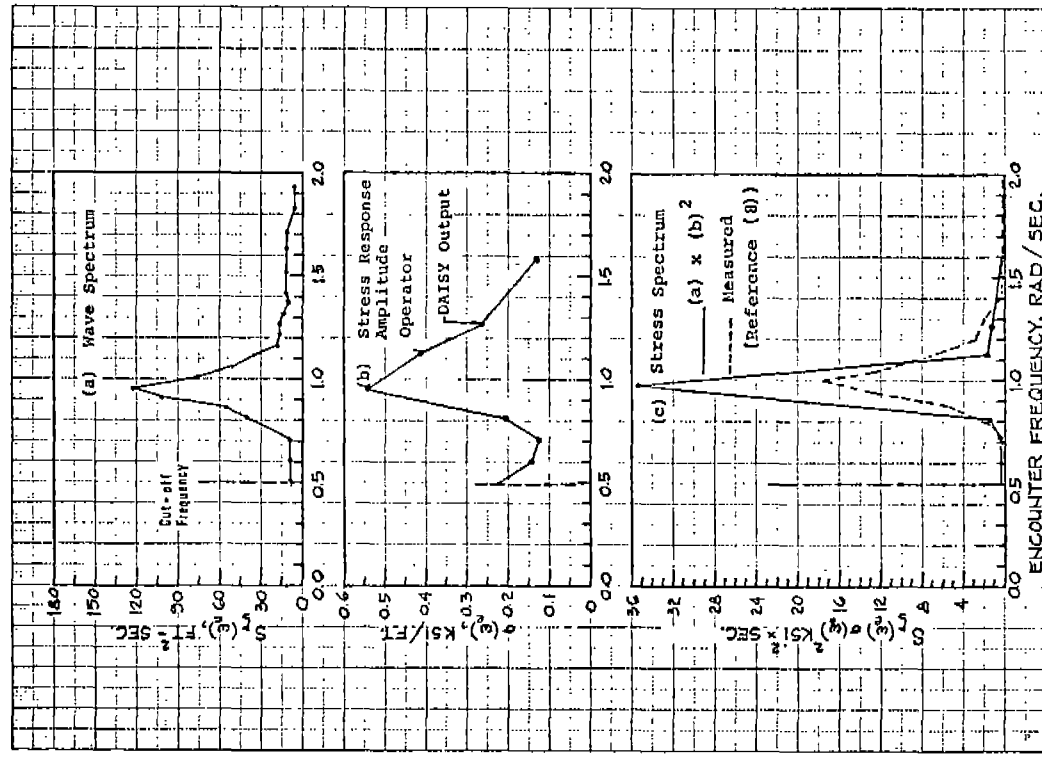
FIGURE 33 – MIDSHIP BENDING STRESS (SENSORS LSBP AND LSBS) RESPONSES TO IRREGULAR SEA, WAVE CONDITION 6
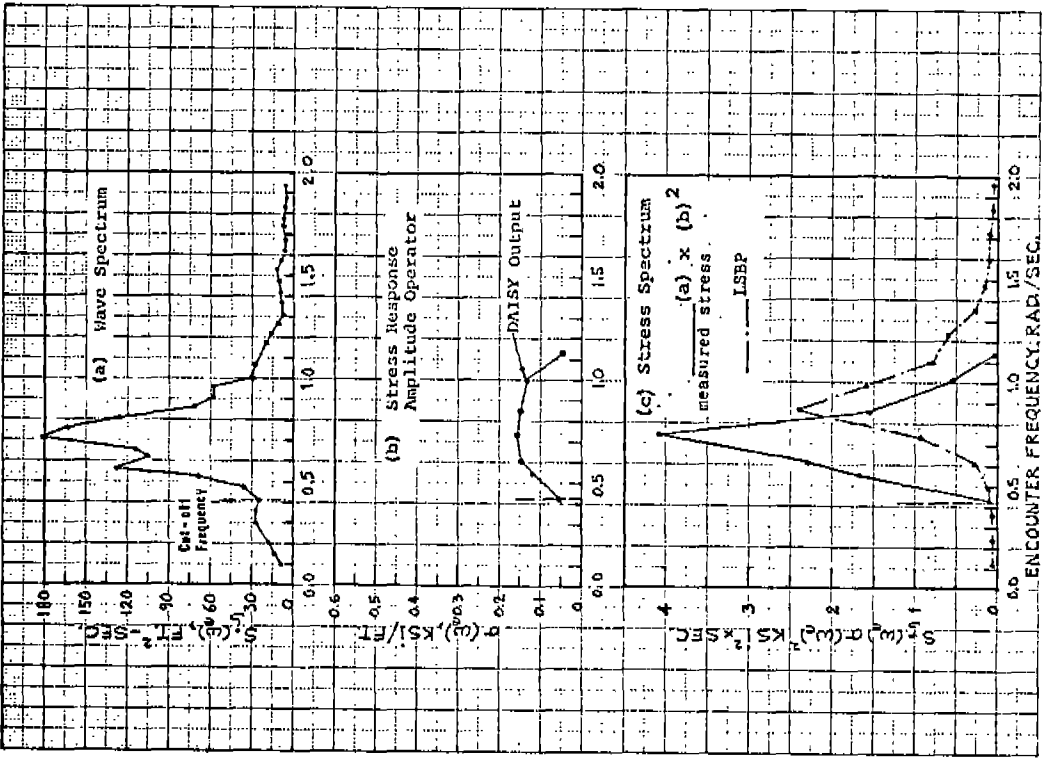
FIGURE 32 – MIDSHIP BENDING STRESS (SENSORS LSBP) RESPONSES TO IRREGULAR SEA, WAVE CONDITION 5

48

FIGURE 35 - MEAN MIDSHIP VERTICAL BENDING STRESS (SENSOR LVB) RESPONSES
TO IRREGULAR SEA, WAVE CONDITION 8
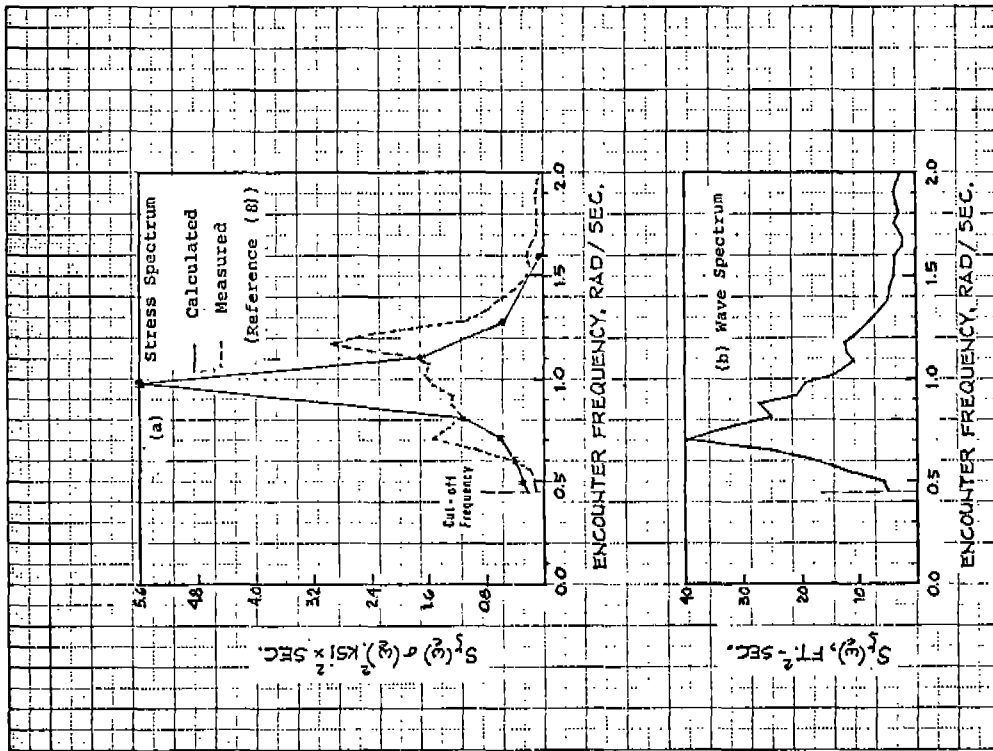
FIGURE 34 - MEAN MIDSHIP VERTICAL BENDING STRESS (SENSOR LVB) RESPONSES
TO IRREGULAR SEA, WAVE CONDITION 7

49

FIGURE 37 - MEAN MIDSHIP VERTICAL BENDING STRESS (SENSOR LVB) RESPONSES
TO IRREGULAR SEA, WAVE CONDITION 10
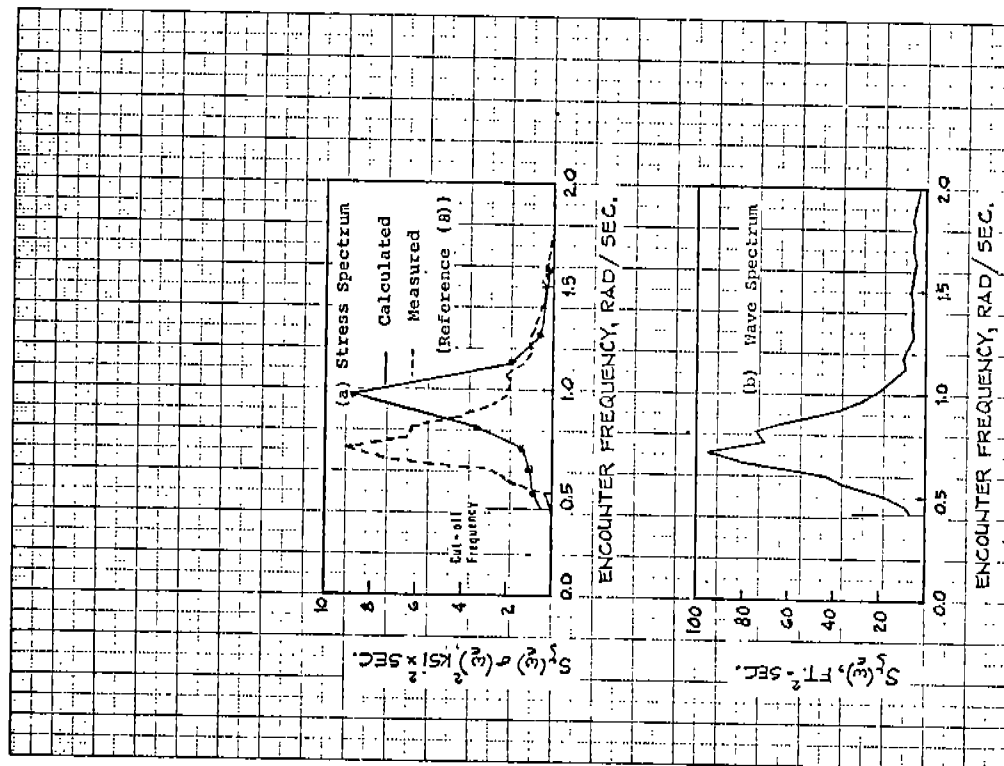
FIGURE 36 - MEAN MIDSHIP VERTICAL BENDING STRESS (SENSOR LVB) RESPONSES
TO IRREGULAR SEA, WAVE CONDITION 9

50
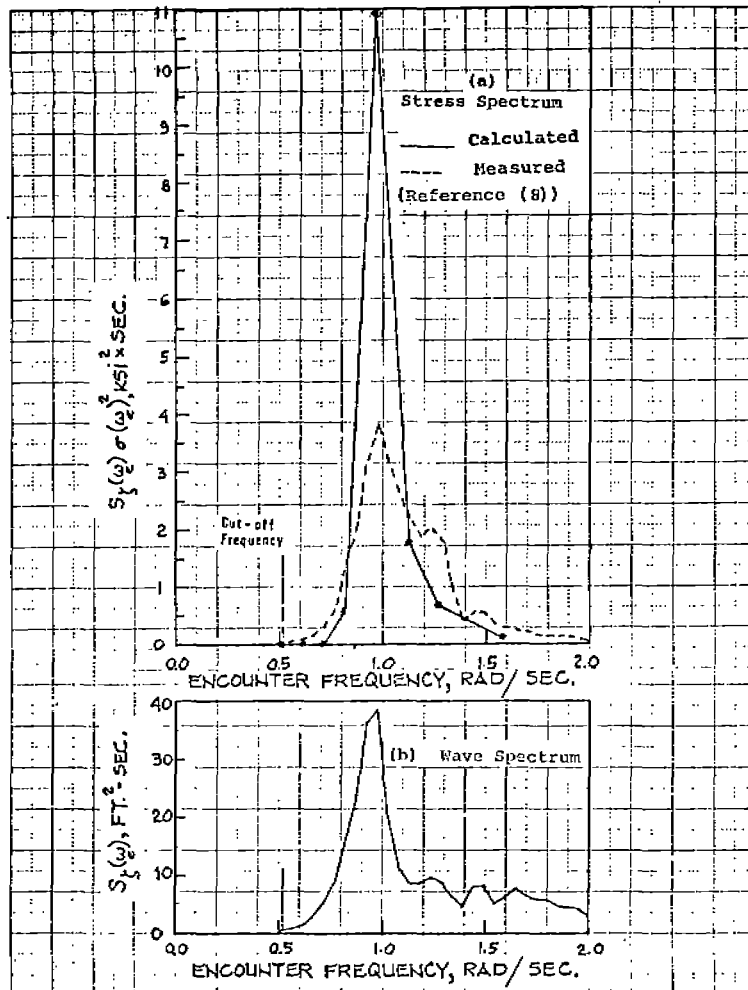
FIGURE 38 - MEAN MIDSHIP VERTICAL BENDING STRESS (SENSOR LVB) RESPONSES TO IRREGULAR SEA, WAVE CONDITION 11
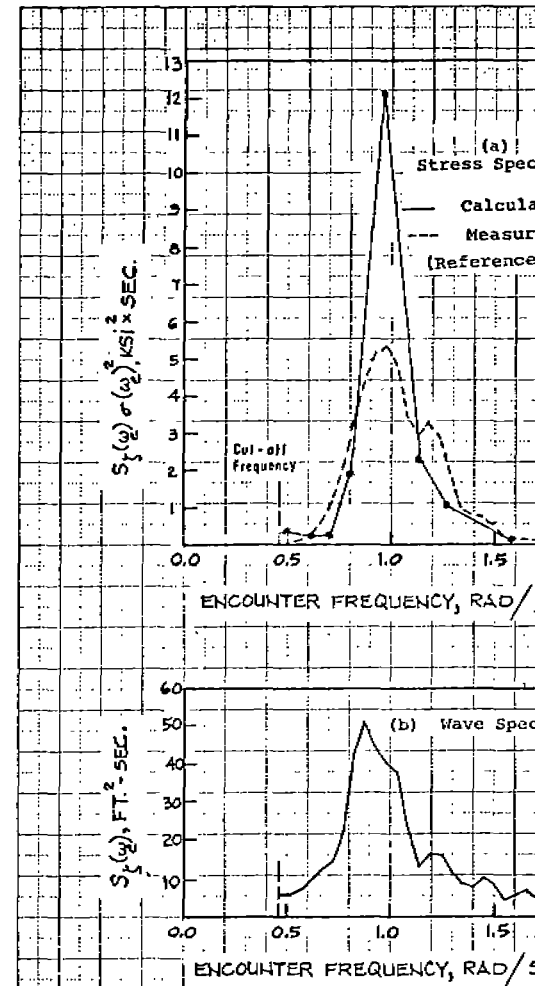
FIGURE 39 - MEAN MIDSHIP VERTICAL BENDING STRESS TO IRREGULAR SEA, WAVE CONDITION 12

FIGURE 41 - MEAN MIDSHIP VERTICAL BENDING STRESS (SENSOR LVB) RESPONSES TO IRREGULAR SEA, WAVE CONDITION 14

FIGURE 40 - MEAN MIDSHIP VERTICAL BENDING STRESS (SENSOR LVB) RESPONSES TO IRREGULAR SEA, WAVE CONDITION 13

TASK III - INSTANTANEOUS STRESS COMPARISON IN HEAD SEAS

1. Selection of Record Intervals

Two record intervals were selected for this phase of the study. The detailed environmental information on these two selected intervals is shown in Figures 42 and 43, as obtained from Reference [8]. The selected time span for stress correlation covers two complete encounter cycles, shown shaded within a circle on the time history of the radar wave elevation, Figures 42 and 43.

2. Ship Motion Calculation

To facilitate the wave-load calculations, the recorded wave elevation within the time period of two complete cycles was approximated by a regular wave with a mean encounter frequency, an average height and an equivalent wave length (See the enlarged scale in Figures 42 and 43).

The wave particulars for the two selected conditions are shown in Table 16. Once the wave particulars were established, a ship motion calculation was performed using the ABS/SHIPMOTION program to compute motions, accelerations, shearing forces and bending moments for three positions of the wave crest along the length of the vessel, namely, at the midship and two quarter-length stations.

TABLE 16   WAVE CHARACTERISTICS AND SHIP MOTION DATA - TASK III

Wave Cond.	Load-ing Cond.	Ship Speed (knots)	Wave Length (ft.)	Wave Height (Peak-to-Trough)	Heave (ft.)	Pitch (deg.)	Location of Wave Crest Forward From A.P. (ft.)
15	43	10.9	1651.0	51.2	-15.9	-2.8	220.0
	44	10.9	1651.0	51.2	20.4	1.48	440.0
	45	10.9	1651.0	51.2	11.4	4.79	660.0
16	46	28.1	808.5	30.6	14.35	0.48	220.0
	47	28.1	808.5	30.6	4.64	5.40	440.0
	48	28.1	808.5	30.6	-15.64	-1.99	660.0

LOG BOOK DATA

DATE AND TIME	01-10-74 2400	
POSITION	43-29 N 24-51 W	
COURSE AND SPEED	250 . 10.9 KNOTS	
SEA STATE	7	
WAVE HEIGHT	25 FEET	
" REL DIR	2 PORT	
SWELL HEIGHT	20 FEET	
" REL DIR	2 PORT	

---- VISUAL WEATHER / COMMENTS ----
OCAST /

WAVE HEIGHT STATISTICS (FEET)

	TUCKER/DYN.		HEAD/RADAR
P-T SAMPLE SIZE	90	70	121
MAXIMUM HEIGHT	15.9	43.4	57.2
10TH HIGHEST HTS	15.0	39.0	39.7
3RD HIGHEST HTS	13.0	33.8	32.5
4.0 RMS(SPECTRA)	13.3	34.0	33.5
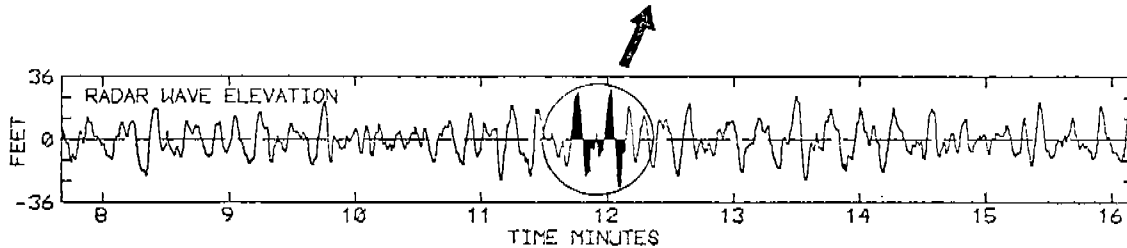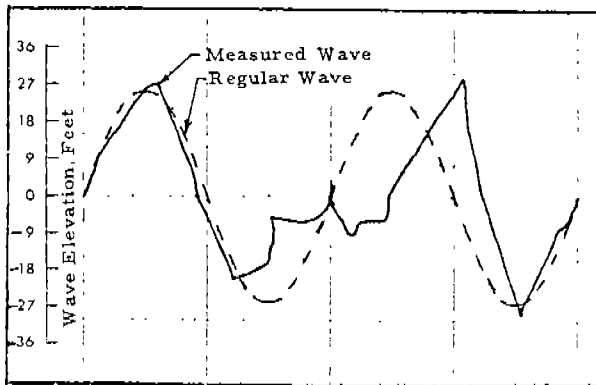
FIGURE 42 - CONDITION 15 - VOYAGE 32W -- TAPE 145 -- INDEX 18 -- INTERVAL 5 - RUN 405

LOG BOOK DATA

DATE AND TIME	01-12-74 1630	
POSITION	41-07 N 40-08 W	
COURSE AND SPEED	245 . 28.1 KNOTS	
SEA STATE	9	
WAVE HEIGHT	25 FEET	
" REL DIR	2 STBD	
SWELL HEIGHT	20 FEET	
" REL DIR	2 STBD	

---- VISUAL WEATHER / COMMENTS ----
OCAST /

WAVE HEIGHT STATISTICS (FEET)

	TUCKER/DYN.		HEAD/RADAR
P-T SAMPLE SIZE	239	179	222
MAXIMUM HEIGHT	8.3	8.9	58.0
10TH HIGHEST HTS	5.9	7.0	33.7
3RD HIGHEST HTS	4.6	5.4	26.4
4.0 RMS(SPECTRA)	5.5	6.3	29.4
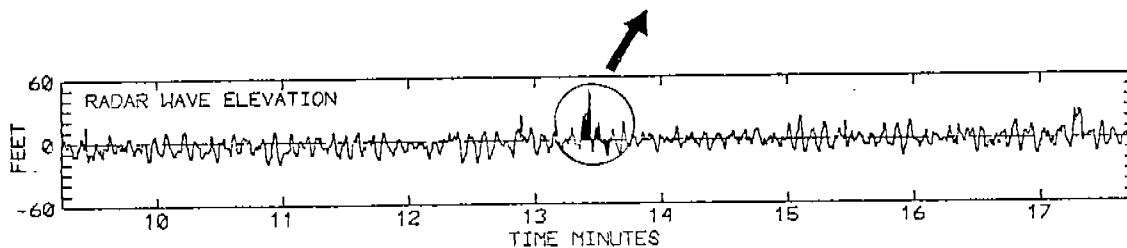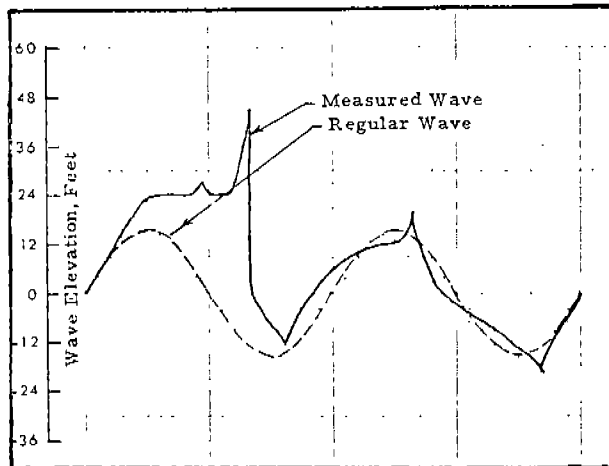
FIGURE 43 - CONDITION 16 - VOYAGE 32W -- TAPE 145 -- INDEX 29 -- INTERVAL 50 - RUN 450

54

3. Input to DAISY Model

A modification of hydrodynamic pressure coefficients, described as Method 1B in Task II, was carried out to make the wave-induced vertical shearing forces and bending moments acting on the DAISY model generally identical to those calculated directly by the SHIPMOTION program. A sample comparison is shown in Figure 44.
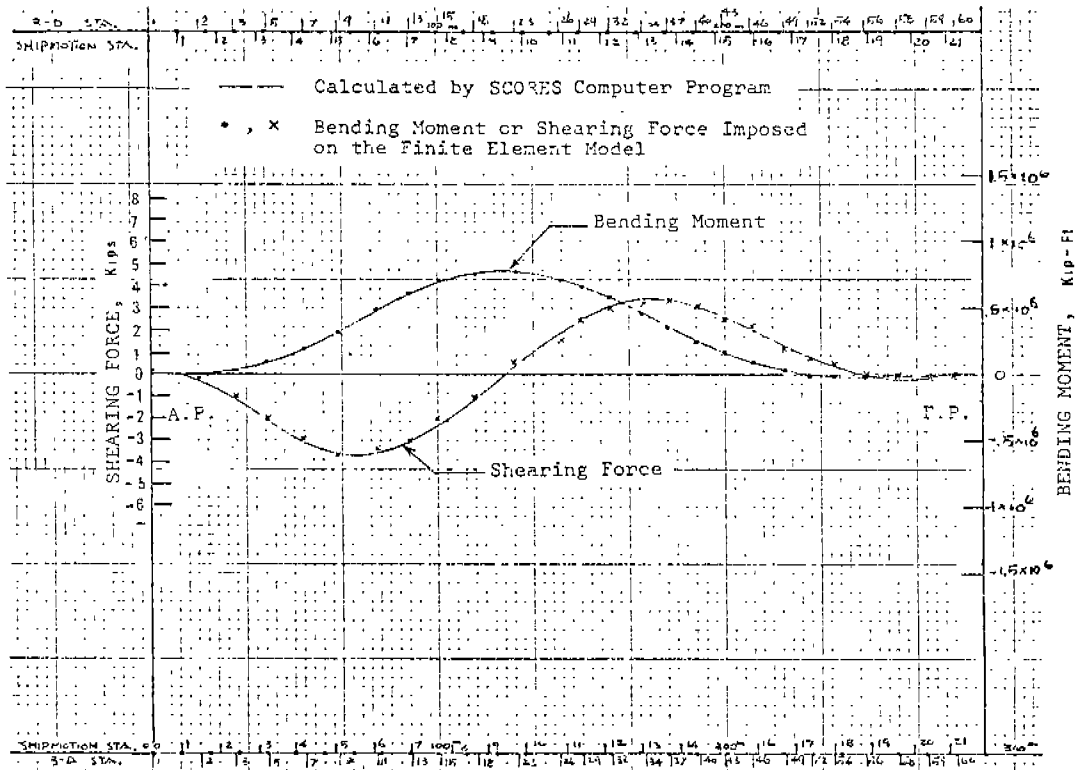
FIGURE 44 - WAVE-INDUCED BENDING MOMENTS AND SHEARING FORCES

4. Comparison of Calculated Stresses and Measured Data

For each wave condition, three values of stress were calculated, corresponding to the three wave-crest positions described above. In order to construct a diagram of stress-time history based on the three calculated values, it was assumed that the computed stress follows a sinusoidal curve

55

with a frequency equal to the wave-encounter frequency. It was further assumed that the stress variation is directly proportional to the dominant wave-load component, the phase angle of which can be obtained from the ship motion calculations. For longitudinal stresses in the deck or bottom regions, the dominant wave-load component was assumed to be the vertical bending moment. A mean stress amplitude obtained from these three calculated stress values, with proper phase angles, was then utilized to plot an idealized stress curve (See Figures 45 and 46).

A. Mean Midship Vertical Bending Stress - Sensor LVB

The calculated and measured mean midship vertical bending stresses (Sensor LVB) are shown in Figures 45 and 46 for Wave Conditions 15 and 16 respectively. The measured stress-time history was selected within the same time period used for the selection of wave data. Recognizing the difference between the recorded wave elevation and the idealized wave profile, it can be seen that the comparison of the calculated stresses and the measured data is very good.

B. Other Stress Gages at Midship for Wave Condition 15

In addition to the mean midship vertical bending stress (Sensor LVB), the following stresses at the midship were also recorded at the same instant as the selected wave data:

    LSTP - Longitudinal Stress Top Port
    LSBP - Longitudinal Stress Bottom Port
    LSBS - Longitudinal Stress Bottom Starboard

The measured and calculated longitudinal stresses at the locations of Sensors LSTP and LSBP, as shown in Figures 47 and 48, exhibit a good agreement. However, the comparison of measured and calculated stresses at the location of Sensor LSBS, Figure 49, is relatively poor. The measured stresses of LSBP and LSBS should be generally comparable in head seas. The difference between the measured stresses of LSBP and LSBS may be attributed to irregularity of the encounter wave and possibly irregularity of gage signals.

It should be noted that all the stress data other than the mean midship vertical bending stress (LVB) was generally recorded on Recorder No. 2, whereas the wave data and LVB were recorded on Recorder No. 1. In addition, all the stress data other than LVB was reduced separately from that of the wave data.
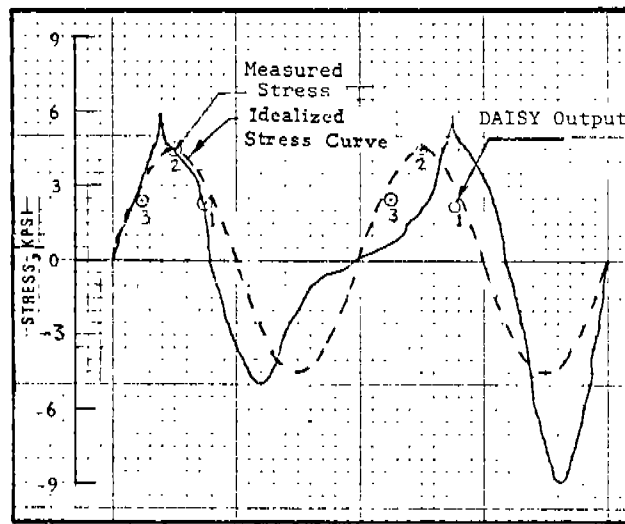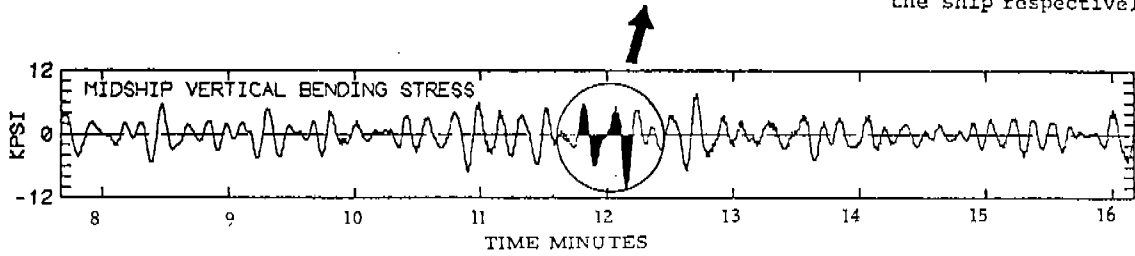
FIGURE 45 - COMPARISON OF THE CALCULATED AND MEASURED MEAN MIDSHIP
VERTICAL BENDING STRESSES (SENSOR LVB), WAVE CONDITION 15
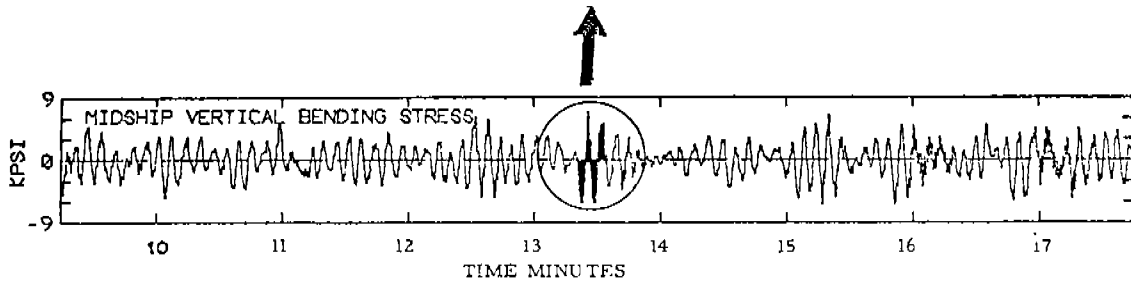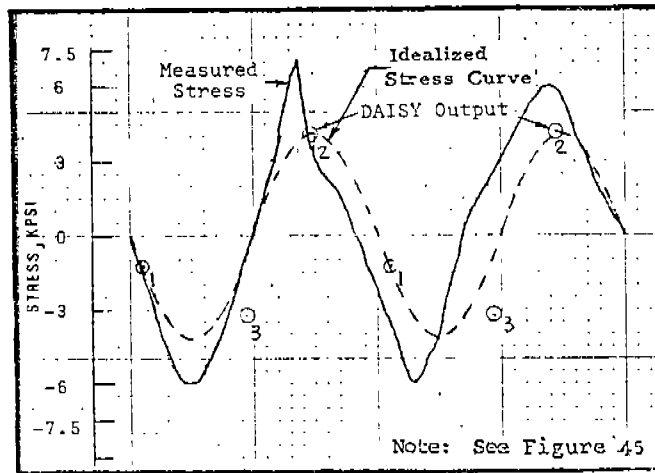
FIGURE 46 - COMPARISON OF THE CALCULATED AND MEASURED MEAN MIDSHIP
VERTICAL BENDING STRESSES (SENSOR LVB), WAVE CONDITION 16

57

C. Three-arm Rosette Gages at Frame 143-144 for
Wave Condition 16

Other sensors recording simultaneously with the selected
wave data for Wave Condition 16 are rosette gages on the deck
at Frame 143-144. The longitudinal elements of these rosettes
are designated by AR1A, AR2A, AR3A and AR4A.

Since an element of the rosette measures strain in one
direction only, the measured stress reflects a straight product
of the strain component and Young's modulus (E), but not the
true stress. For purposes of comparison, it is essential to
calculate stresses on a consistent basis. Therefore, the
computed stresses shown in Figures 50-53 are the product of
the longitudinal strain component and Young's modulus.

The comparison of the measured and calculated stresses
at locations of Sensors AR1A, AR2A, AR3A and AR4A as shown
in Figures 50 through 53 are generally good.

5. Conclusions

Based on the results discussed above, the following
conclusions can be established for Task III:

A. The comparison of the measured and calculated longitudinal
stresses for a selected period of time in head seas is gener-
ally good. The calculated stress amplitudes agree well with
the mean values of the selected two stress cycles, with the
exception of two gage locations.

B. For the selected cases, the wave data are generally
consistent with the stress data.

C. To calculate structural responses in head seas, irregular
waves can be approximated by regular waves with equivalent
amplitude and frequency.

FIGURE 47 - COMPARISON OF THE CALCULATED AND MEASURED INSTANTANEOUS
LONGITUDINAL STRESSES (SENSOR LSTP), WAVE CONDITION 15

FIGURE 48 - COMPARISON OF THE CALCULATED AND MEASURED INSTANTANEOUS
LONGITUDINAL STRESSES (SENSOR LSBP), WAVE CONDITION 15

59

FIGURE 49 - COMPARISON OF THE CALCULATED AND MEASURED INSTANTANEOUS
LONGITUDINAL STRESSES (SENSOR LSBS), WAVE CONDITION 15

FIGURE 50 - COMPARISON OF THE CALCULATED AND MEASURED INSTANTANEOUS
LONGITUDINAL STRESSES (SENSOR AR1A), WAVE CONDITION 16

60

FIGURE 51 — COMPARISON OF THE CALCULATED AND MEASURED INSTANTANEOUS LONGITUDINAL STRESSES (SENSOR AR2A), WAVE CONDITION 16

FIGURE 52 — COMPARISON OF THE CALCULATED AND MEASURED INSTANTANEOUS LONGITUDINAL STRESSES (SENSOR AR3A), WAVE CONDITION 16

61

FIGURE 53 – COMPARISON OF THE CALCULATED AND MEASURED INSTANTANEOUS
LONGITUDINAL STRESSES (SENSOR AR4A), WAVE CONDITION 16

1. Method of Approach

Due to the complexity of the wave load pattern in oblique seas, difficulties were experienced in dealing with the hydro-dynamic pressures and balancing of the structural model. To improve the consistency between the external pressures and the ship motion calculation, hydrodynamic pressure coefficients were modified for lateral moments in addition to the modifications for vertical moments described in Task II.

To investigate the feasibility of performing an instantaneous stress comparison in oblique seas, two record intervals were selected for test runs. The detailed information for the selected intervals and the radar wave data as obtained from Reference [8] are shown in Table 17.

TABLE 17   WAVE CONDITION SELECTED FROM REFERENCE [8] FOR THE COMPARISON OF INSTANTANEOUS STRESSES IN OBLIQUE SEAS

Wave Condition	Tape	Index	Interval	Run No.	Ship Speed (knots)	Wave Relative Dir. (deg.)	Heading Angle (deg.)
17	143	11	44	345	32.3	64 Port	116
18	143	12	48	349	31.8	41 Port	139

For instantaneous stress comparison, two complete cycles of the recorded wave elevation were selected and approximated by a regular wave with a mean encounter frequency, an average height and an equivalent wave length, (see the enlarged scale in Figures 54 and 55).

For each wave, three wave-crest positions, at midship and the two quarter-length points, were utilized to calculate wave loads. Each wave-crest position was treated as a separate loading condition. The particulars of these loading conditions are shown in Table 18.

```
LOG BOOK DATA
DATE AND TIME    01-09-74  2000
     POSITION    45-08 N    13-30 W
COURSE AND SPEED 267  .  32.3 KNOTS
   SEA STATE     8
  WAVE HEIGHT    10 FEET
     REL DIR     64 PORT
 SWELL HEIGHT    10 FEET
     REL DIR     64 PORT
---- VISUAL WEATHER / COMMENTS ----
CLDY /
```

WAVE HEIGHT STATISTICS (FEET)			
	TUCKER/DYN.	HEAD/RADAR	
P-T SAMPLE SIZE	201	128	235
MAXIMUM HEIGHT	8.4	13.0	36.4
10TH HIGHEST HTS	6.0	9.4	28.3
3RD HIGHEST HTS	4.5	7.5	21.9
4.0 RMS(SPECTRA)	5.2	7.9	22.9
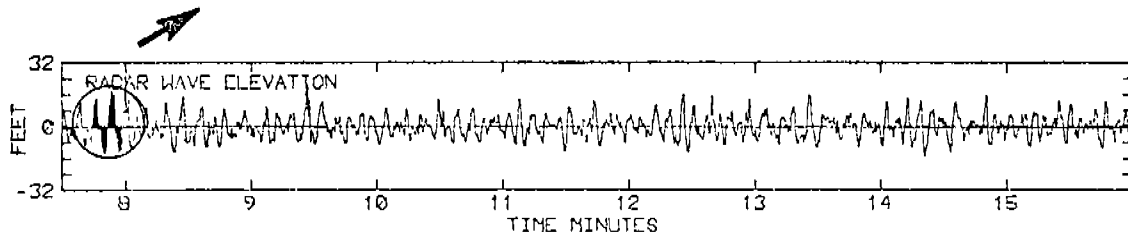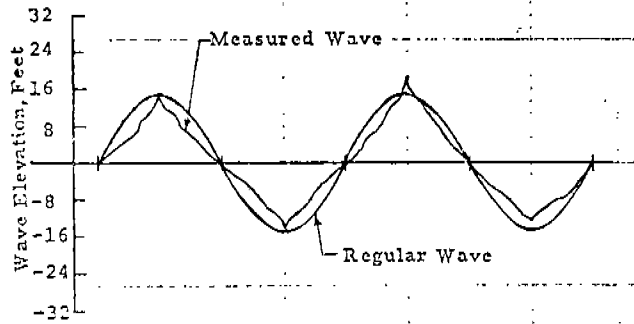
FIGURE 54 - CONDITION 17 - VOYAGE 32W - TAPE 143 - INDEX 11 - INTERVAL 44 -
             RUN 345

```
LOG BOOK DATA
DATE AND TIME    01-09-74  2400
     POSITION    45-08 N    13-30 W
COURSE AND SPEED 266  .  31.8 KNOTS
   SEA STATE     9
  WAVE HEIGHT    15 FEET
     REL DIR     41 PORT
 SWELL HEIGHT    10 FEET
     REL DIR     41 PORT
---- VISUAL WEATHER / COMMENTS ----
OCAST /
```

WAVE HEIGHT STATISTICS (FEET)			
	TUCKER/DYN.	HEAD/RADAR	
P-T SAMPLE SIZE	137	103	146
MAXIMUM HEIGHT	9.9	19.1	40.7
10TH HIGHEST HTS	7.8	15.1	37.8
3RD HIGHEST HTS	6.3	12.5	33.0
4.0 RMS(SPECTRA)	6.8	13.2	33.5
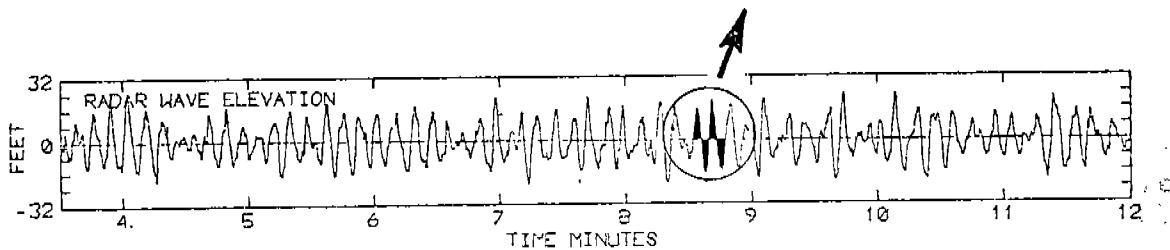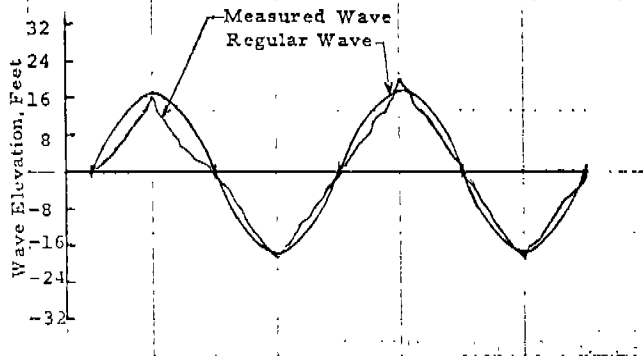
FIGURE 55 -   CONDITION 18 - VOYAGE 32W - TAPE 143 - INDEX 12 - INTERVAL 48 -
              RUN 349

64

TABLE 18 WAVE CHARACTERISTICS AND SHIP MOTION DATA - TASK IV

Wave Cond.	(a) Loading Cond.	Ship Speed (knots)	Wave Length (ft.)	Wave Height (Peak-to-Trough) (ft.)	(b) Heading Angle (deg.)	(c) Roll (deg.)	(d) Heave (ft.)	(e) Pitch (deg.)	Location of Wave Crest Forward From A.P. (ft.)
17	49	32.3	540.15	30.18	116	-0.27	21.45	3.15	220.0
	50	32.3	540.15	30.18	116	1.40	3.97	5.76	440.0
	51	32.3	540.15	30.18	116	1.495	-18.0	1.85	660.0
18	52	31.8	888.29	33.46	139	-0.457	17.5	-0.95	220.0
	53	31.8	888.29	33.46	139	1.252	20.4	5.317	440.0
	54	31.8	888.29	33.46	139	1.40	-1.8	5.05	660.0

Notes:

a, b, and c   see sign convention under Table 7

d Heading angle is measured counterclockwise from ship centerline to wave direction

e Roll is positive starboard deck edge down

2. Calculation of Wave-induced Loads

To determine the wave-induced loads for input to DAISY, the SHIPMOTION and DYNPRE programs were used. In oblique seas, the wave-induced moments consist generally of three components, namely vertical, lateral and torsional moments. Since the wave-induced loads obtained by integration of a set of hydrodynamic pressures and the corresponding inertia forces would generally not agree with those obtained from the ship motion calculation, a correction coefficient for the hydrodynamic pressure was introduced to modify the vertical and lateral moments for the external pressures. After this modification, the torsional moments may not be in agreement with those obtained from the ship motion calculation.

Because of the complexity of the wave-load pattern in oblique seas and the difficulty in balancing the DAISY model in the lateral direction, the external pressures were not extended up or deleted down to the wave surface for this task.

65

3. Structural Analysis

The procedures utilized for calculating structural responses for this task are generally the same as those in Tasks II and III, except that the asymmetric wave load was divided into symmetric and anti-symmetric components which were then treated as separate loading conditions in DAISY. The combination of the symmetric and anti-symmetric cases gives the total response for both the port and starboard sides. (See Figure 5).

For each wave, in addition to the three dynamic loading conditions corresponding to three wave-crest positions, a static case reflecting the still-water condition was also included in the analysis. The wave-induced stresses were then obtained by subtracting the still-water stresses from the total responses for each dynamic loading condition.

4. Calculated Results

In order to generate a stress-time history curve based on the calculated stresses at three different wave-crest positions, the following two assumptions were made:

a. The curve was assumed to be sinusoidal.

b. The calculated longitudinal wave-induced stress was assumed to be in phase with the effective moment (M_e) combining the wave-induced vertical and lateral bending moments, expressed in terms of

$$M_e = \left[M_V + \frac{M_L}{(SM_L/SM_V)} \right] \tag{5}$$

where M_V, M_L = wave-induced vertical and lateral bending moments respectively, at the location under consideration.

SM_V, SM_L = hull-girder section modulus with respect to vertical and lateral bending moments respectively, at the location under consideration.

The phase angles of M_V and M_L were obtained directly from the ship motion calculation, and the effective moment, M_e, was then determined graphically. A sample plot is shown in Figure 56.

66
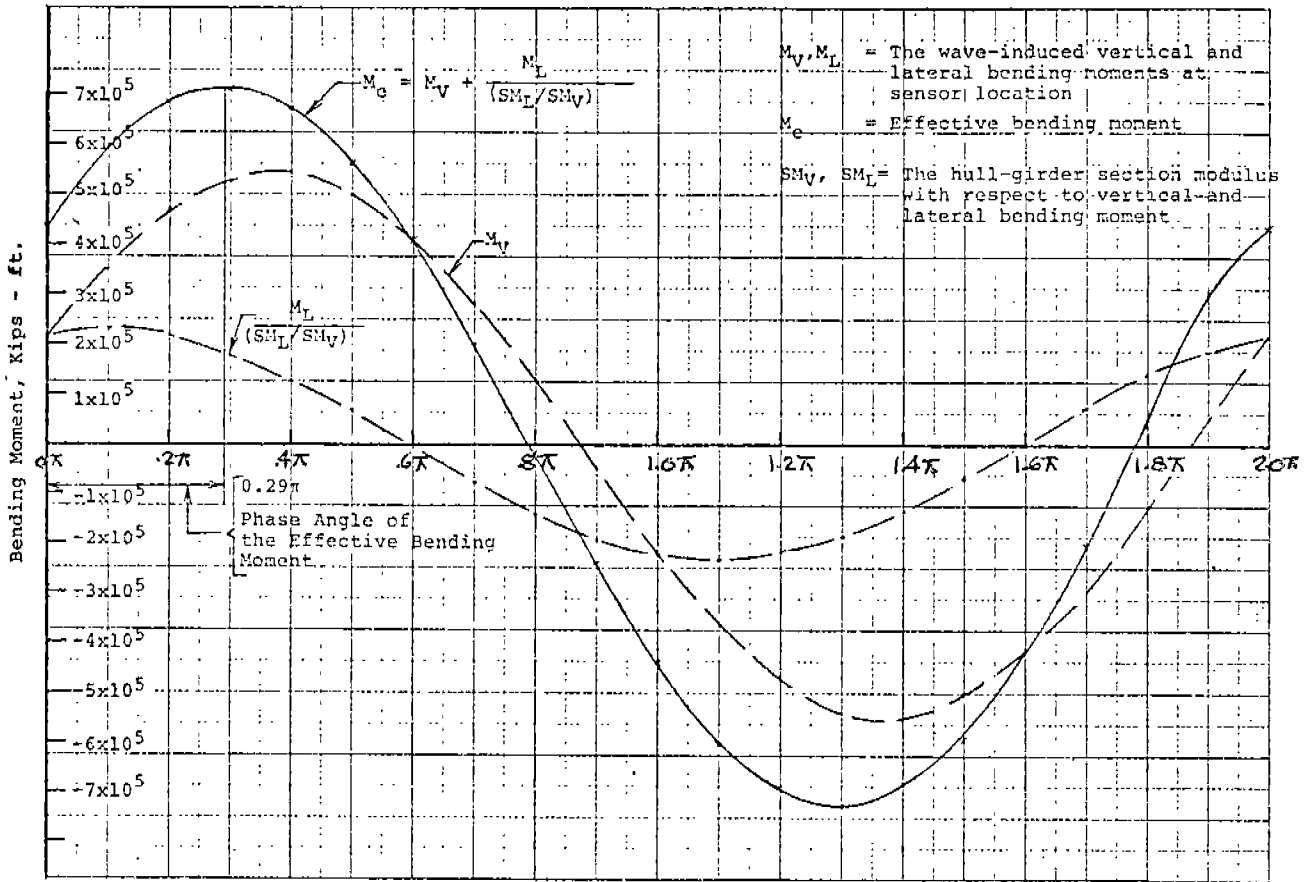
FIGURE 56 — GRAPHIC SOLUTION FOR THE PHASE ANGLE OF THE EFFECTIVE BENDING MOMENT

5. Comparison of Calculated Stresses and Measured Data

For each wave condition, three values of stress were calculated, corresponding to the three wave-crest positions described above. In order to construct a diagram of stress-time history based on the three calculated values, it was assumed that the computed stress follows a sinusoidal curve with a frequency equal to the wave-encounter frequency. It was further assumed that the stress variation is in direct proportion with the dominant wave-load component, and that the phase angle for combined wave-induced vertical and lateral bending moments can be obtained using the method described in the previous section. A mean stress amplitude obtained from these three calculated stress values with proper phase angles was then utilized to plot idealized stress curves as shown in Figures 57 through 67.

Based on the results shown in Figures 57 through 67, it can be seen that the calculated stress-time histories generally agree with the measured data, except for Sensor AR4A in Figure 67. Text contained on page 74.
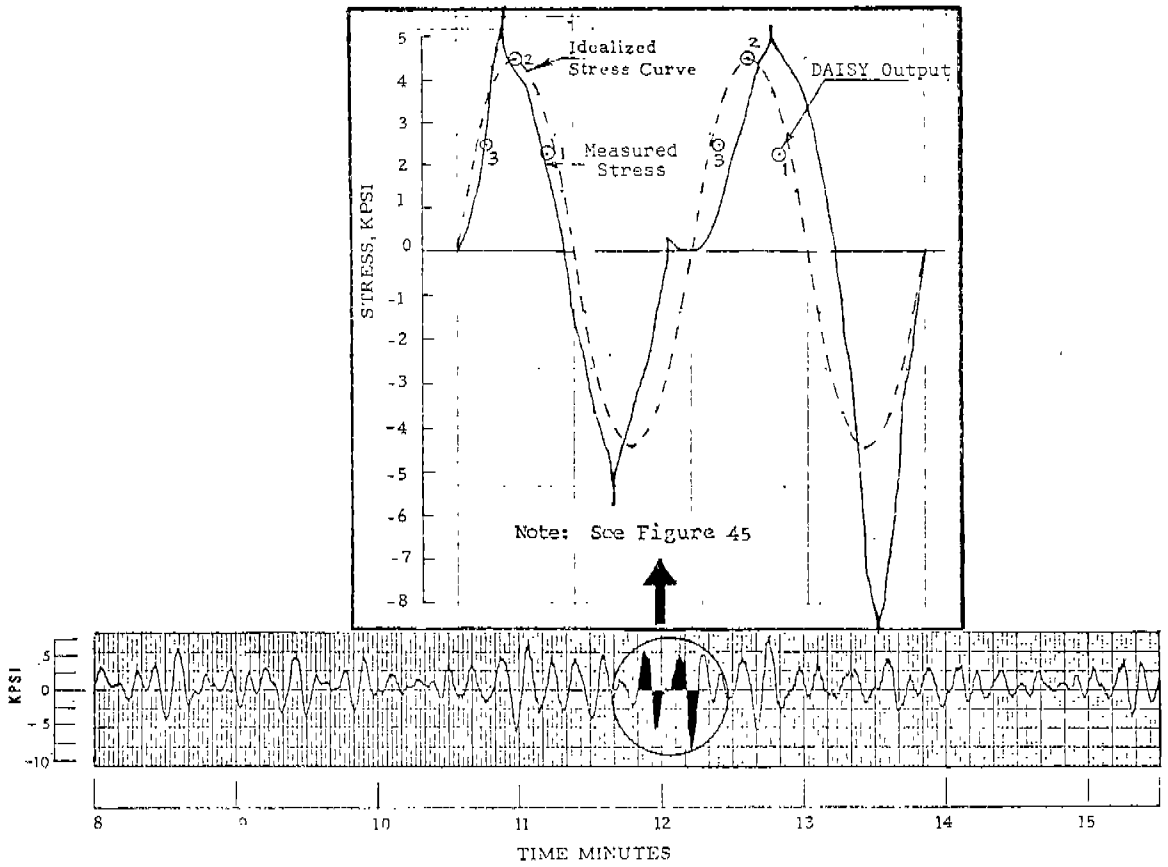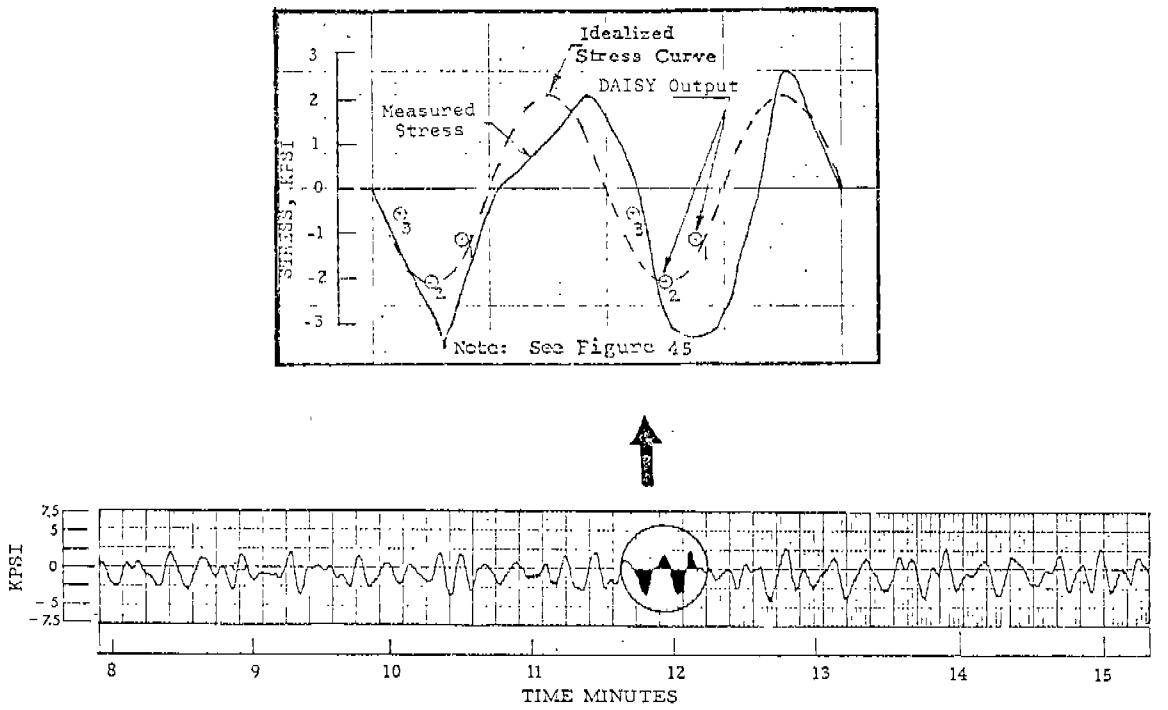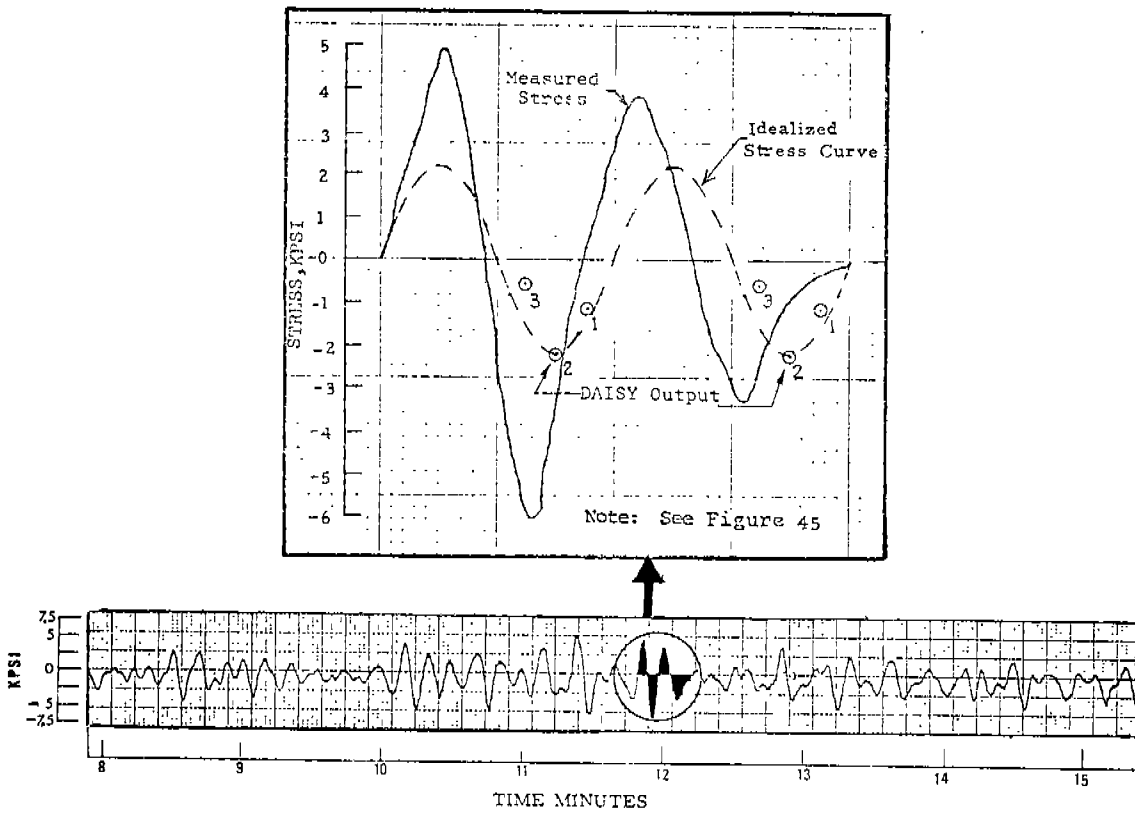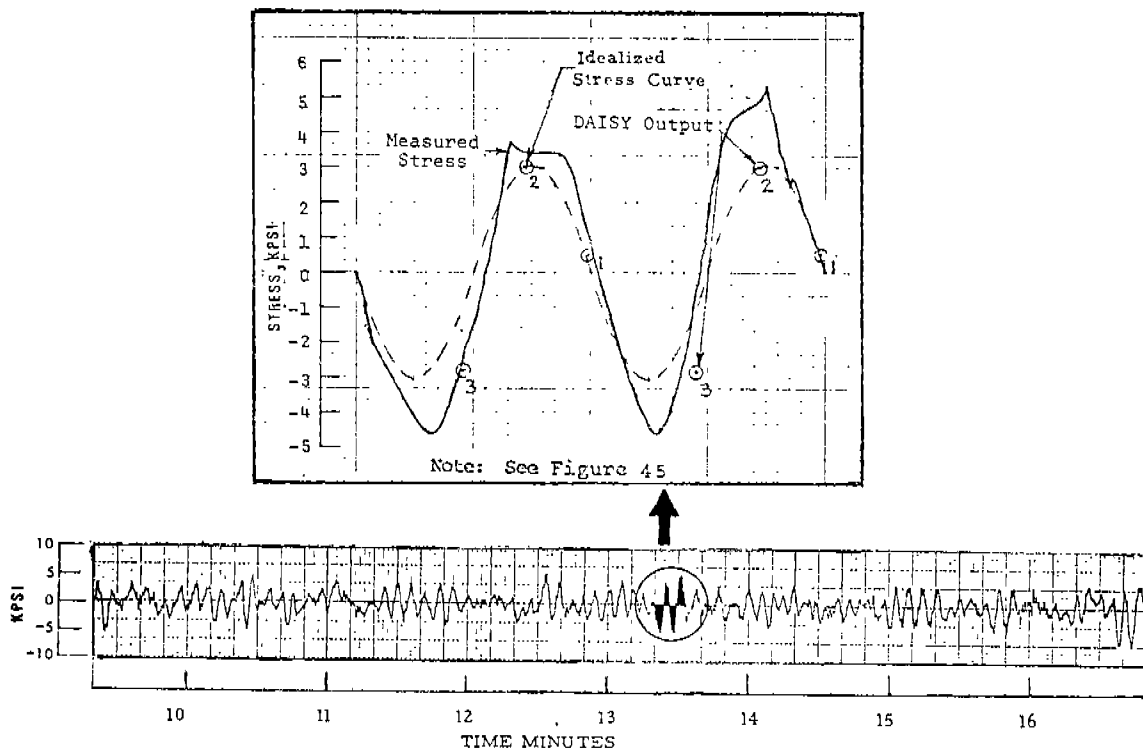
67
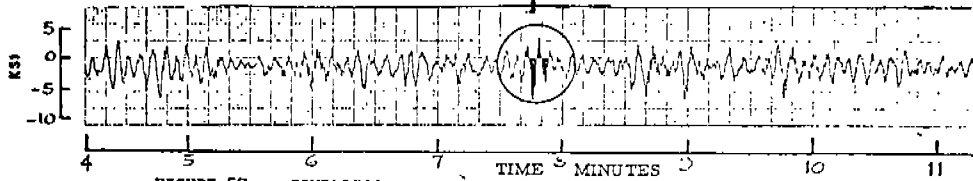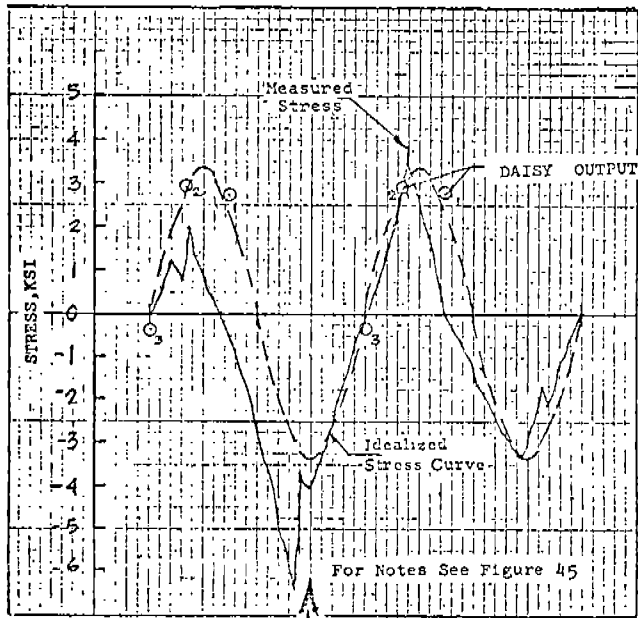
FIGURE 57 - COMPARISON OF THE CALCULATED AND MEASURED INSTANTANEOUS
LONGITUDINAL STRESSES (SENSOR LSTP), WAVE CONDITION 17
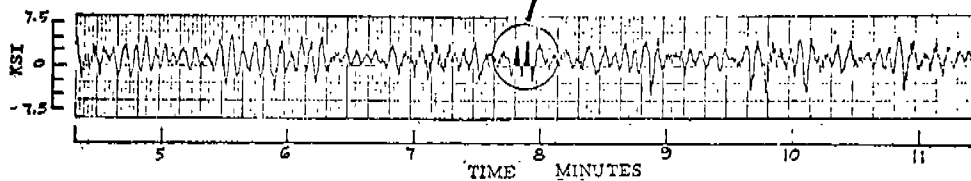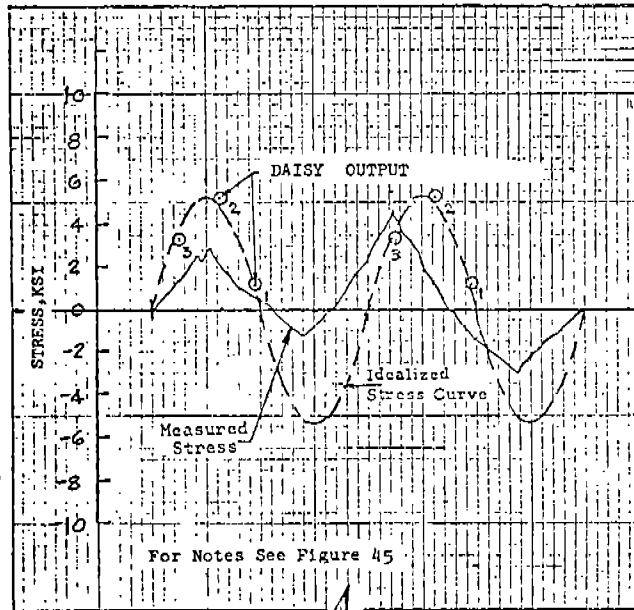
FIGURE 58 - COMPARISON OF THE CALCULATED AND MEASURED INSTANTANEOUS
LONGITUDINAL (SENSOR LSTS), WAVE CONDITION 17

68
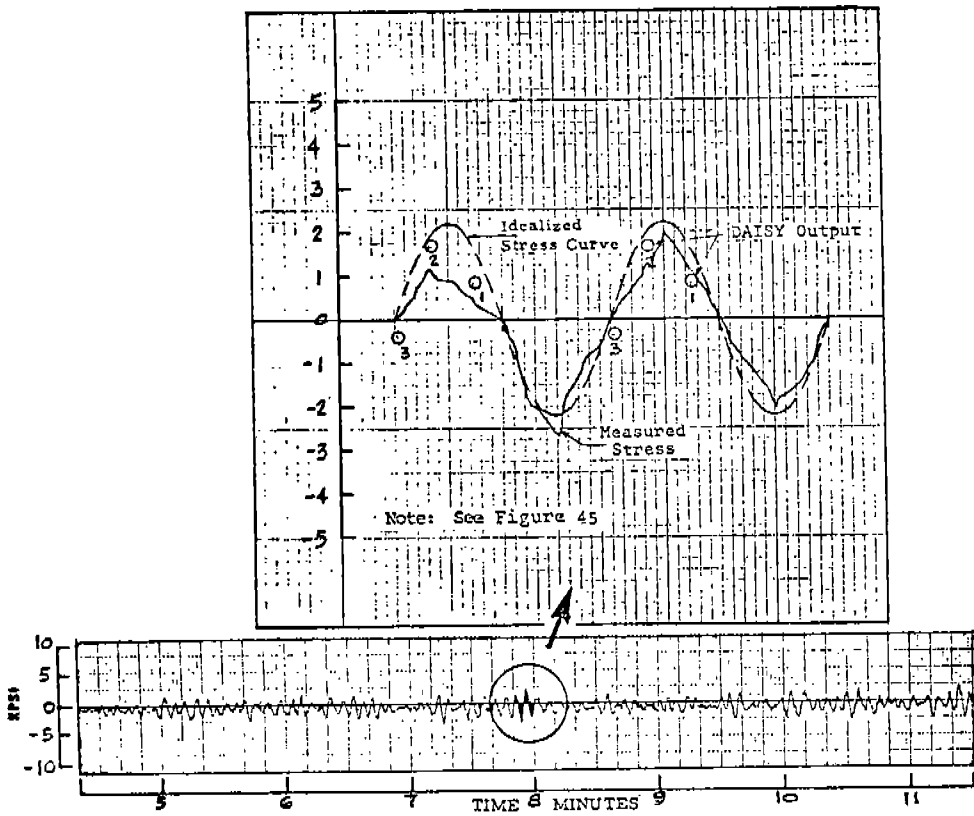
FIGURE 59 - COMPARISON OF THE CALCULATED AND MEASURED INSTANTANEOUS
LONGITUDINAL STRESSES (SENSOR LSBP), WAVE CONDITION 17
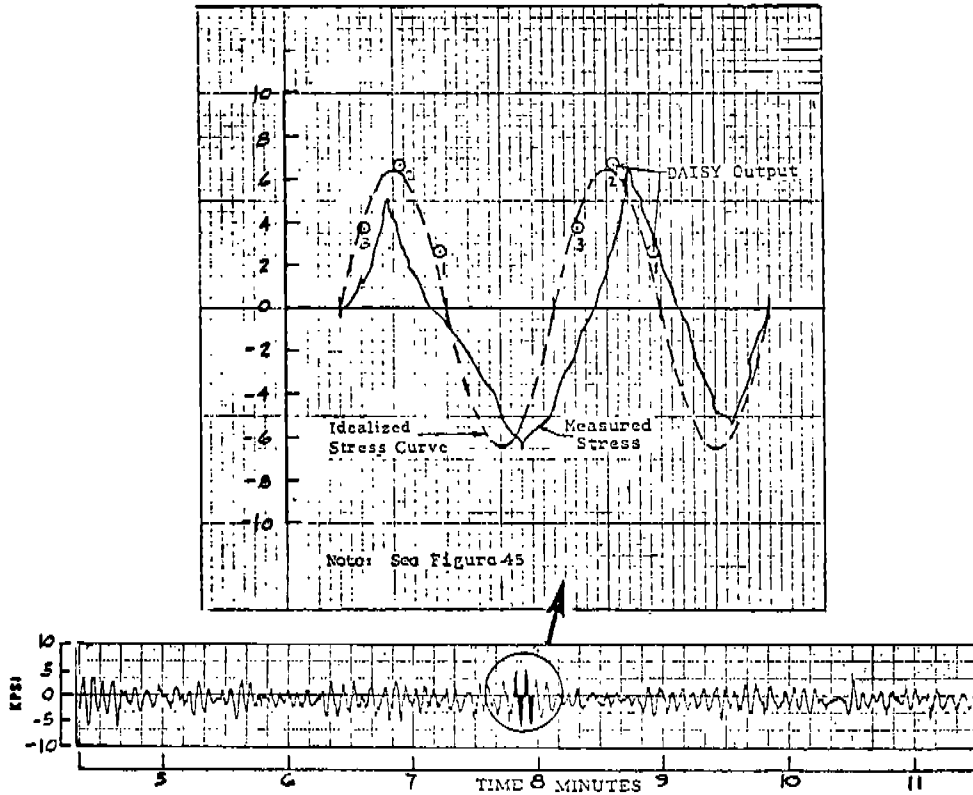
FIGURE 60 - COMPARISON OF THE CALCULATED AND MEASURED INSTANTANEOUS
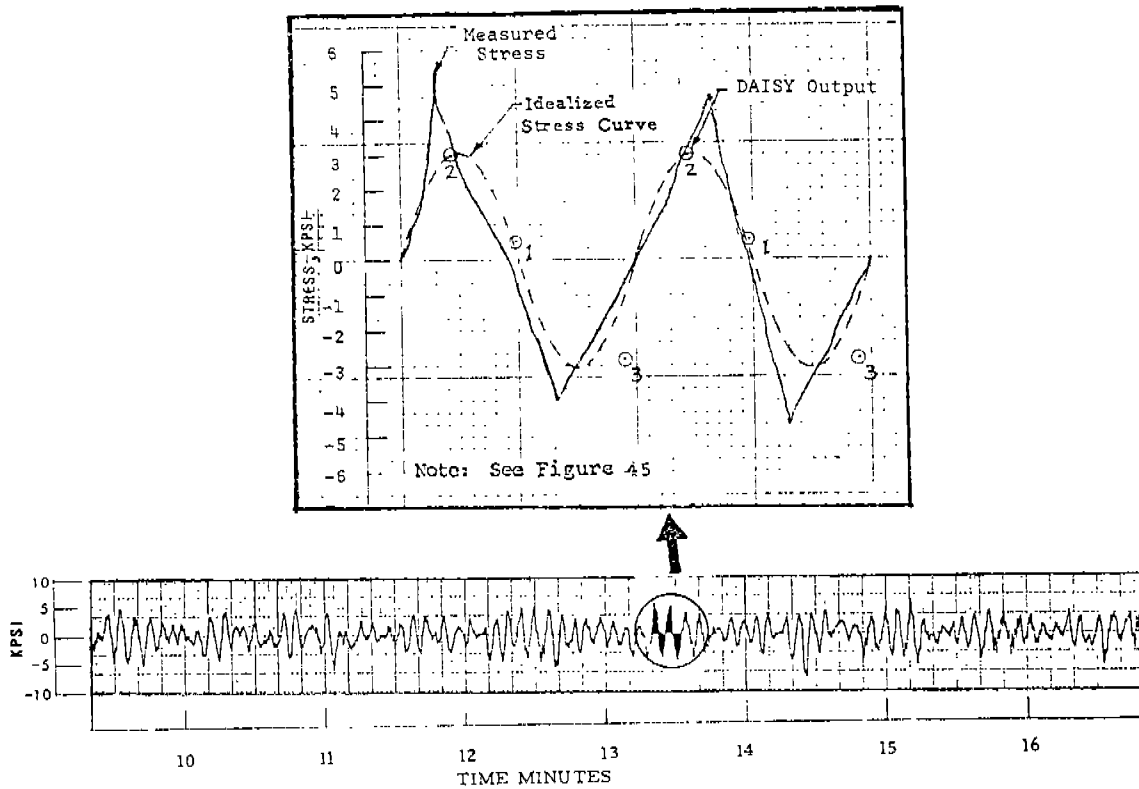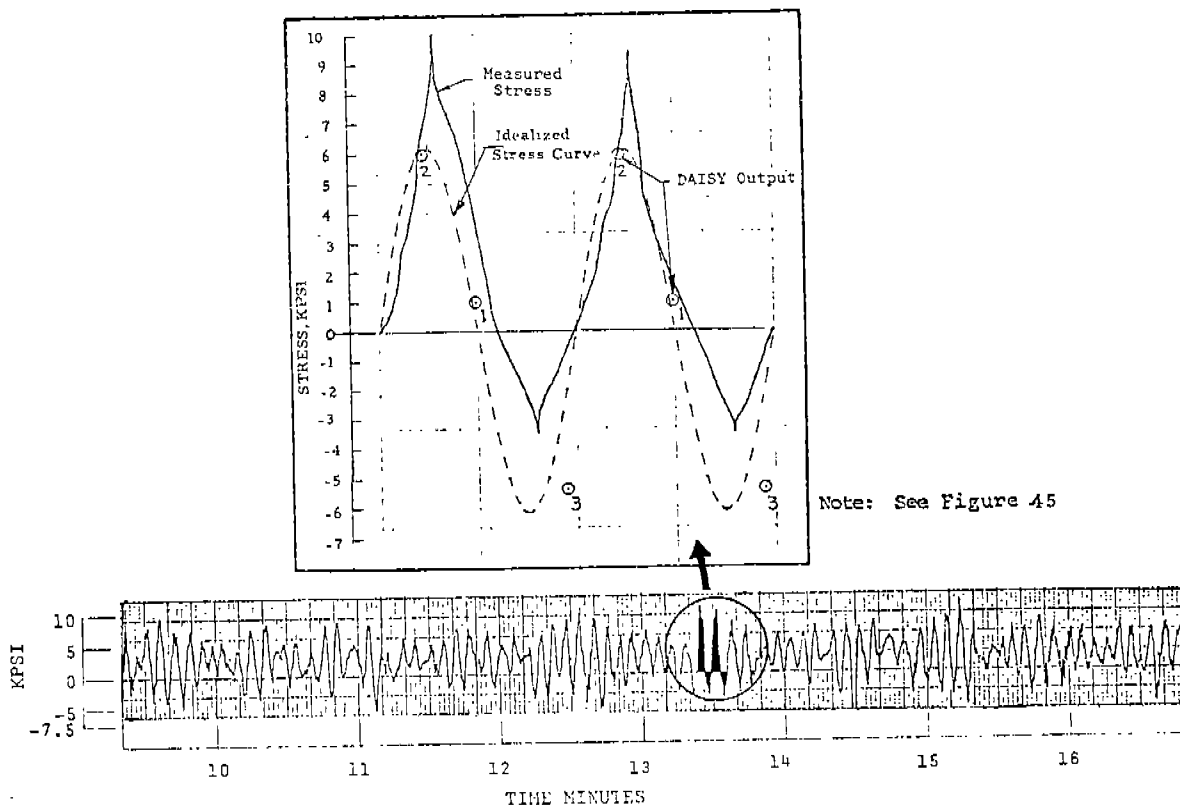LONGITUDINAL STRESSES (SENSOR AR1A), WAVE CONDITION 17

69
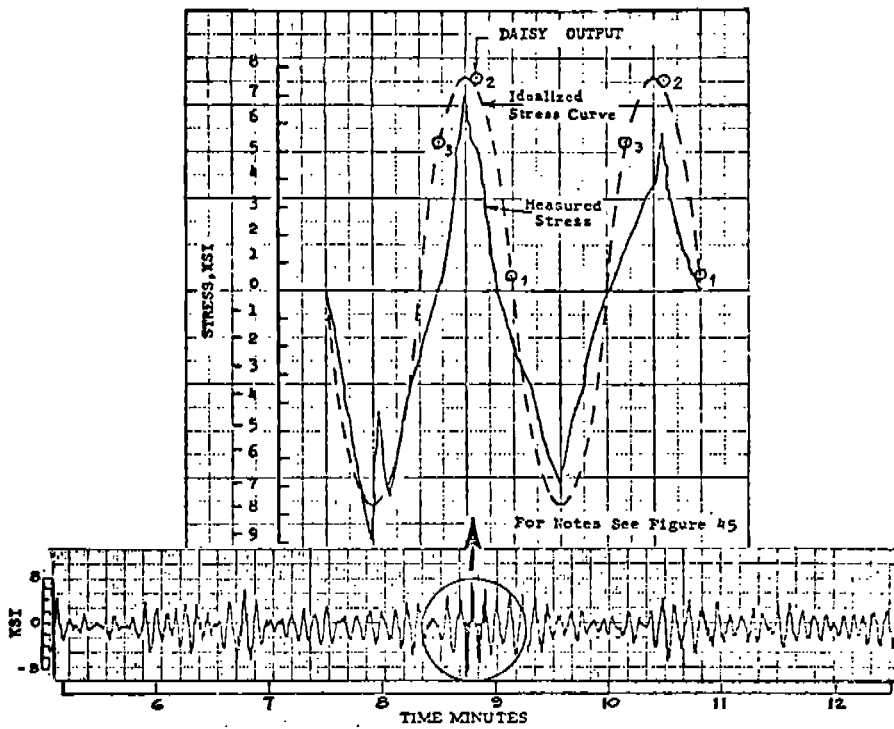
FIGURE 61 - COMPARISON OF THE CALCULATED AND MEASURED INSTANTANEOUS
LONGITUDINAL (SENSOR LSTP), WAVE CONDITION 18
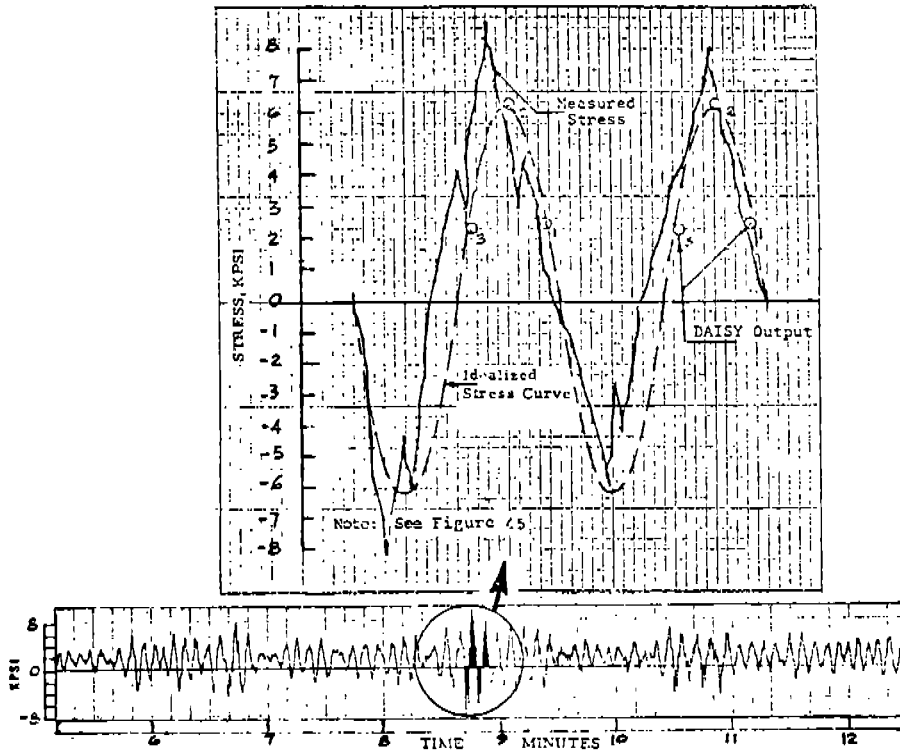
FIGURE 62 - COMPARISON OF THE CALCULATED AND MEASURED INSTANTANEOUS
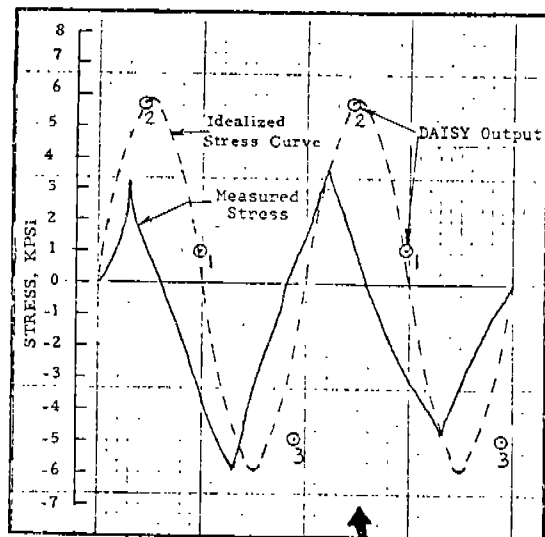LONGITUDINAL STRESSES (SENSOR LSTS), WAVE CONDITION 18
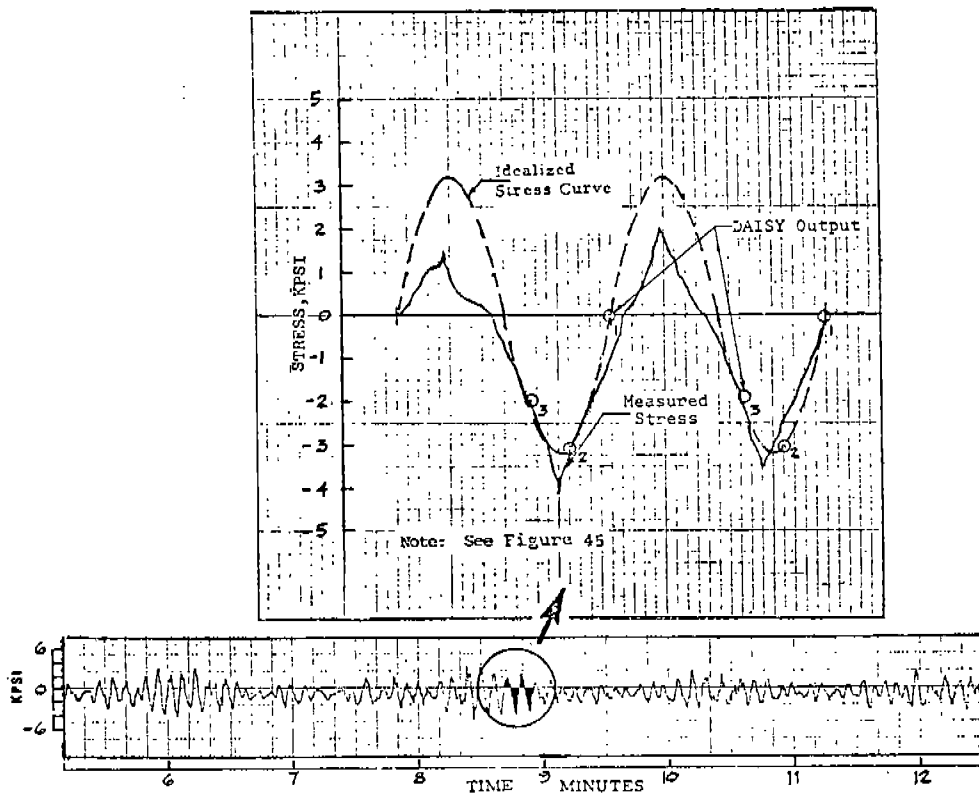
FIGURE 63 - COMPARISON OF THE CALCULATED AND MEASURED INSTANTANEOUS
LONGITUDINAL STRESSES (SENSOR LSBP), WAVE CONDITION 18

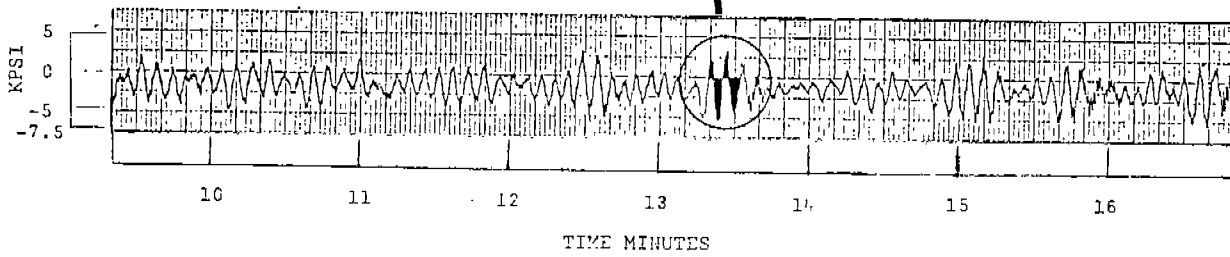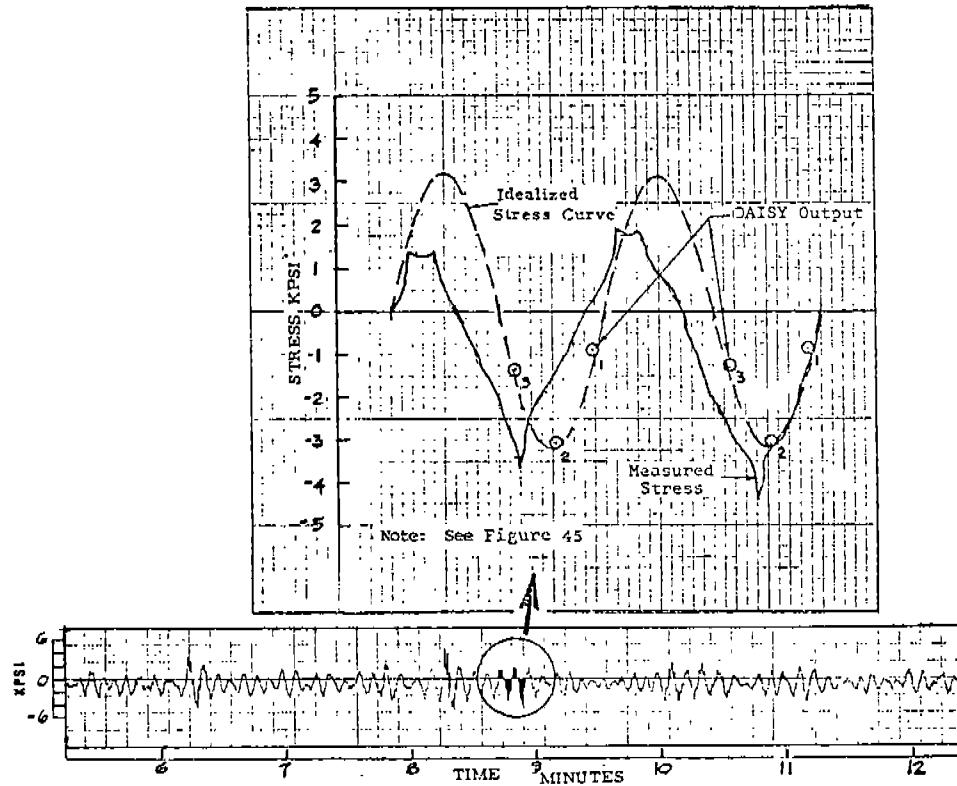FIGURE 64 - COMPARISON OF THE CALCULATED AND MEASURED INSTANTANEOUS
LONGITUDINAL STRESSES (SENSOR LSBS), WAVE CONDITION 18

71
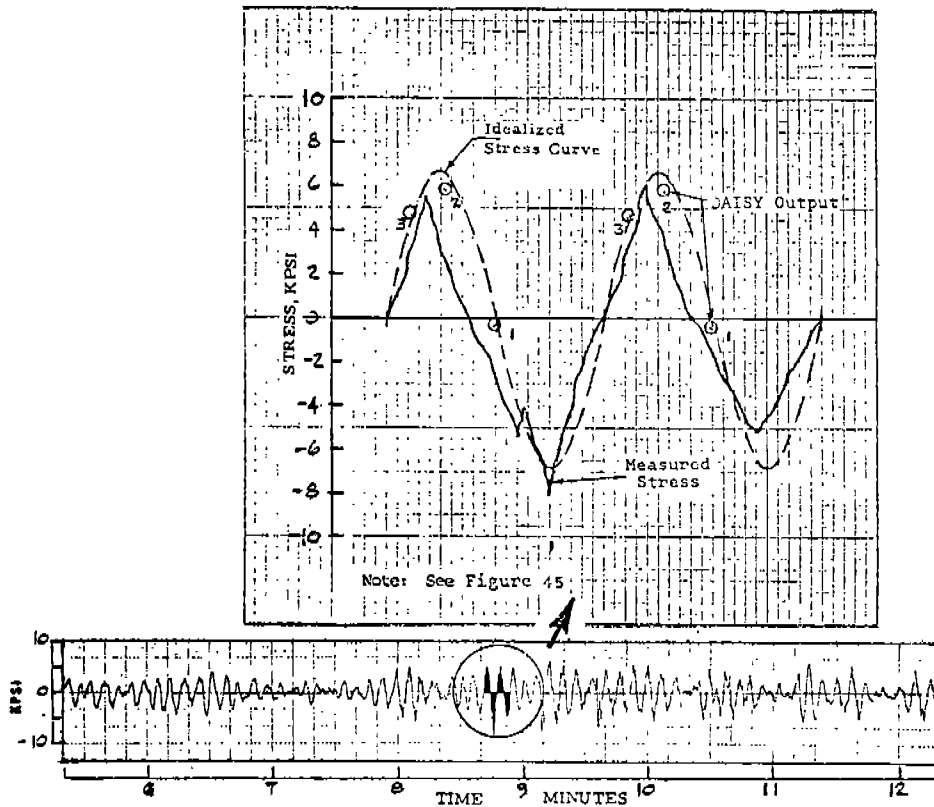
FIGURE 65 - COMPARISON OF THE CALCULATED AND MEASURED INSTANTANEOUS
LONGITUDINAL STRESSES (SENSOR AR1A), WAVE CONDITION 18
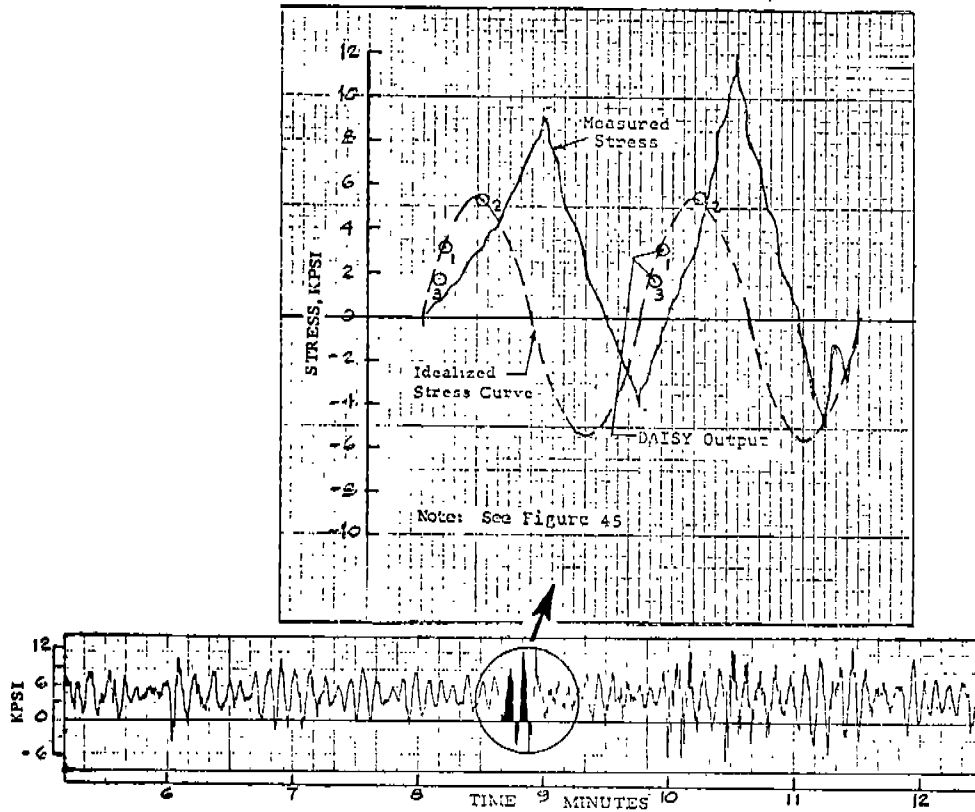
FIGURE 66 - COMPARISON OF THE CALCULATED AND MEASURED INSTANTANEOUS
LONGITUDINAL STRESSES (SENSOR AR3A), WAVE CONDITION 18

72
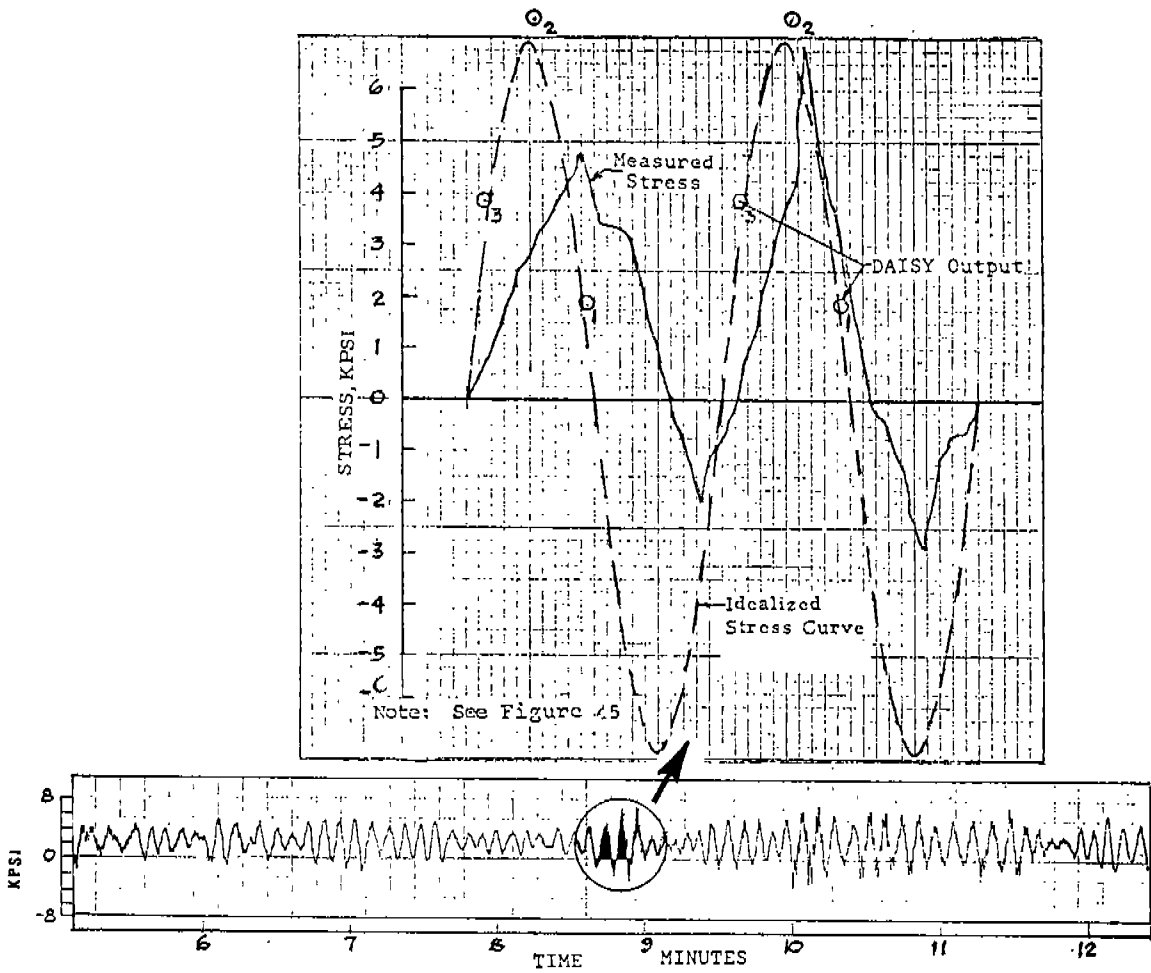
FIGURE 67 - COMPARISON OF THE CALCULATED AND MEASURED INSTANTANEOUS
LONGITUDINAL STRESSES (SENSOR AR4A), WAVE CONDITION 18

73

CALCULATED TOTAL STRESSES

In the structural analysis, a total of 46 wave-loading conditions, with wave heights up to 51.2 feet, were taken into consideration. The detailed characteristics of these wave conditions are shown in Tables 7, 9, 12, 16 and 18. To examine the overall structural responses to the various wave conditions, the fine-mesh results were scanned for stresses greater than 11,360 psi (800 kg/cm^2). Some sample selective stress outputs which exhibit the maximum values for all the wave-loading conditions are shown in Tables C1 through C5 in Appendix C. In those tables all the direct, shear, principal and Hencky-von Mises stresses are given. The printed values represent the total stresses (still-water plus wave) in kg/cm^2.

The maximum total stresses in the selected fine-mesh models which represent the most critical regions of the hull girder are generally less than 20,000 psi (1408 kg/cm^2). The only exceptions are the plate element Nos. 329, 333 and 347 of fine-mesh model 5 (Table C-4 and Figure 12), where the highest stress reaches 21,513 psi (1515 kg/cm^2). Most of the high stresses occur at the hatch corner region where the structural discontinuity causes significant stress concentration.

The strength deck of the SL-7 class containership was constructed of ABS H33 higher-strength steel. In accordance with the current ABS Rules, the permissible hull-girder bending stress for this vessel is 30,100 psi. Therefore, the highest calculated total stress, which includes stress concentration, is approximately 71% of the permissible hull-girder bending stress.

Based on these calculated stresses and the full-scale stress data measured to date, no stresses greater than the permissible limit have been found.

CONCLUSIONS

1.   The overall comparison between calculated and measured
stresses for the dockside calibration is generally inconclusive
because of significant temperature differentials during the
test and the low magnitudes of the applied loads. However,
good agreement between the calculated and measured stresses
was obtained when thermal effects were small. For future cali-
bration tests, it is recommended that complete temperature data
be recorded and that appreciable mechanical strains be generated
in the structure.

2.   The comparison of calculated and measured RMS stresses in
head seas is generally satisfactory, using both the spectrum
analysis approach and the equivalent regular wave approach. The
correlation using the former approach which takes into account
the variation in response to different wave frequencies, shows
better agreement than that obtained from the latter approach.
However, it should be noted that the spectrum analysis approach
is valid only near the midship section where the wave-induced
stresses are generally in direct proportion to wave heights.

3.   The agreement of calculated and measured instantaneous
stresses in head seas is generally good; the calculated stress
amplitudes agree well with the mean values of the measured
stresses over a time-span of two complete encounter cycles.

4.   The agreement of calculated and measured instantaneous
stresses in oblique seas is also generally good for the wave
conditions considered.

5.   Based on the results obtained from this project, it can be
concluded that the existing analytical tools for predicting wave
loads and structural responses are suitable to assess the overall
strength of the hull girder. All the measured stress data reduced
to date from the SL-7 instrumentation program and all the calcula-
ted hull-girder stresses from the present study were found to be
of low magnitude. Consequently, no modifications to the present
hull girder strength standard are deemed necessary.

6.   Regarding the structural responses, the ABS/DAISY system in
its present form is considered satisfactory for performing static
analyses for either quasi-static or dynamic loads.

7.   In order to assess the strength of local structures and also
to improve the current methodology, further research is deemed
necessary to improve the calculation method for external pressures
(possibly verified by model experiments) and to improve the ship
motion program (SCORES) to account for three-dimensional effects
and possibly for non-linear effects with respect to wave heights.

REFERENCES

1. Siekierka, W.J., Johnson, R.A., and Loosmore, C.S., "SL-7 Instrumentation Program Background and Research Plan", Ship Structure Committee Report SSC-257, 1976.

2. Fain, R.A., "Design and Installation of a Ship Response Instrumentation System Aboard the SL-7 Class Containership S.S. Sea-Land McLean", Ship Structure Committee Report SSC-238, 1974.

3. Elbatouti, A.M., Liu, D., and Jan, H.Y., "Structural Analysis of SL-7 Containership under Combined Loading of Vertical, Lateral and Torsional Moments Using Finite Element Techniques", Ship Structure Committee Report SSC-243, 1974.

4. American Bureau of Shipping, "ABS/DAISY System of Computer Programs for Ship Structural Analysis", 1975.

5. Webster, W.C. and Payer, H.G., "Structural Tests of SL-7 Ship Model", Ship Structure Committee Report SSC-269, 1977.

6. Boentgen, R.R. and Wheaton, J.W., "Static Structural Calibration of Ship Response Instrumentation System Aboard the Sea-Land McLean", Ship Structure Committee Report SSC-263, 1976.

7. Wheaton, J.W. and Boentgen, R.R., "Ship Response Instrumentation Aboard the SL-7 Containership S.S. Sea-Land McLean", Results from the First, Second and Third Operational Seasons in North Atlantic Service, Teledyne Materials Research Technical Reports TR-1559 (f), 1973: TR-1559 (j), 1975: and TR-2058 (d), 1975.

8. Dalzell, J.F., "Correlation and Verification of Wave Meter Data from the SL-7", Davidson Laboratory Report Nos. SIT-DL-77-1931, 1933 and 1934, January and February 1977.

9. Elbatouti, A.M., Jan, H.Y. and Stiansen, S.G., "Structural Analysis of a Containership Steel Model and Comparison with the Test Results", SNAME Transactions, 1976.

10. Raff, A.I., "Program SCORES - Ship Structural Response in Waves", Ship Structure Committee Report SSC-230, 1972.

11. Dalzell, J.F. and Chiocco, M.J., "Wave Loads in a Model of the SL-7 Containership Running at Oblique Headings in Regular Waves", Ship Structure Committee Report SSC-239, 1974.

12. Kaplan, P., Sargent, T.A., and Cilmi, J., "Theoretical Estimates of Wave Loads on the SL-7 Containership in Regular and Irregular Seas", Ship Structure Committee Report SSC-246, 1974.

13. Kaplan, P., Sargent, T.A. and Silbert, M., "A Correlation Study of SL-7 Containership Loads and Motions - Model Test and Computer Simulation", Ship Structure Committee Report SSC-271, 1977.

ACKNOWLEDGEMENT

The primary components of the DAISY computer program system are the preprocessor programs, the DAISY finite element program itself and the postprocessor programs. The flow chart of the system is shown in Figure A-1.

Preprocessor System

Seven principal computer programs form the nucleus of the three-dimensional ship structure preprocessing system. Each program performs a specific function and is used in a particular sequence so that the output of one program can be used as input to another. The seven programs are listed below in the order of their use:

1. SHIPMOM (SHIP MOMENT) calculates hull-girder shear forces, bending moments and vertical deflections for a vessel in still water or statically poised on a wave.

   With the vessel's hull geometry and a description of lightship weight and cargo weights as inputs, the equilibrium draft and trim are calculated for a ship in a still-water condition or in any sinusoidal or trochoidal wave. The sinusoidal waves are directly applicable to ship dynamics and their effect on the static response of the vessel differs very little from that of the trochoidal waves traditionally used. The program calculates quasi-static lateral bending moments and torsional moments if the vessel is poised in an oblique wave. Computer line plots of the shear force diagrams, bending moment diagrams and deflections are automatically generated.

2. SHIPMOTION (ABS version of SCORES program) based upon the two-dimensional ship theory for six degrees of freedom predicts a vessel's motions (velocity and acceleration) in a seaway, longitudinal and lateral wave-induced bending moments and shear forces, as well as torsional moments due to waves. The seaway can be regular sinusoidal waves, irregular long-crested waves, or regular and irregular short-crested seas. The sea condition can also be represented by measured wave data. The program computes the ship motions and the dynamic components of bending moment and shear force resulting from the sea state chosen, as well as long-term values, using probability theory based on the intended service of the vessel. A sample comparison of the RAO for the vertical and lateral bending moments with model experimental data are shown in Figures A-2 and A-3.

3. DYNPRE (DYNAMIC PRESSURE) converts the data generated by SHIPMOTION into dynamic load inputs to the DAISY finite element program. DYNPRE converts the hydrodynamic pressure distribution generated by SHIPMOTION into a pressure distribution at the nodal points of the finite element structural model and modifies the pressures to compensate for certain discrepancies in the SHIPMOTION hydrodynamic pressure calculation.

4. EXAM generates the ship structural finite element model for either a portion of or for the entire hull structure. Basic data generated by the program consists of nodal points and loadings applied to the elements and nodes. The program can generate a finite element model of any type of vessel.

   With the vessel's hull geometry finite element nodal point locations are generated with a minimum of user input. Structural properties of bending or membrane plates, beams and/or rod members are input in a convenient tabular form from which the program automatically generates appropriate elements to represent the ship structure. The elements are generated and connected in a way that minimizes the bandwidth of the structural stiffness matrix.

   EXAM automatically calculates the symmetric and anti-symmetric components of a general seaway loading. Loads in the form of pressure heads are automatically calculated and applied to the elements according to the vessel's hydrostatic cargo and sea loadings described in SHIPMOM. The user also has the capability to input additional loads on elements and nodes.

5. EXPLOT (EXAM PLOT) provides plots of the finite element structural model generated by EXAM. The plots are isometric or two-dimensional projections. They can indicate nodal points, elements and freedom patterns. Plots of any or all of the structural portions of the vessel can be made.

6. LOADER calculates the statically consistent nodal point loads from the element pressures provided by EXAM and from the structure's own weight. Additional dynamic forces due to ship motion are calculated within the program. LOADER also calculates the out-of-balance forces for all loading conditions, and

the coefficients necessary to compute a set of pseudo-inertia forces necessary to balance the structural model. The out-of-balance forces are small in magnitude, since the vessel has been balanced in SHIPMOM, but some small re-balancing is needed to avoid artificial reaction forces from developing at the points of rigid body support.

LOADER also takes the EXAM output and rearranges it in a manner suitable for input to the DAISY program.

7. CATCH edits the data, allowing the user to make modifications to the LOADER output before input into the DAISY program. The user is able to make changes to any previously defined input data by means of additional deletions or modifications.

DAISY

DAISY (Displacement Automated Integrated SYstem) is a general purpose program which performs linear elastic structural analyses of two- or three-dimensional structures of almost any degree of complexity under statically applied generalized forces and thermal loads.

The DAISY program has a library of fourteen elements which can be divided into six categories: bars, beams, membrane plates, bending plates, solids and substructures.

Some special features of DAISY are:

1. Inputs to DAISY can be in standard fixed formats or in any format desired by the user. The user may also interface his own preprocessor and postprocessor programs with DAISY.

2. Intermediate results such as element stiffnesses, assembled stiffness matrices and loads, can be output on magnetic tape or disk file. Similarly, computed results such as displacements and stresses can be output on magnetic tape or disk file for further processing.

3. DAISY automatically generates the total number of degrees of freedom at each nodal point, exclusive of rigid body supports, based on the elements connected at each node.

4. DAISY is capable of generating planes of symmetry and/or antisymmetry.

A-3

5. DAISY has a RESTART capability designed to break down long computations into a series of shorter runs.

POSTPROCESSOR SYSTEM

The standard postprocessor system consists of DAISYOUT, a general purpose output program which prints the results calculated by DAISY with the selective output of element stresses and strains, and DAISYPLOT, which produces plots of nodal displacements and stress contours. The output data file produced by DAISY may print all or part of the results. Selective output may be printed listing all elements which are stressed above certain user-prescribed limits. Normal stresses, shear stresses and stress concentrations (Hencky-von Mises stresses) are calculated and printed.

HULL GEOMETRY   MODEL   MODEL   MODEL   DATA
& LOAD DATA   GENERATION   PLOT   LOADING   MODIFICATION   ANALYSIS

```
┌──────────┐      ┌──────┐          ┌────────┐                      ┌───────┐
│ SHIPMOM  │─────▶│ EXAM │─────▶────▶│ LOADER │──────▶────────▶─────│ DAISY │
└──────────┘      └──────┘    │     └────────┘          ▲           └───────┘
      │                       ▼          ▲              │              │    │
      ▼                  ┌─────────┐     │        ┌──────────┐         ▼    ▼
┌──────────────┐         │ EXPLOT  │     │        │  CATCH   │   ┌─────────┐ ┌──────────┐
│  SHIPMOTION  │         └─────────┘     │        └──────────┘   │DAISYOUT │ │DAISYPLOT │
└──────────────┘                         │                       └─────────┘ └──────────┘
      │                                  │
      ▼                                  │
┌──────────┐                             │
│  DYNPRE  │                             │
└──────────┘                             │
      │                                  │
      └──────────────────────────────────┘
```
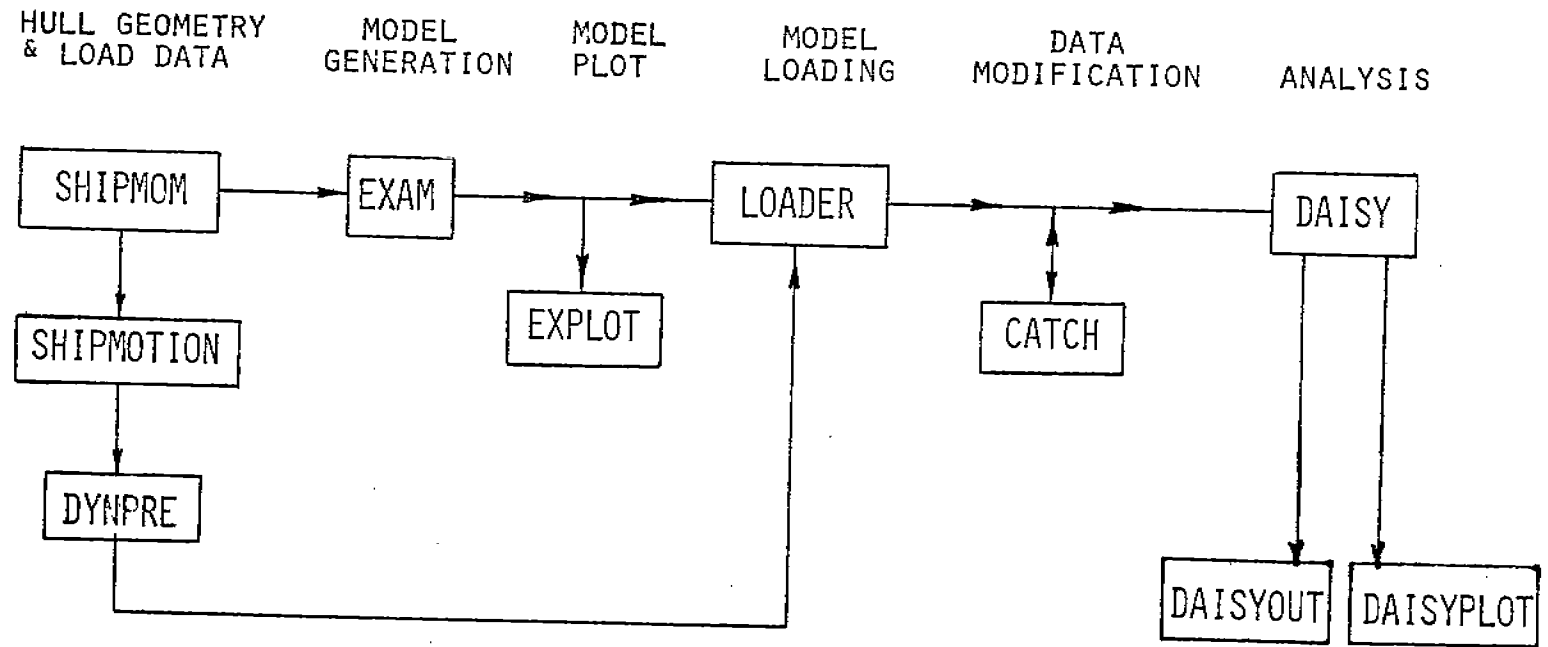
FIGURE A-1   FLOW CHART OF ABS/DAISY FINITE ELEMENT
STRUCTURAL ANALYSIS SYSTEM

○   25 Kt. Heavy Displacement
♂   30 Kt. Heavy Displacement
△   25 Kt. Light Displacement
⧊   30 Kt. Light Displacement

Calculated Results:

———— ABS/SHIPMOTION ⎫ 25 Kt. Loading Condition 1
— — — Oceanics ⎭ (Near Light Displacement)

VERTICAL MOMENT AMPLITUDE, $\frac{ft.-tons}{ft.}$ / WAVE AMPLITUDE

50,000

40,000

30,000

20,000

10,000

.2   .4   .6   .8   1.0   1.2   1.4   1.6   1.8   2.0

WAVE LENGTH/SHIP LENGTH

FIGURE A-2   RAO OF MIDSHIP VERTICAL WAVE BENDING MOMENTS 180° HEADING

Model test data (From Reference [11])

○   25 Kt. Heavy Displacement
♂   30 Kt. Heavy Displacement
△   25 Kt. Light Displacement
⧊   30 Kt. Light Displacement

Calculated Results:

———— ABS/SHIPMOTION ⎫ 25 Kt. Loading Condition 1
— — — Oceanics ⎭ (Near Light Displacement)

LATERAL MOMENT AMPLITUDE, $\frac{ft.-tons}{ft.}$ / WAVE AMPLITUDE

50,000

40,000

30,000

20,000

10,000

.2   .4   .6   .8   1.0   1.2   1.4   1.6   1.8   2.0

WAVE LENGTH/SHIP LENGTH
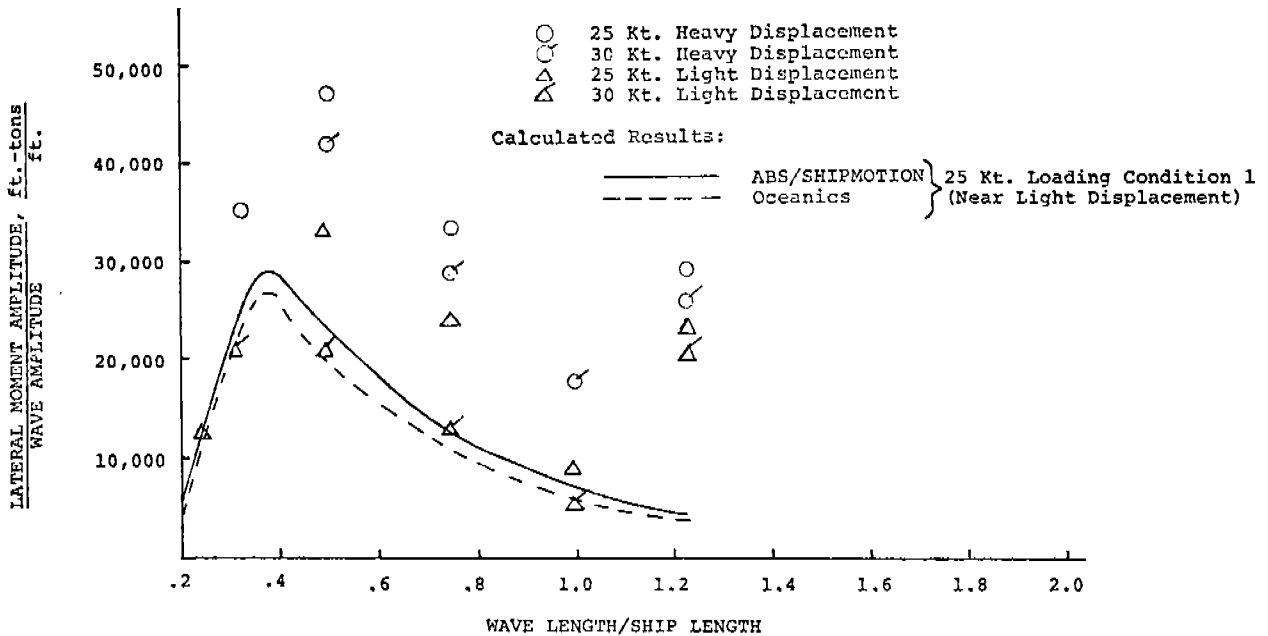
FIGURE A-3   RAO OF MIDSHIP LATERAL WAVE BENDING MOMENTS 60° HEADING

A-6

APPENDIX B - STRAIN GAGE SENSORS INSTALLED ON THE SL-7
CONTAINERSHIP
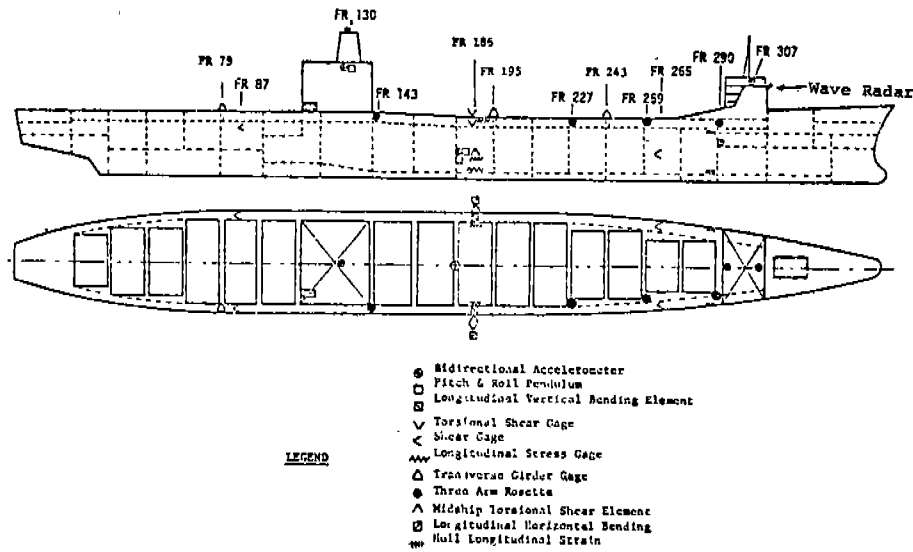
FIGURE B-1   GENERAL SENSORS LAYOUT (FROM REFERENCE [6])

FRAME 186^1/4 (FM 1)

FRAME 194-195 1/2(FM 2)

FRAME 186^1/4 (FM 3)

FRAME 226-227 (FM 4)

FRAME 143 (FM 5)

FRAME 290 (FM 6)
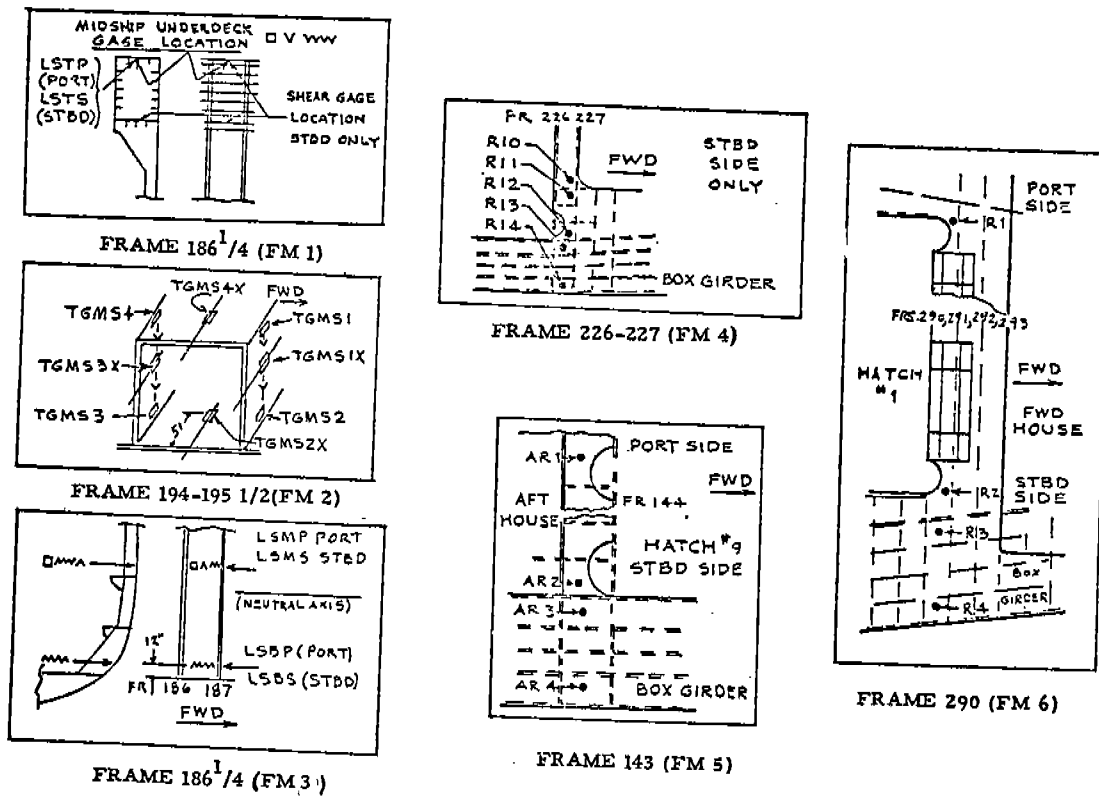
FIGURE B-2   DETAILS OF STRAIN GAGE LAYOUT
(FROM REFERENCE [2])

TABLE B-1   (FROM REFERENCE [6])

TABLE X

SENSOR LIST

72/73 Season and Calibration

Sensor No.	Sensor Nom.	Location (2)		Config.	Orient	Sensitive to	Recorder	Channel	Mode	Full Cal	Units	Circuit No.
		Frame	Position									
1 (1)	LVB	$186\frac{1}{4}$	Tunnel Tops	Dyadic	Long.	V. Bend.	1	1	-	8214	PSI	1
2	TSX	$186\frac{1}{4}$	Side N/A	Shear	Vert.	H.T. Shear	1	2	-	4991	PSI	3
3	Wave Ht.	300	Fwd Deckhouse (Stbd)	Radar	Angled	Range(3)	1	3	-	3.6	Volt	-
4	Roll	178	26" Fwd 31' ATT	Pend.	Trans.	Roll	1	4	-	20	Deg.	-
5	Pitch	178	26" Fwd 31' ATT	Pend.	Long.	Pitch	1	5	-	20	Deg.	-
6	MAV	178	23" Fwd 31' ATT	Mass	Vert.	V. Accel.	1	6	-	1	g	-
7	MAT	178	23" Fwd 31' ATT	Mass	Trans.	T. Accel.	1	7	-	1	g	-
8	FAV	290	14" Fwd 59' ATT	Mass	Vert.	V. Accel.	1	8	-	1	g	-
9	FAT	290	14" Fwd 59' ATT	Mass	Trans.	T. Accel.	1	9	-	1	g	-
10	Op Para.	-	RPM, Rud, Wind S&D	Multiplex	-	Transmitters	1	10	-	3.6	Volt	-
11	LHB	$186\frac{1}{4}$	Side NA	Dyadic	Long.	H. Bend	1	11	-	8214	PSI	2
12	SFP	265	P Side 32' ATT	Shear	Vert.	Shear	1	12	-	5000	PSI	4
13	SFS	265	S Side 32' ATT	Shear	Vert.	Shear	1	13	-	5000	PSI	4
14 (1)	LVB						2	1	A			
15	LSTS	186	S Tunnel Top	Dyadic	Long.	N. Stress	2	2	A	8240	PSI	5
16	LSYS	186	S Side N.A.	Dyadic	Long.	N. Stress	2	3	A	8240	PSI	5
17	LSBS	186	S Side Bottom	Dyadic	Long.	N. Stress	2	4	A	8240	PSI	5
18	LSTP	186	P Tunnel Top	Dyadic	Long.	N. Stress	2	5	A	8240	PSI	5
19	LSYP	186	P Side NA	Dyadic	Long.	N. Stress	2	6	A	8240	PSI	5
20	LSBP	186	P Side Bottom	Dyadic	Long.	N. Stress	2	7	A	8240	PSI	5
21	SAP	87	P Side 26' ATT	Shear	Vert.	Shear	2	8	A	5000	PSI	4
22	SAS	87	S Side 26' ATT	Shear	Vert.	Shear	2	9	A	5000	PSI	4

TABLE B-1 (CONT'D)

SENSOR LIST

72/73 Sensor and Calibration

Sensor No.	Sensor Nom.	Location (2) Frame	Location (2) Position	Config.	Orient	Sensitive to	Recorder	Channel	Mode	Full Cal	Units	Circuit No.
23	FDLV	307	Level 04 CL	Mass	Vert.	V. Accel.	2	10	A	+1 (4)	g	-
24	FDHT	307	Level 04 CL	Mass	Trans.	T. Accel.	2	11	A	+1	g	-
25	ADHL	130	Level 05 1" P	Mass	Long.	L. Accel.	2	10 (a)	A	+1	g	-
26	ADHT	130	Level 05 1" P	Mass	Trans	T. Accel.	2	11 (a)	A	+1	g	-
27	BGST	$186\frac{1}{4}$	S Tunnel Top	Shear	Long.	Shear	2	12	A	5000	PSI	4
28	BGSB	$186\frac{1}{4}$	S Tunnel Bot	Shear	Long.	Shear	2	13	A	5000	PSI	4
29 (1)	LVB						2	1	B			
30	AR-1A	143	Port Side Girder	Single	Long.	N. Strain	2	2	B	334.6	µ"/"	6
31	AR-1B	143	Near Deck Cutout	Single	Diag.	N. Strain	2	3	B	334.6	µ"/"	6
32	AR-1C	143	Under Deck	Single	Trans.	N. Strain	2	4	B	334.6	µ"/"	6
33	AR-2A	143	Stbd Side Girt.	Single	Long.	N. Strain	2	5	B	334.6	µ"/"	6
34	AR-2B	143	Near Deck Cutout	Single	Diag.	N. Strain	2	6	B	334.6	µ"/"	6
35	AR-2C	143	Under Deck	Single	Trans.	N. Strain	2	7	B	334.6	µ"/"	6
36	AR-3A	143	Stbd Tunnel	Single	Long.	N. Strain	2	8	B	334.6	µ"/"	6
37	AR-3B	143.	In Board	Single	Diag.	N. Strain	2	9	B	334.6	µ"/"	6
38	AR-3C	143	Under Deck	Single	Trans.	N. Strain	2	10	B	334.6	µ"/"	6
39	AR-4A	143	Stbd Tunnel	Single	Long.	N. Strain	2	11	B	334.6	µ"/"	6
40	AR-4B	143	Out Board	Single	Diag.	N. Strain	2	12	B	334.6	µ"/"	6
41	AR-4C	.143	Under Deck	Single	Trans.	N. Strain	2	13	B	334.6	µ"/"	6

TABLE B-1 (CONT'D)

SENSOR LIST

72/73 Season and Calibration

Sensor No.	Sensor Nom.	Location(2) Frame	Location(2) Position	Config.	Orient	Sensitive to	Recorder	Channel	Mode	Full Cal	Units	Circuit No.
42 (1)	LVB			·			2	1	C			6
43	R1A	291	Port Side Gird	Single	Long.	N. Strain	2	2-13	C	334.6	μ"/"	6
44	P1B	291	Near Deck Cutout	Single	Diag.	N. Strain	2	VIA	C	334.6	μ"/"	6
45	P1C	291	Under Deck	Single	Trans.	N. Strain	2	RSB	C	334.6	μ"/"	6
46	R2A	291	Stbd Side Gird	Single	Long.	N. Strain	2	2-13	C	334.6	μ"/"	6
47	R2B	291	Near Deck Cutout	Single	Diag.	N. Strain	2	VIA	C	334.6	μ"/"	6
48	R3C	291	Under Deck	Single	Trans.	N. Strain	2	RSB	C	334.6	μ"/"	6
49	R3A	291	Stbd Tunnel	Single	Long.	N. Strain	2	2-13	C	334.6	μ"/"	6
50	R3B	291	In Board	Single	Diag.	N. Strain	2	VIA	C	334.6	μ"/"	6
51	R3C	291	Under Deck	Single	Trans.	N. Strain	2	RSB	C	334.6	μ"/"	6
52	R4A	291	Stbd Tunnel	Single	Long.	N. Strain	2	2-13	C	334.6	μ"/"	6
53	R4B	291	Out Board	Single	Diag.	N. Strain	2	VIA	C	334.6	μ"/"	6
54	R4C	291	Under Deck	Single	Trans.	N. Strain	2	RSB	C	334.6	μ"/"	6
55	R5A	258	Stbd Side Gird	Single	Long.	N. Strain	2	2-13	C	334.6	μ"/"	6
56	R5B	258	In Corn. Hat 2	Single	Diag.	N. Strain	2	VIA	C	334.6	μ"/"	6
57	R5C	258	Under Deck	Single	Trans.	N. Strain	2	RSB	C	334.6	μ"/"	6
58	R6A	258	Stbd Side Gird	Single	Long.	N. Strain	2	2-13	C	334.6	μ"/"	6
59	R6B	258	Out Corn. Hat 2	Single	Diag.	N. Strain	2	VIA	C	334.6	μ"/"	6
60	R6C	258	Under Deck	Single	Trans.	N. Strain	2	RSB	C	334.6	μ"/"	6
61	R7A	258	Stbd Side Gird	Single	Long.	N. Strain	2	2-13	C	334.6	μ"/"	6
62	R7B	258	Near Deck Cutout	Single	Diag.	N. Strain	2	VIA	G	334.6	μ"/"	6
63	R7C	258	Under Deck	Single	Trans.	N. Strain	2	RSB	C	334.6	μ"/"	6
64	R8A	258	Stbd Tunnel	Single	Long.	N. Strain	2	2-13	C	334.6	μ"/"	6
65	R8B	258	In Board	Single	Diag.	N. Strain	2	VIA	C	334.6	μ"/"	6
66	R8C	258	Under Deck	Single	Trans.	N. Strain	2	RSB	C	334.6	μ"/"	6

TABLE B-1   (CONT'D)

SENSOR LIST
72/73 Season and Calibration

Sensor No.	Sensor Nom.	Frame	Position	Config.	Orient	Sensitive to	Recorder	Channel	Mode	Full Cal	Units	Circ No
67	R9A	258	Stbd Tunnel	Single	Long.	N. Strain	2	2-13	C	334.6	µ"/"	6
68	R9B	258	Out Board	Single	Diag.	N. Strain	2	VIA	C	334.6	µ"/"	6
69	R9C	258	Under Deck	Single	Trans.	N. Strain	2	RSB	C	334.6	µ"/"	6
70	R10A	226	Stbd Side Gird	Single	Long.	N. Strain	2	2-13	C	334.6	µ"/"	6
71	R10B	226	In Corn. Hat 4	Single	Diag.	N. Strain	2	VIA	C	334.6	µ"/"	6
72	R10C	226	Under Deck	Single	Trans.	N. Strain	2	RSB	C	334.6	µ"/"	6
73	R11A	226	Stbd Side Gird	Single	Long.	N. Strain	2	2-13	C	334.6	µ"/"	6
74	R11B	226	Out Corn Hat 4	Single	Diag.	N. Strain	2	VIA	C	334.6	µ"/"	6
75	R11C	226	Underdeck	Single	Trans.	N. Strain	2	RSB	C	334.6	µ"/"	6
76	R12A	226	Stbd Side Gird	Single	Long.	N. Strain	2	2-13	C	334.6	µ"/"	6
77	R12B	226	Near Deck Cutout	Single	Diag.	N. Strain	2	VIA	C	334.6	µ"/"	6
78	R12C	226	Underdeck	Single	Trans.	N. Strain	2	RSB	C	334.6	µ"/"	6
79	R13A	226	Stbd Tunnel	Single	Long.	N. Strain	2	2-13	C	334.6	µ"/"	6
80	R13B	226	In Board	Single	Diag.	N. Strain	2	VIA	C	334.6	µ"/"	6
81	R13C	226	Under Deck	Single	Trans.	N. Strain	2	RSB	C	334.6	µ"/"	6
82	R14A	226	Stbd Tunnel	Single	Long.	N. Strain	2	2-13	C	334.6	µ"/"	6
83	R14B	226	Out Board	Single	Diag.	N. Strain	2	VIA	C	334.6	µ"/"	6
84	R14C	226	Under Deck	Single	Trans.	N. Strain	2	RSB	C	334.6	µ"/"	6
85 (1)	LV3						2	1	D			
86	TGTS1	244	Fwd Top	Single	Trans.	N. Stress	2	2	D	10038	PSI	6

TABLE B-1 (CONT'D)

SENSOR LIST

72/73 Season and Calibration

Sensor No.	Sensor Nom.	Location (2)		Config.	Orient	Sensitive to	Recorder	Channel	Mode	Full Cal
		Frame	Position							
87	HLSST	289	S Side 1' BT	Single	Long.	N. Stress	2	2 (a)	D	10038
83	TGFS2	244	Fwd Bot.	Single	Trans.	N. Stress	2	3	D	10038
89	HLSSB	289	S Side 1' ATT	Single	Long.	N. Stress	2	3 (a)	D	10038
90	TGFS3	242	Aft Bot	Single	Trans.	N. Stress	2	4	D	10038
91	HLSPT	289	P Side 1' BT	Single	Long.	N. Stress	2	4 (a)	D	10038
92	TGFS4	242	Aft Top	Single	Trans.	N. Stress	2	5	D	10038
93	HLSPB	289	P Side 1' ATT	Single	Long.	N. Stress	2	5 (a)	D	10038
94	TGMS1	196	Fwd Gird. Top	Single	Trans.	N. Stress	2	6	D	10038
95	TGMS2	196	Fwd Gird Bot.	Single	Trans.	N. Stress	2	7	D	10038
96	TGMS3	194	Aft Gird Bot.	Single	Trans.	N. Stress	2	8	D	10038
97	TGMS4	194	Aft Gird Top	Single	Trans.	N. Stress	2	9	D	10038
98	TGMS1X	194	Fwd Gird Mid	Single	Trans.	N. Stress	2	6 (a)	D	10038
99	TGMS2X	195	Bot Gird Mid	Single	Trans.	N. Stress	2	7 (a)	D	10038
100	TGMS3X	194	Aft Gird Mid	Single	Trans.	N. Stress	2	8 (a)	D	10038
101	TGMS4X	195	Top Gird Mid	Single	Trans.	N. Stress	2	9 (a)	D	10030
102	TGSS1X	196	Fwd Gir Q Top	Shear	Trans.	Shear	2	6 (a)	D	5000
103	TGSS2X	196	Fwd Gir Q Bot	Shear	Trans.	Shear	2	7 (a)	D	5000
104	TGSS3X	194	Aft Gir Q Bot	Shear	Trans.	Shear	2	8 (a)	D	5000
105	TGSS4X	194	Aft Gir Q Top	Shear	Trans.	Shear	2	9 (a)	D	5000
106	TGAS1	80	Fwd Top	Single	Trans.	N. Stress	2	10	D	10038
107	TGAS2	80	Fwd Bot	Single	Trans.	N. Stress	2	11	D	10038
108	TGAS3	78	Aft Bot	Single	Trans.	N. Stress	2	12	D	10038
109	TGAS4	78	Aft Top	Single	Trans.	N. Stress	2	13	D	10038

TABLE C-1   FINE MESH #1, PORT.

SELECTIVE STRESS OUTPUT FOR LOAD CASE 17
****

ELEM NO	CORNER POINTS 1ST 2ND 3RD 4TH	L.C.	TOP BOT	SIGMA X	SIGMA Y	SIGMA Z	TAU	SIGMA 1	SIGMA 2	TAU MAX	HENCKY-VON MIS.STRESS	ANG S [d] .....

STRESSES IN QUADRILATERAL BENDING PLATE (QUAB4 ELM)

ELEM NO	CORNER POINTS 1ST 2ND 3RD 4TH	L.C.	TOP BOT	SIGMA X	SIGMA Y	SIGMA Z	TAU	SIGMA 1	SIGMA 2	TAU MAX	HENCKY-VON MIS.STRESS	ANG S
416	[a] 1999 1998 2098 2099	17	T	99.8	871.8	0.0	-68.7	877.9	93.7	392.1	834.9	LCL X-85 [b]
			B	53.3	944.9	0.0	-68.8	950.2	48.0	451.1	927.1	-85
417	2000 1999 2099 2100	17	T	30.9	1038.8	0.0	-65.2	1043.0	26.7	508.2	1029.9	LCL X-86
			B	60.9	1069.6	0.0	-107.9	1081.1	49.5	515.8	1057.2	-84
422	1980 2000 2100 2080	17	T	0.0	-31.2	968.4	-56.4	971.6	-34.3	503.0	989.2	GLB Y-86
			B	0.0	90.6	985.0	-92.4	994.4	81.2	456.6	956.4	-84
423	2086 2096 1996 1986	17	T	0.0	-140.1	997.0	1.1	997.0	-140.1	560.5	1073.9	GLB Y 89 [c]
			B	0.0	181.6	1090.3	-5.0	1090.4	181.6	454.4	1011.9	-89

STRESSES IN BENDING TRIANGULAR PLATES (TRIB3 ELM)

ELEM NO	CORNER POINTS 1ST 2ND 3RD	L.C.	TOP BOT	SIGMA X	SIGMA Y	SIGMA Z	TAU	SIGMA 1	SIGMA 2	TAU MAX	HENCKY-VON MIS.STRESS	ANG S
430	1986 2076 2086	17	T	0.0	-20.0	958.6	-0.8	958.6	-20.0	489.3	968.7	GLB Y-90
			B	0.0	-18.2	955.6	-5.4	955.6	-18.2	486.9	964.8	-89
431	1996 2096 2081	17	T	0.0	-86.8	1087.3	-5.8	1087.3	-86.9	587.1	1133.3	GLB Y-89
			B	0.0	-51.0	1091.6	-32.3	1092.5	-51.9	572.2	1119.3	-88

STRESSES IN QUADRILATERAL BENDING PLATE (QUAB4 ELM)

ELEM NO	CORNER POINTS 1ST 2ND 3RD 4TH	L.C.	TOP BOT	SIGMA X	SIGMA Y	SIGMA Z	TAU	SIGMA 1	SIGMA 2	TAU MAX	HENCKY-VON MIS.STRESS	ANG S
432	2026 2036 2037 2027	17	T	22.0	-213.2	0.0	515.3	433.0	-624.2	528.6	920.5	GLB X 38
			B	57.4	-200.2	0.0	511.3	455.8	-598.7	527.3	916.0	37
439	2059 2069 2070 2060	17	T	244.8	-115.3	0.0	445.5	545.2	-415.6	480.5	834.8	GLB X 34
			B	275.4	-119.4	0.0	440.0	560.3	-404.3	482.3	839.0	32
440	2066 2076 2048 2067	17	T	685.3	-75.2	0.0	-583.9	1001.8	-391.7	696.8	1244.8	GLB X-28
			B	719.9	-12.7	0.0	-589.1	1047.3	-340.1	693.7	1252.5	-29
441	2069 2068 2080 2070	17	T	667.5	64.2	0.0	593.6	1031.7	-300.0	665.8	1209.9	GLB X 31
			B	706.5	101.6	0.0	593.7	1070.3	-262.2	666.3	1222.7	31
457	2097 2096 2196 2197	17	T	102.4	1026.5	0.0	-27.3	1027.3	101.6	462.8	980.5	LCL X-88
			B	44.1	1007.3	0.0	-46.7	1009.5	41.8	483.9	989.3	-87
458	2098 2097 2197 2198	17	T	77.0	853.3	0.0	-31.1	854.5	75.8	389.4	819.3	LCL X-87
			B	66.9	929.0	0.0	-38.4	930.7	65.2	432.8	899.9	-87
459	2099 2098 2198 2199	17	T	98.0	864.3	0.0	-59.7	868.9	93.4	387.8	826.2	LCL X-85
			B	48.7	935.1	0.0	-50.4	937.9	45.8	446.1	915.9	-86

NOTES

[a] Each nodal point is represented by a four-digit number, the first two digits indicate the station number of the finite element model and the last two digits are the local nodal number.

[b] Where the local coordinate system is used, SIGMA X is the direct stress in the direction from first to second nodal point. SIGMA Y is the direct stress orthogonal with SIGMA X.

[c] Where the global coordinate system is used, SIGMA X, SIGMA Y and SIGMA Z are stress in the directions as shown in Figure 3.

[d] If the global angle is printed, the coordinate stresses are in global system. If not, they are in element local coordinate system the first line indicates stresses and angles at the top of the plate, the second line indicates the results at the plate bottom.

TABLE C-1   FINE MESH #1
(Cont'd)

SELECTIVE STRESS OUTPUT FOR LOAD CASE 53   STRESS : KG/CM**2
****

ELEM NO	1ST	2ND	3RD	4TH	L.C. DAISY	TOP BOT	SIGMA X	SIGMA Y	SIGMA Z	TAU	SIGMA 1	SIGMA 2	TAU MAX	HENCKY-VON MIS.STRESS	A

STRESSES IN QUADRILATERAL BENDING PLATE (QUAB4 ELM)

460	2100	2099	2199	2200	17	T	13.2	1022.0	0.0	-75.5	1027.6	7.6	510.0	1023.8	LCL X
						B	76.0	1061.9	0.0	-52.5	1064.7	73.2	495.7	1030.0	
465	2080	2100	2200	2180	17	T	0.0	-14.2	974.7	-122.0	909.5	-29.0	509.3	1004.3	GLB Y
						B	0.0	75.4	977.2	-170.2	1011.1	41.5	484.8	991.1	
466	2186	2196	2096	2086	17	T	0.0	-141.1	985.8	47.1	987.7	-143.1	565.4	1066.5	GLB Y
						B	0.0	170.2	1077.4	60.4	1001.4	174.1	453.6	1005.7	

STRESSES IN BENDING TRIANGULAR PLATES (TRIB3 ELM)

473	2070	2180	2080		17	T	0.0	27.1	786.5	95.3	798.3	15.4	391.5	790.7	GLB Y
						B	0.0	72.1	814.0	115.7	831.6	54.4	388.6	805.8	
476	2076	2186	2086		17	T	0.0	-21.7	950.7	72.5	956.1	-27.0	491.5	969.9	GLB Y
						B	0.0	-22.2	944.1	85.2	951.5	-29.7	490.6	966.7	
477	2096	2196	2081		17	T	0.0	-91.8	1072.0	94.7	1079.7	-99.5	589.6	1132.7	GLB Y
						B	0.0	-55.2	1076.1	125.3	1089.9	-68.9	579.4	1125.9	
485	2196	2281	2081		17	T	0.0	-38.8	1197.2	74.0	1201.6	-43.3	622.4	1223.8	GLB Y
						B	0.0	-25.6	1139.0	92.1	1146.2	-32.9	589.5	1163.0	

STRESSES IN QUADRILATERAL BENDING PLATE (QUAB4 ELM)

489	2197	2196	2296	2297	17	T	20.2	1014.9	0.0	10.0	1015.0	20.1	497.5	1005.1	LCL X
						B	28.0	1025.6	0.0	-20.2	1026.0	27.6	499.2	1012.5	
490	2198	2197	2297	2298	17	T	77.5	972.9	0.0	-29.3	973.8	76.6	448.6	937.9	LCL X
						B	25.4	952.7	0.0	-38.3	954.3	23.8	465.2	942.6	
491	2199	2198	2298	2299	17	T	104.1	993.2	0.0	-67.0	998.3	99.1	449.6	952.6	LCL X
						B	-9.7	945.1	0.0	-58.9	948.7	-13.3	481.0	955.5	
492	2200	2199	2299	2300	17	T	-20.9	1033.5	0.0	-113.2	1045.5	-32.9	539.2	1062.4	LCL X
						B	64.8	1053.3	0.0	-75.8	1059.1	59.1	500.0	1030.9	
497	2180	2200	2300	2280	17	T	0.0	-25.0	970.1	-102.3	980.5	-35.5	508.0	998.7	GLB Y
						B	0.0	75.8	993.8	-150.5	1017.9	51.8	483.1	993.0	
498	2286	2296	2196	2186	17	T	0.0	-140.0	969.3	45.0	971.2	-141.8	556.5	1049.3	GLB Y
						B	0.0	125.6	1036.9	58.8	1040.7	121.8	459.4	985.4	

TABLE C-1   FINE MESH #1
(Cont'd)

SELECTIVE STRESS OUTPUT FOR LOAD CASE 53
***************************************   STRESS : KG/CM**2

ELEM NO	CORNER POINTS 1ST	2ND	3RD	4TH	L.C. DAISY	TOP BOT	SIGMA X	SIGMA Y	SIGMA Z	TAU	SIGMA 1	SIGMA 2	TAU MAX	HENCKY-VON MIS.STRESS	ANG ....

STRESSES IN BENDING TRIANGULAR PLATES (TRIB3 ELM)

503	2180	2270	2280		17	T	0.0	-49.8	824.0	102.0	835.8	-61.6	448.7	868.2	GLB Y 83
						B	0.0	140.7	909.7	93.5	920.9	129.5	395.7	863.5	83
505	2186	2276	2286		17	T	0.0	-12.8	940.4	30.6	941.4	-13.8	477.6	948.4	GLB Y 88
						B	0.0	28.2	956.2	51.3	959.0	25.4	466.8	946.6	86
506	2196	2296	2281		17	T	0.0	-43.7	1054.0	102.4	1063.5	-53.2	558.3	1091.1	GLB Y 84
						B	0.0	-2.8	1057.3	113.2	1069.3	-14.8	542.0	1076.7	84

STRESSES IN QUADRILATERAL BENDING PLATE (QUA84 ELM)

508	2297	2296	2396	2397	17	T	-16.6	1010.5	0.0	23.5	1011.0	-17.2	514.1	1019.7	LCL X 88
						B	13.5	1045.0	0.0	-5.1	1045.0	13.4	515.8	1038.3	-89
509	2298	2297	2397	2398	17	T	45.5	1075.1	0.0	-25.2	1075.7	44.9	515.4	1054.0	LCL X-88
						B	-53.3	1023.0	0.0	-30.8	1023.9	-54.2	539.0	1052.1	-88
510	2299	2298	2398	2399	17	T	75.8	1094.5	0.0	-71.3	1099.4	70.8	514.3	1065.8	LCL X-86
						B	-84.2	1025.9	0.0	-69.9	1030.3	-88.6	559.5	1077.3	-85
511	2300	2299	2399	2400	17	T	-62.7	1035.7	0.0	-124.7	1049.7	-76.7	563.2	1090.1	LCL X-83
						B	54.6	1100.9	0.0	-88.1	1108.3	47.3	530.5	1085.4	-85
517	2280	2300	2400	2380	17	T	0.0	-50.6	994.0	-86.9	1001.2	-57.8	529.5	1031.3	GLB Y-85
						B	0.0	72.9	1036.0	-113.3	1049.2	59.7	494.7	1020.6	-83
518	2386	2396	2296	2286	17	T	0.0	-173.3	928.5	72.5	933.2	-178.1	555.7	1033.8	GLB Y 86
						B	0.0	176.3	1078.7	44.8	1080.9	174.1	453.4	1005.2	87
525	2250	2350	2360	2260	17	T	0.0	-0.3	780.9	107.3	795.3	-14.7	405.0	802.8	GLB Y 82
						B	0.0	92.1	849.8	115.0	866.9	75.0	395.9	831.9	81
526	2240	2340	2350	2250	17	T	0.0	-31.7	712.9	108.0	728.2	-47.1	387.7	752.9	GLB Y 81
						B	0.0	130.8	798.9	107.7	815.8	113.9	351.0	765.2	81
527	2270	2370	2380	2280	17	T	0.0	-56.1	879.7	80.2	886.5	-62.9	474.7	919.6	GLB Y 85
						B	0.0	121.5	985.8	92.2	995.5	111.7	441.9	944.6	84
529	2246	2346	2356	2256	17	T	0.0	43.1	819.9	63.8	825.1	37.9	393.6	806.8	GLB Y 85
						B	0.0	-53.5	748.7	60.9	753.3	-58.1	405.7	784.0	85

TABLE C- 2   FINE MESH #3, PORT

SELECTIVE STRESS OUTPUT FOR LOAD CASE 53
***********************************✶✶✶✶✶✶

STRESS : KG/CM**2

ELEM NO	1ST	2ND CORNER POINTS 3RD	4TH	L.C. DAISY	TOP BOT	SIGMA X	SIGMA Y	SIGMA Z	TAU	SIGMA 1	SIGMA 2	TAU MAX	HENCKY-VON MIS.STRESS	ANG

STRESSES IN BENDING TRIANGULAR PLATES (TRIB3 ELM)

| 251 | 1701 | 1704 | 1801 | 17 | T | -214.5 | -879.9 | 0.0 | -342.3 | -69.8 | -1024.5 | 477.3 | 991.4 | LCL X-22 |
| | | | | | B | -123.7 | -847.6 | 0.0 | -324.6 | 0.5 | -971.8 | 486.2 | 972.1 | -20 |

STRESSES IN QUADRILATERAL BENDING PLATE (QUAB4 ELM)

| 272 | 1801 1806 1706 1701 | 17 | | T | 0.0 | -161.6 | -806.9 | 9.2 | -161.4 | -807.0 | 322.8 | 739.7 | GLB Y |
| | | | | B | 0.0 | -163.4 | -805.2 | 8.3 | -163.3 | -805.3 | 321.0 | 737.3 | |

STRESSES IN BENDING TRIANGULAR PLATES (TRIB3 ELM)

| 291 | 1801 | 1804 | 1901 | 17 | T | -123.8 | -839.3 | 0.0 | -234.3 | -53.9 | -909.2 | 427.7 | 883.5 | LCL X-16 |
| | | | | | B | -101.5 | -853.3 | 0.0 | -222.9 | -40.3 | -914.4 | 437.0 | 894.9 | -15 |

STRESSES IN QUADRILATERAL BENDING PLATE (QUAB4 ELM)

| 310 | 1901 1906 1806 1801 | 17 | | T | 0.0 | -155.4 | -802.0 | 21.6 | -154.7 | -802.7 | 324.0 | 737.6 | GLB Y |
| | | | | B | 0.0 | -149.3 | -800.9 | 26.5 | -148.2 | -801.9 | 326.9 | 739.1 | |

STRESSES IN BENDING TRIANGULAR PLATES (TRIB3 ELM)

| 319 | 1901 | 1904 | 2001 | 17 | T | -124.8 | -855.7 | 0.0 | -187.9 | -79.3 | -901.2 | 411.0 | 864.3 | LCL X-1 |
| | | | | | B | -114.2 | -839.1 | 0.0 | -192.6 | -66.1 | -887.1 | 410.5 | 855.9 | -1 |

TABLE C-3   FINE MESH #4

STRESS : KG/CM**2

SELECTIVE STRESS OUTPUT FOR LOAD CASE 15
****

ELEM NO	CORNER POINTS 1ST 2ND 3RD 4TH	L.C. DAISY	TOP BOT	SIGMA X	SIGMA Y	SIGMA Z	TAU	SIGMA 1	SIGMA 2	TAU MAX	HENCKY-VON MIS.STRESS	ANG ....
STRESSES IN QUADRILATERAL BENDING PLATE (QUAD4 ELM)												
320	3197 3196 3296 3297	5	T	10.0	798.8	0.0	-26.8	799.7	9.1	395.3	795.2	LCL X-8
			B	13.6	824.5	0.0	-32.8	825.8	12.3	406.8	819.7	-8
342	3178 3196 3296 3278	5	T	0.0	131.1	906.7	43.4	909.1	128.7	390.2	852.1	GLB Y 5
			B	0.0	-138.8	849.6	54.6	852.6	-141.8	497.2	931.7	8
343	3297 3296 3396 3397	5	T	42.7	841.7	0.0	-24.1	842.5	42.0	400.2	822.3	LCL X-8
			B	-46.5	785.6	0.0	-15.8	785.9	-46.8	416.3	810.3	-8
362	3278 3296 3396 3378	5	T	0.0	21.7	724.0	174.7	765.1	-19.3	392.2	774.9	GLB Y 7
			B	0.0	-180.5	680.3	132.4	700.2	-200.4	450.3	819.0	8
363	3397 3396 3496 3497	5	T	70.4	879.1	0.0	-10.3	879.2	70.3	404.5	846.3	LCL X-5
			B	5.5	856.3	0.0	13.5	858.5	5.3	426.6	855.9	6
427	3497 3496 3596 3597	5	T	98.5	862.6	0.0	49.3	865.7	95.4	385.1	822.1	LCL X 8
			B	99.6	844.3	0.0	46.6	847.2	96.7	375.2	803.2	8
STRESSES IN BENDING TRIANGULAR PLATES (TRIB3 ELM)												
439	3596 3496 3587	5	T	1028.9	230.7	0.0	-471.2	1247.2	12.3	617.5	1241.1	LCL X-
			B	1024.6	231.7	0.0	-474.8	1246.7	9.6	618.6	1242.0	-
461	3596 3496 3486	5	T	1029.4	185.8	0.0	-20.4	1029.9	185.3	422.3	950.9	LCL X
			B	993.4	174.4	0.0	-14.8	993.7	174.1	409.8	919.1	
STRESSES IN QUADRILATERAL BENDING PLATE (QUAB4 ELM)												
484	3586 3687 3596 3587	5	T	353.6	973.5	0.0	562.7	1306.0	21.1	642.4	1295.5	LCL X
			B	380.0	966.8	0.0	567.7	1312.4	34.4	639.0	1295.6	
STRESSES IN BENDING TRIANGULAR PLATES (TRIB3 ELM)												
486	3597 3596 3687	5	T	170.1	977.7	0.0	-10.2	977.8	170.0	403.9	904.9	LCL X-
			B	170.6	962.8	0.0	-10.1	962.9	170.4	396.2	890.0	-

TABLE C-3   FINE MESH #4, STBD
(Cont'd)   STRESS : KG/CM**2

SELECTIVE STRESS OUTPUT FOR LOAD CASE 53
****

ELEM NO	CORNER POINTS 1ST 2ND 3RD 4TH	L.C. DAISY	TOP BOT	SIGMA X	SIGMA Y	SIGMA Z	TAU	SIGMA 1	SIGMA 2	TAU MAX	HENCKY-VON MIS.STRESS	A

STRESSES IN QUADRILATERAL BENDING PLATE (QUAB4 ELM)

| 427 | 3497 3496 3596 3597 | 17 | T | 127.6 | 852.1 | 0.0 | 47.1 | 855.2 | 124.6 | 365.3 | 800.2 | LCL |
| | | | B | 124.3 | 834.9 | 0.0 | 44.8 | 837.7 | 121.5 | 358.1 | 784.1 | |

STRESSES IN BENDING TRIANGULAR PLATES (TRIB3 ELM)

| 439 | 3596 3496 3587 | 17 | T | 1003.0 | 210.0 | 0.0 | -455.4 | 1210.4 | 2.7 | 603.8 | 1209.0 | LCL |
| | | | B | 1001.4 | 209.8 | 0.0 | -457.0 | 1210.2 | 1.1 | 604.6 | 1209.7 | |

STRESSES IN QUADRILATERAL BENDING PLATE (QUAB4 ELM)

440	3420 3410 3610 3620	17	T	480.0	164.1	0.0	523.0	868.3	-224.3	546.3	999.5	LCL
			B	-469.1	96.1	0.0	475.9	367.0	-739.9	553.5	976.6	
441	3420 3620 3640 3440	17	T	110.0	-184.4	0.0	-520.6	503.8	-578.2	541.0	937.8	LCL
			B	358.3	75.2	0.0	-566.9	801.0	-367.5	584.3	1035.0	

STRESSES IN BENDING TRIANGULAR PLATES (TRIB3 ELM)

| 461 | 3596 3496 3486 | 17 | T | 1017.2 | 187.4 | 0.0 | -49.3 | 1020.1 | 184.5 | 417.8 | 941.5 | LCL |
| | | | B | 968.5 | 170.1 | 0.0 | -40.3 | 970.5 | 168.0 | 401.3 | 898.4 | |

STRESSES IN QUADRILATERAL BENDING PLATE (QUAB4 ELM)

465	3402 3702 3732 3632	17	T	0.0	-674.2	-126.8	-342.6	38.0	-839.0	438.5	858.7	GLB
			B	0.0	-675.1	-129.8	-342.7	35.5	-840.4	438.0	858.7	
484	3586 3687 3596 3587	17	T	342.4	936.5	0.0	528.0	1245.3	33.7	605.8	1228.8	LCL
			B	355.9	929.2	0.0	530.1	1245.2	39.9	602.6	1225.7	

TABLE C-4 FINE MESH #5, PORT

SELECTIVE STRESS OUTPUT FOR LOAD CASE 50
****

STRESS : KG/CM**2

ELEM NO	1ST	CORNER POINTS 2ND	3RD	4TH DAISY	L.C.	TOP BOT	SIGMA X	SIGMA Y	SIGMA Z	TAU	SIGMA 1	SIGMA 2	TAU MAX	HENCKY-VON MIS.STRESS

STRESSES IN QUADRILATERAL BENDING PLATE (QUAB4 ELM)

ELEM NO	1ST	2ND	3RD	4TH	DAISY	TOP/BOT	SIGMA X	SIGMA Y	SIGMA Z	TAU	SIGMA 1	SIGMA 2	TAU MAX	HENCKY-VON MIS.STRESS
307	1994	1992	2092	2094	14	T	230.9	1297.4	0.0	-10.1	1297.5	230.8	533.4	1198.9 L
						B	225.1	1255.9	0.0	-7.2	1256.0	225.0	515.5	1160.0
308	1996	1994	2094	2096	14	T	248.0	1079.1	0.0	93.1	1089.4	237.6	425.9	992.2 L
						B	198.3	1019.6	0.0	105.4	1032.9	185.0	423.9	953.9
309	1998	1996	2096	2098	14	T	180.5	941.4	0.0	122.1	960.5	161.4	399.5	890.8 L
						B	146.1	884.1	0.0	126.5	905.2	125.0	390.1	849.6
310	2000	1998	2098	2100	14	T	88.0	932.0	0.0	135.5	953.2	66.8	443.2	921.6 L
						B	95.0	888.4	0.0	157.1	918.4	65.1	426.7	887.6
320	1980	2080	2100	2000	14	T	0.0	277.9	847.0	215.1	919.1	205.8	356.7	835.5 G
						B	0.0	232.5	825.0	209.8	891.8	165.7	363.1	821.6
324	1942	2042	2052	1952	14	T	0.0	159.6	870.2	-2.3	870.2	159.6	355.3	802.4 G
						B	0.0	111.2	827.3	-20.2	827.8	110.7	358.6	778.4
325	1952	2052	2072	1972	14	T	0.0	155.6	1009.7	55.2	1013.3	152.0	430.6	946.5 G
						B	0.0	141.5	963.5	54.7	967.1	137.9	414.6	906.1
326	1972	2072	2092	1992	14	T	0.0	131.7	1258.9	231.1	1304.4	86.2	609.1	1263.5 G
						B	0.0	143.8	1229.2	231.0	1276.3	96.7	589.8	1230.8
329	1986	2086	2092	1992	14	T	765.3	343.3	0.0	723.7	1308.1	-199.5	753.8	1418.4 L
						B	754.3	384.7	0.0	684.4	1278.4	-139.4	708.9	1353.5
333	2094	2092	2192	2194	14	T	415.9	1511.6	0.0	-64.8	1515.4	412.1	551.6	1357.1 L
						B	408.2	1503.8	0.0	-45.4	1505.7	406.3	549.7	1349.3
334	2096	2094	2194	2196	14	T	308.9	997.9	0.0	-7.8	998.0	308.8	344.6	884.9 L
						B	289.6	1005.0	0.0	2.1	1005.0	289.6	357.7	896.0
335	2098	2096	2196	2198	14	T	193.4	884.2	0.0	30.0	885.5	192.1	346.7	806.8 L
						B	191.3	897.8	0.0	36.8	899.7	189.4	355.2	821.5
347	2172	2192	2092	2072	14	T	0.0	121.7	1484.3	113.0	1493.6	112.4	690.6	1440.7 G
						B	0.0	135.1	1438.0	117.8	1448.5	124.5	662.0	1390.5
348	2152	2172	2072	2052	14	T	0.0	184.8	1006.6	64.4	1011.6	179.8	415.9	934.8 G
						B	0.0	123.3	954.0	65.8	959.2	118.2	420.5	905.9
349	2142	2152	2052	2042	14	T	0.0	143.6	870.7	39.0	872.8	141.5	365.6	811.4 G
						B	0.0	129.5	840.1	36.9	842.0	127.6	357.2	786.0

TABLE C-4 FINE MESH #5, PORT
(Cont'd)
SELECTIVE STRESS OUTPUT FOR LOAD CASE 50

STRESS : KG/CM**2

ELEM NO	1ST	2ND	3RD	4TH	L.C. DAISY	TOP BOT	SIGMA X	SIGMA Y	SIGMA Z	TAU	SIGMA 1	SIGMA 2	TAU MAX	HENCKY-VON MIS.STRESS	ANG SIGI .....AXIS

STRESSES IN BENDING TRIANGULAR PLATES (TRIB3 ELM)

ELEM NO	1ST	2ND	3RD	4TH	L.C. DAISY	TOP BOT	SIGMA X	SIGMA Y	SIGMA Z	TAU	SIGMA 1	SIGMA 2	TAU MAX	HENCKY-VON MIS.STRESS	ANG SIGI .....AXIS
374	2124	2132	2122		14	T	17.8	-131.4	0.0	466.2	415.3	-528.9	472.1	819.7	GLB X 40.5
						B	39.4	-121.2	0.0	469.4	435.3	-517.1	476.2	825.9	40.1
378	2186	2116	2192		14	T	714.1	-219.2	0.0	415.0	872.5	-377.6	625.0	1110.5	GLB X 20.8
						B	801.8	-278.1	0.0	441.4	959.3	-435.6	697.4	1236.1	19.6

STRESSES IN QUADRILATERAL BENDING PLATE (QUAB4 ELM)

ELEM NO	1ST	2ND	3RD	4TH	L.C. DAISY	TOP BOT	SIGMA X	SIGMA Y	SIGMA Z	TAU	SIGMA 1	SIGMA 2	TAU MAX	HENCKY-VON MIS.STRESS	ANG SIGI .....AXIS
384	2141	2191	2183	2173	14	T	281.9	3.9	0.0	464.1	627.3	-341.5	484.4	851.1	GLB X 36.7
						B	260.1	-53.6	0.0	464.4	593.4	-386.9	490.2	855.2	35.7
385	2173	2183	2186	2174	14	T	327.3	-151.5	0.0	400.2	554.2	-378.4	466.3	812.5	GLB X 29.6
						B	271.9	-237.1	0.0	387.4	480.9	-446.1	463.5	803.0	28.3
388	2194	2192	2292	2294	14	T	232.1	1384.5	0.0	-140.7	1401.4	215.2	593.1	1307.2	LCL X-83.1
						B	218.6	1357.6	0.0	-159.7	1379.5	196.7	591.4	1292.5	-82.2
389	2196	2194	2294	2296	14	T	244.6	1049.7	0.0	-111.2	1064.8	229.5	417.7	970.6	LCL X-82.3
						B	208.7	1030.1	0.0	-109.1	1044.4	194.5	425.0	962.0	-82.6
390	2198	2196	2296	2298	14	T	142.5	876.1	0.0	-48.2	879.3	139.3	370.0	818.6	LCL X-86.3
						B	147.3	878.2	0.0	-41.0	880.5	145.0	367.8	817.7	-86.8
392	2104	2102	2202	2204	14	T	188.4	0.0	767.5	169.1	813.3	142.7	335.3	752.2	GLB Z 15.1
						B	175.4	0.0	757.3	172.9	804.8	127.9	338.4	749.1	15.4
402	2272	2292	2192	2172	14	T	0.0	38.8	1348.8	178.2	1372.6	15.0	678.8	1365.2	GLB Y 82.4
						B	0.0	71.3	1323.9	197.9	1354.5	40.8	656.8	1334.5	81.2
403	2252	2272	2172	2152	14	T	0.0	139.5	1037.6	135.6	1057.7	119.5	469.1	1003.3	GLB Y 81.6
						B	0.0	51.5	974.6	159.6	1001.4	24.7	488.4	989.3	80.5
404	2242	2252	2152	2142	14	T	0.0	116.7	889.5	181.2	929.9	76.3	426.8	894.2	GLB Y 77.4
						B	0.0	95.5	852.7	168.8	880.7	59.5	414.6	860.4	70.0
405	2232	2242	2142	2132	14	T	0.0	101.0	804.8	126.5	826.8	79.0	373.9	790.3	GLB Y 80.1
						B	0.0	84.1	773.9	134.2	799.1	58.9	370.1	771.3	79.4

TABLE C-5 SL-7, FINE MESH #6, STBD

SELECTIVE STRESS OUTPUT FOR LOAD CASE 51

STRESS : KG/CM**2

***************************************.

ELEM NO	CORNER POINTS 1ST 2ND 3RD 4TH DAISY				L.C.	TOP BOT	SIGMA X	SIGMA Y	SIGMA Z	TAU	SIGMA 1	SIGMA 2	TAU MAX	HENCKY-VON MIS.STRESS	ANG ...

FORCES AND STRESSES IN FLANGES OR RODS (ROD2 ELM)

ELEM NO	CORNER POINTS START END		LOAD CASE	AXIAL FORCE	AXIAL STRESS
124	4484	4485	15	0.9197D-01	919.67

STRESSES IN QUADRILATERAL BENDING PLATE (QUAB4 ELM)

ELEM NO	CORNER POINTS 1ST 2ND 3RD 4TH				L.C.	TOP BOT	SIGMA X	SIGMA Y	SIGMA Z	TAU	SIGMA 1	SIGMA 2	TAU MAX	HENCKY-VON MIS.STRESS	ANG
408	4484	4521	4465	4485	15	T	433.1	0.0	694.9	397.8	982.7	145.2	418.8	918.8 GLB	Z 3
						B	244.6	0.0	447.5	297.7	660.5	31.6	314.5	645.3	3

STRESSES IN BENDING TRIANGULAR PLATES (TRIB3 ELM)

ELEM NO	CORNER POINTS 1ST 2ND 3RD			L.C.	TOP BOT	SIGMA X	SIGMA Y	SIGMA Z	TAU	SIGMA 1	SIGMA 2	TAU MAX	HENCKY-VON MIS.STRESS	ANG
409	4521	4486	4465	15	T	428.7	0.0	670.8	-304.8	883.2	224.3	329.5	795.2 GLB	Z-3
					B	39.3	0.0	248.3	-262.8	426.6	-139.0	282.8	510.4	-3
410	4465	4495	4485	15	T	137.9	0.0	672.5	-319.4	821.7	-11.3	416.5	827.5 GLB	Z-2
					B	244.2	0.0	648.9	-361.9	861.1	32.0	414.6	845.6	-3
420	4523	4486	4521	15	T	427.8	0.0	690.5	-235.0	828.4	289.9	269.2	728.1 GLB	Z-3
					B	53.1	0.0	279.5	-191.4	388.7	-56.1	222.4	419.5	-2

SHIP STRUCTURE COMMITTEE PUBLICATIONS

SL-7 PUBLICATIONS TO DATE

SL-7-1, (SSC-238) - *Design and Installation of a Ship Response Instrumentation System Aboard the SL-7 Class Containership S.S. SEA-LAND McLEAN* by R. A. Fain. 1974. AD 780090.

SL-7-2, (SSC-239) - *Wave Loads in a Model of the SL-7 Containership Running at Oblique Headings in Regular Waves* by J. F. Dalzell and M. J. Chiocco. 1974. AD 780065.

SL-7-3, (SSC-243) - *Structural Analysis of SL-7 Containership Under Combined Loading of Vertical, Lateral and Torsional Moments Using Finite Element Techniques* by A. M. Elbatouti, D. Liu, and H. Y. Jan. 1974. AD-A002620.

SL-7-4, (SSC-246) - *Theoretical Estimates of Wave Loads on the SL-7 Containership in Regular and Irregular Seas* by P. Kaplan, T. P. Sargent, and J. Cilmi. 1974. AD-A004554.

SL-7-5, (SSC-257) - *SL-7 Instrumentation Program Background and Research Plan* by W. J. Siekierka, R. A. Johnson, and CDR C. S. Loosmore, USCG. 1976. AD-A021337.

SL-7-6, (SSC-259) - *Verification of the Rigid Vinyl Modeling Techniques: The SL-7 Structure* by J. L. Rodd. 1976. AD-A025717.

SL-7-7, (SSC-263) - *Static Structural Calibration of Ship Response Instrumentation System Aboard the SEA-LAND McLEAN* by R. R. Boentgen and J. W. Wheaton. 1976. AD-A031527.

SL-7-8, (SSC-264) - *First Season Results from Ship Response Instrumentation Aboard the SL-7 Class Containership S.S. SEA-LAND McLEAN in North Atlantic Service* by R. R. Boentgen, R. A. Fain, and J. W. Wheaton. 1976. AD-A039752.

SL-7-9, *Second Season Results from Ship Response Instrumentation Aboard the SL-7 Class Containership S. S. SEA-LAND McLEAN in North Atlantic Service* by J. W. Wheaton and R. R. Boentgen. 1976. AD-A034162.

SL-7-10, *Third Season Results from Ship Response Instrumentation Aboard the SL-7 Class Containership S. S. SEA-LAND McLEAN in North Atlantic Service* by R. R. Boentgen. 1976. AD-A034175.

SL-7-11, (SSC-269) - *Structural Tests of SL-7 Ship Model* by W. C. Webster and H. G. Payer. 1977. AD-A047117.

SL-7-12, (SSC-271) - *A Correlation Study of SL-7 Containership Loads and Motions - Model Tests and Computer Simulation* by P. Kaplan, T. P. Sargent, and M. Silbert. 1977. AD-A049349.

SL-7-13, *A Report on Shipboard Waveheight Radar System* by D. Chen and D. Hammond. 1978. AD-A053379.

SL-7-14, (SSC-277) - *Original Radar and Standard Tucker Wavemeter SL-7 Containership Data Reduction and Correlation Sample* by J. F. Dalzell. 1978. AD-A062394.

SL-7-15, (SSC-278) - *Wavemeter Data Reduction Method and Initial Data for the SL-7 Containership* by J. F. Dalzell. 1978. AD-A062391.

SL-7-16, *Radar and Tucker Wavemeter Data from S. S. SEA-LAND McLEAN - Voyage 32* by J. F. Dalzell. 1978. AD-A057154.

SL-7-17, *Radar and Tucker Wavemeter Data from S. S. SEA-LAND McLEAN - Voyage 33* by J. F. Dalzell. 1978. AD-A057155.

SL-7-18, *Radar and Tucker Wavemeter Data from S. S. SEA-LAND McLEAN - Voyage 34* by J. F. Dalzell. 1978. AD-A057156.

SL-7-19, *Radar and Tucker Wavemeter Data from S. S. SEA-LAND McLEAN - Voyages 35 and 36E* by J. F. Dalzell. 1978. AD-A057157.

SL-7-20, (SSC-279) - *Modified Radar and Standard Tucker Wavemeter SL-7 Containership Data* by J. F. Dalzell. 1978. AD-A062393.

SL-7-21, *Radar and Tucker Wavemeter Data from S. S. SEA-LAND McLEAN - Voyage 60* by J. F. Dalzell. 1978. AD-A057004.

SL-7-22, *Radar and Tucker Wavemeter Data from S. S. SEA-LAND McLEAN - Voyage 61* by J. F. Dalzell. 1978. AD-A057005.

SL-7-23, (SSC-280) - *Results and Evaluation of the SL-7 Containership Radar and Tucker Wavemeter Data* by J. F. Dalzell. 1978. AD-A062392.

SL-7-24, (SSC-282) - *Comparison of Stresses Calculated Using the DAISY System to Those Measured on the SL-7 Containership Program* by H-Y Jan, K-T Chang, and M. E. Wojnarowski. 1979.